S O U T H   F L O R I D A   W A T E R   M A N A G E M E N T   D I S T R I C T

Technical Publication
WR-2014-004

STORMWATER TREATMENT AREA WATER AND PHOSPHORUS BUDGET IMPROVEMENTS

PHASE I:

STA-3/4 CELLS 3A AND 3B WATER BUDGETS

Ceyda Polatel, Wossenu Abtew, Steve Krupa and Tracey Piccone

South Florida Water Management District
3301 Gun Club Road
West Palm Beach, FL 33406

November 2014

sfwmd.gov

Summary

The analyses conducted during Phase I of the Stormwater Treatment Area (STA) Water and Phosphorus Budget Improvements Study are presented in this report. Phase I of the study focused on identifying the sources of errors in STA water budgets and methods to reduce these errors, as well as developing improved cell-by-cell water budgets for Cells 3A and 3B of STA-3/4. Currently used and alternative methods to estimate the components of the water budgets were reviewed for potential improvements. Phase II of the study will extend water budget analysis to other cells of STA-3/4 and STA-2, which were selected as a result of a resource prioritization effort to focus on treatment cells most relevant to the successful completion of the Restoration Strategies for Clean Water for the Everglades Science Plan studies. Phase II of the study will also include improvements to phosphorus budgets based on improvements to the water budgets for the selected treatment cells.

In this first phase of the study, all components of the cell-by-cell water budgets for Cells 3A and 3B were reviewed. The spatial and temporal variability of rainfall and evapotranspiration data and the differences in data from various sources were investigated. A comparison of next generation radar (NEXRAD) and rain gauge data found a notable difference in the rainfall estimates by these two methods. It is currently not possible to determine which data set is superior; therefore, it is recommended that STA water budget analyses continue using rain gauges when available with NEXRAD data used to fill gaps. The results of ongoing efforts (external to this study) to address the question of whether the rain gauge or NEXRAD data better represents the actual volume of rainfall over an area can be applied to future water budget analyses. Comparison of satellite and lysimeter-based evapotranspiration methods revealed no significant difference in the effect of the two methods on the annual water budgets. Updated cell effective treatment areas were used in the analyses.

Available methods to estimate seepage were reviewed and applied to Cells 3A and 3B of STA-3/4. A seepage estimation method based on reconciliation of the water budget for historical "no flow, no rainfall" periods was developed and used to quantify the effect of seepage on water budget. Data collection and surface water flow computation protocols and procedures were reviewed. Historical stage and flow data were examined for errors. Corrections were applied to stage data for flow-way inflow (G-380) and mid-levee (G-384) structures. Datum adjustment and sensor calibration corrections were applied to stage data at G-384 by the Hydro Data Management Section staff. Corrections due to a clogged well were applied at G-380. The accuracy of the current flow ratings at water control structures was reviewed. A computational fluid dynamics-based flow rating equation was developed for the G-384A-F culverts. Errors in change in storage estimation were evaluated as a function of errors in water depth measurements.

Low head differentials at the G-384 internal control structures were identified as the main source of high residual errors and spurious flow data in Cells 3A and 3B water budgets. Three methods to fix the historical flow rate data, one based on data correction and two on back calculation, were used to improve water budgets for these cells. The back calculation method produced the most improvement with a resulting annual residual error ranging from less than 1% to 9%, well below the target annual residual of 10% or less. Phase II of this study will involve more thorough analysis and development of improved flow data for the structures in STA-3/4. The improved flow data will then be loaded in DBHYDRO, the South Florida Water Management District's (District's) corporate environmental database, for use in developing improved water and total phosphorus budgets.

An uncertainty analysis was performed to estimate the expected uncertainties in the water budget residual by propagating the uncertainties in each component through the water budget equation. Based on the uncertainty analysis, the expected residual error for the considered cells was 17% or less for any given water year and 9% or less for a four-year period of record. The biggest source of uncertainties in the residuals was identified as the surface water flows. Despite constituting a small fraction of the water budget, due to large uncertainties in its estimates, seepage was found to be a major contributor to the residual uncertainty. It is expected that future efforts of reducing uncertainties in seepage estimates will help improve water budgets. Attempts to reduce the errors and uncertainties in each of the water budget terms should be made where feasible in order to improve the reliability of the data to characterize treatment performance of the STA cells.

Based on the results of the Phase I test case, applied corrections to the stage and flow rate data and estimated seepage rates for Cells 3A and 3B are sufficient for cell-by-cell water budgets with acceptable residual errors. Should further improvements to STA annual water budgets be desired, a series of potential activities could be implemented. To prevent the occurrence of unfavorably low head differentials in the future, operational modifications such as automating the gate operations as a function of the head differential are suggested. Flow uncertainty curves were provided to guide the operation of mid-levee culverts to minimize error in the computed flows. Structural changes could include augmenting internal structures with pumps and retrofitting culvert inlets to install v-notch weirs. More field measurements at low head conditions, provided they are within the accuracy limits of field instruments, are recommended to improve the accuracy of the flow estimates. Considering the sensitivity of the estimated flows to small variations in stage records, conducting periodic structure and stilling well surveys is advised. Changes in data acquisition and analysis, including installation of more than one set of stage sensors for internal structures, changes in the sampling protocols, use of differential head measurements, and periodic inspection and calibrations of the sensors are recommended. Tagging the flows computed with very low head differential to warn users of potentially erroneous flow rates can also be considered. Improvements in the data analysis including reporting uncertainty limits or quality indicators for flow data and using “PREF DBKEYs” for internal structures are also suggested. It must be noted here that these recommendations can be capital intensive, and a feasibility analysis is recommended to determine potential cost of implementation.

In the second phase of the study, investigation of methods to eliminate and correct for spurious flow computations in the mid-levees will continue. The presented analysis will be expanded to other cells of STA-3/4 and STA-2 and phosphorus budgets will also be developed. The variables and equations used in the District’s Water Budget Tool will be reviewed and capability to compute seepage for individual cells will be added.

The mid-levee flows (G-384) used in the analyses are provisional and subject to revision.

Presented water budget analyses will be revisited after G-384 flows are corrected.

Acknowledgements

The authors wish to express appreciation to the following individuals (in alphabetical order) for providing comments and/or data: Marjorie Coley, Jamie Crandall, Emile Damisse, Tibebe Dessalegne, Delia Ivanoff, Kang-Ren Jin, Harold Hennessey-Correa, Neil Larson, Richard Miessau, Ron Pinak, Anier Sosa, Felipe Zamorano, Lichun Zhang and Liqiong Zhang. All data analyses presented in this report were performed by the authors unless otherwise stated. The authors extend special thanks to Matahel Ansar, Hal Hennessey-Correa, Scott Huebner, Pamela Lehr, Sashi Nair, Anurag Nayak, Sarah Noorjahan, Jose Otero, John Raymond, Garth Redfield, Larry Schwartz, Mark Wilsnack, Gary Wu, and Shi Xue for their reviews.

Table of Contents

SUMMARY I

ACKNOWLEDGEMENTS III

LIST OF FIGURES VI

LIST OF TABLES VIII

LIST OF SYMBOLS X

LIST OF ACRONYMS AND ABBREVIATIONS XI

1 INTRODUCTION 1

2 OBJECTIVE AND SCOPE 3

3 WATER BUDGET ANALYSES FOR STORMWATER TREATMENT AREAS 5

3.1 Cells 3A and 3B Water Budget Analyses in the 2013 SFER 6

4 EFFECTIVE TREATMENT AREAS 8

5 SURFACE WATER INFLOW AND OUTFLOW 9

5.1 Flow Computations at Culverts 9
5.2 Rating Status for Flow-way 3 Water Control Structures 10
5.3 Mid-Levee Culverts Flow Data Review 12
5.4 Correcting Flow Data for Mid-Levee Culverts 14
5.4.1 Method 1: Correcting Mid-Levee Flows by Setting Small Head Differentials to Zero 15
5.4.2 Method 2: Back-Calculating Mid-Levee Flow Rates by Redistributing Flow-way 3 Water Budget Residuals 18
5.4.3 Method 3: Back-Calculating Mid-Levee Flow Rates As the Weighted Average of Flow-way 3 Inflows and Outflows 21

6 SEEPAGE 23

6.1 Seepage Estimation Methods 23
6.1.1 Application of Flux Measurements from ENR 25
6.1.2 Seep2D Model for STA-3/4 26
6.1.3 Seepage Study for STA-3/4 Design 29
6.1.4 Combined Water and Solute Mass Balance 30
6.1.5 Analysis of Historical No Flow/No Rainfall Periods for Seepage Estimation 30
6.1.6 Water Budget Tool 35
6.1.7 Direct Measurements 35
6.2 Effect of Seepage on Water Budget 35

7 RAINFALL 40

7.1 Comparison of Rainfall Estimation Methods 40
7.2 Rainfall Data for Cells 3A and 3B 48

8 EVAPOTRANSPIRATION 52

8.1 Spatial Variations 53
8.2 Comparison of Evapotranspiration Estimation Methods 54
8.3 Relative Magnitude of Rainfall and ET in STA Water Budgets 56

9 CHANGE IN STORAGE 58

10 STA WATER BUDGET UNCERTAINTY ANALYSIS 59

10.1 Flow Rate Uncertainty Analysis 59
10.1.1 Law of Propagation of Uncertainty 60

10.1.2 Propagation of Uncertainty for Culverts Flowing Full *60*
10.2 Managing Flow Rate Uncertainty for Culverts Flowing Full 62
10.3 Propagation of Uncertainties to the Water Budget Residual 64
11 KEY FINDINGS AND IMPROVED WATER BUDGETS 68
12 CONCLUSIONS 70
13 REFERENCES 72
APPENDIX: LIST OF COMPLETED TASKS AND RECOMMENDATIONS 74

List of Figures

Figure 1. STA-3/4 site plan (from SFWMD 2007). 2
Figure 2. Comparison of existing and updated ratings for G-384 (Zhang 2013). 11
Figure 3. G-384 head differential histogram for WY2009–WY2012 based on 15-minute interpolated data. 12
Figure 4. G-384 gate opening histogram for WY2009–2012 based on 15-minute interpolated data. 12
Figure 5. Δh vs Q per culvert curves for G-384A–F for the new (Cd = 0.754) and old ratings (Cd = 0.85) (with G = 8 ft, n = 0.012). 13
Figure 6. Historical inflow and outflow discharges for Cell 3A. 15
Figure 7. Historical inflow and modified outflow (Method 1) discharges for Cell 3A. 15
Figure 8. Modified inflow (Method 1) and historical outflow discharges for Cell 3B. 16
Figure 9. Components of water budgets for Flow-way 3 and Cells 3A and 3B. 19
Figure 10. Comparison of mid-levee flows computed by Methods 2 and 3. 21
Figure 11. Locations of stage recorders in the vicinity of Flow-way 3. 24
Figure 12. Locations and seepage coefficients for STA-3/4 cross-sections by Sangoyomi et al. (2011). (Note: ft^3/d/ft-levee/ft-head – cubic feet per day times height of levee time height of head.) 27
Figure 13. Approximate dimensions in acres (ac) and miles (mi) for Cells 3A and 3B. 28
Figure 14. Holey Land and average Cell 3A stages since May 2008. 31
Figure 15. Holey Land and average Cell 3B stages since May 2008. 31
Figure 16. Holey Land and average cell stages for December 2008 to June 2009. 34
Figure 17. STA-1W rainfall gauges and NEXRAD pixels. 41
Figure 18. Difference between NEXRAD and gauge monthly average areal rainfall in STA-1W. 42
Figure 19. Mean monthly NEXRAD and gauge areal average rainfall for STA-1W (WY2001–WY2012). 43
Figure 20. August 2004 NEXRAD rainfall estimate (10.05 inches) for STA-1W when gauge Thiessen average estimate was 5.08 inches. 44
Figure 21. Mean monthly difference in a NEXRAD pixel and a gauge rainfall. 46
Figure 22. a) August 2012 NEXRAD rainfall estimates, for STA-1E (20.52 inches) and for STA-1W (14.67 inches); b) main rainfall band on STA-1E (Tropical Storm Isaac August 25–28, 2014). 47
Figure 23. Rain stations in the vicinity of STA-3/4 Cell 3A. 48
Figure 24. Variations in rainfall from various rain stations for STA-3/4 Cell 3A for WY2012. 49
Figure 25. NEXRAD pixels covering Cells 3A and 3B. 50
Figure 26. Map of available ET stations in the vicinity of Flow-way 3. 52
Figure 27. Comparison of monthly ET measurements at weather stations in the vicinity of STA-3/4 Cell 3A. 54
Figure 28. Comparison of monthly ET over STA-3/4 Cells 3A and 3B with DBHYDRO ET and satellite-based ET data for January 2008 to December 2012. 55
Figure 29. Rainfall and ET as percentage of inflow a) expected average inflow and b) historical inflows. 57
Figure 30. Errors in change in storage due to depth estimation errors of 0.1, 0.2, 0.3 and 0.4 ft. 58
Figure 31. Histogram of percent uncertainties in G-384 daily flow rates before corrections were applied. 61

Figure 32. Comparison of variation of relative flow rate uncertainty with operating head Δh for fully open gates and G_o= 5 ft for culvert 1 (C1).......... 63
Figure 33. Flow rate uncertainty curves for culverts 1 and 2 (C1 and C2).......... 64

List of Tables

Table 1. Water budget analysis for Cell 3A in the 2013 SFER (cell area = 2,153 acres). 7
Table 2. Water budget analysis for Cell 3B in the 2013 SFER (cell area = 2,427 acres). 7
Table 3. Water budget analysis for Cell 3 (Flow-way 3) in the 2013 SFER (Flow-way Area 4,580 ac). 7
Table 4. Effective treatment areas for Cells 3A and 3B. 8
Table 5. Hydraulic properties for Flow-way 3 culverts. 10
Table 6. Flow rating status for Flow-way 3 structures. 11
Table 7. Revisited Cell 3A water budget with corrected mid-levee (G-384) flows (Method 1). 17
Table 8. Revisited Cell 3B water budget with corrected mid-levee (G-384) flows (Method 1). 17
Table 9. Revisited Cell 3 water budget (unaffected by mid-levee flows). 17
Table 10. Cell 3A water budget with back calculated outflow (Method 2). 20
Table 11. Cell 3B water budget with back calculated inflow (Method 2). 20
Table 12. Cell 3 water budget (unaffected by mid-levee flows) (**Table 9** repeated). 20
Table 13. Cell 3A water budget with back-calculated outflow (Method 3). 22
Table 14. Cell 3B water budget with back-calculated inflow (Method 3). 22
Table 15. Cell 3 water budget (unaffected by mid-levee flows) (Table 9 -Repeated). 22
Table 16. WY2009–WY2012 average stages 25
Table 17. Estimated Seepage for Cells 3A, 3B, and Flow-way 3 using the average ENR fluxes by Harvey et al. (2004). (Note: ft^2 – square feet and ft^3/day – cubic feet per day) 26
Table 18. Converted seepage coefficients reported by Sangoyomi et al. (2011). (Note: ac-ft/yr/mi-levee/ft-head – acre-feet per year times length of levee times height of head.) 28
Table 19. Scenario A seepage results (from Montgomery Watson Americas, Inc. 1999, Table 4.6A). 29
Table 20. Scenario B seepage results (from Montgomery Watson Americas, Inc. 1999, Table 4.6B). 29
Table 21. Application of seepage rates from Montgomery Watson Americas, Inc. (1999) to Cell 3A and Cell 3B. 30
Table 22. Seepage rates for Cells 3A and 3B for WY2009–WY2012 estimated from an analysis of dry periods. 35
Table 23. Seepage coefficient currently in use by the Water Budget Tool for the STA-3/4 and corresponding average yearly seepage rates for Cells 3A and 3B during WY2009–WY2012. 35
Table 24. Estimated average yearly seepage rates by all reviewed methods. 36
Table 25. Summary statistics of the estimated average yearly seepage rates by all reviewed methods. . 36
Table 26. WY2009–WY2012 average yearly water budgets with seepage values at the lower CL. 37
Table 27. WY2009–WY2012 average yearly water budgets with mean seepage values. 37
Table 28. WY2009–WY2012 average yearly water budgets with seepage values at the upper CL. 37
Table 29. WY2009–WY2012 percent contributions of water budget components with seepage values at the lower CL. 37
Table 30. WY2009–WY2012 percentage contributions of water budget components with mean seepage values. 38
Table 31. WY2009–WY2012 percentage contributions of water budget components with seepage values at the upper CL. 38

Table 32. Contribution of seepage to the water budgets for WY2009–WY2012. 38
Table 33. WY2009–WY2012 percentage contributions of water budget components for average rainfall, ET and mean seepage values. 38
Table 34. Comparison of water year rainfall estimates over STA-1W by NEXRAD (8 cells) rainfall and five-gauge Thiessen average. 42
Table 35. Comparison of annual rainfall estimates in STA-1W by NEXRAD (one cell) and ENR308 gauge. 45
Table 36. Comparison of water year NEXRAD rainfall and gauge rainfall estimates over STA-2, STA-5 and STA-6 (From Huebner et al., 2007). 46
Table 37. Variation in total water year rainfall from available stations for Cell 3A (2,415 acres). 49
Table 38. Variation in total water year rainfall from available stations for Cell 3B (2,087 acres). 51
Table 39. Differences in rainfall data measured at the S7 rain station and by NEXRAD for Cells 3A and 3B. 51
Table 40. Weather stations used in ET rate estimates for District STAs. 52
Table 41. Variation in ET rate estimates from different weather stations. 53
Table 42. Variations in annual ET volumes from ROTNWX and satellite-based data for Cell 3B (2,087 acres). 56
Table 43. Input variables and their uncertainties for culverts flowing full. 62
Table 44. Threshold operating head ($\Delta\mathrm{h}$) for various relative flow uncertainties for fully open gates. 63
Table 45. Approximate uncertainties in water budget component estimates for 1 water year. 65
Table 46. Sizes of water budget components relative to $(\sum\mathrm{Out} + \sum\mathrm{In})/2$. 66
Table 47. Approximate uncertainties in water budget residuals for various length of record. 66
Table 48. Contribution of water budget components to residual uncertainty. 67
Table 49. Summary of recommendations for Cells 3A and 3B water budget components. 68
Table 50. Improved Cell 3A water budget (**Table 10** repeated). 69
Table 51. Improved Cell 3B water budget (**Table 11** repeated). 69
Table 52. Improved Flow-way 3 water budget (**Table 12** repeated). 69

List of Symbols

A	Area
A_G	Flow area under culvert gate [L^2]
A_c	Planar effective STA cell treatment area [L^2]
A_g	Cross-sectional area of the groundwater flow [L^2]
A_o	Culvert full barrel cross-sectional area [L^2]
B	Culvert width [L]
C_d	Discharge coefficient [-]
D	Culvert depth [L]
ET	Evapotranspiration [L^3/T]
g	gravitational acceleration
G	Culvert gate opening [L]
h	Water stage [feet National Geodetic Vertical Datum of 1929 (ft NGVD)]
h_{2A}	Cell 2A average stage for WY 2009- WY 2012 [ft NGVD]
h_3	Flow-way 3 average stage for WY 2009- WY 2012 [ft NGVD]
h_{3A}	Cell 3A average stage for WY 2009- WY 2012 [ft NGVD]
h_{3B}	Cell 3A average stage for WY 2009- WY 2012 [ft NGVD]
h_{HL}	Holey Land average stages for WY 2009- WY 2012 [ft NGVD]
h_{IC}	Cell 3A Inflow Canal average stage for WY 2009- WY 2012 [ft NGVD]
h_{OC}	Cell 3B Outflow Canal average stage for WY 2009- WY 2012 [ft NGVD]
h_{SC}	STA-3/4 Seepage Canal average stage for WY 2009- WY 2012 [ft NGVD]
h_a	Water stage in a water body adjacent to an STA cell[ft NGVD]
h_c	Water stage within an STA cell [ft NGVD]
h_t	Average cell stage at a specific time step [ft NGVD]
$h_{t-\Delta t}$	Average cell stage at previous time step [ft NGVD]
HW	Headwater stage [ft NGVD]
k	Coverage factor for 95% confidence level [-]
K_e	Effective hydraulic conductivity [L/T]
K_{sp}	Seepage coefficient [L/T]
L	Culvert length [L]
L_{levee}	Levee length [L]
n	Manning's roughness coefficient [-]
Q_c	Computed flow rate [L^3/T]
$Q_{d/s}$	Surface outflow downstream of a flow-way [L^3/T]
Q_g	Seepage flow lost from the STA cell [L^3/T]
Q_{in}	Surface water inflow [L^3/T]
Q_{mid}	Surface flow through mid-levee structures [L^3/T]
Q_{out}	Surface water outflow [L^3/T]
$Q_{u/s}$	Surface inflow upstream of a flow-way [L^3/T]
r	Water budget residual [L^3/T]
R	Precipitation [L^3/T]
R_o	Full barrel hydraulic radius [L]\
t	time
T	time
TW	Tailwater stage [ft NGVD]
u	Standard uncertainty

U	Expanded (total) uncertainty
ε	Percent water budget residual error [%]
Δh_{c-a}	$h_c - h_a$[L]
Δh_t	Change in stage measurements collected at a location at different times [L]
Δh	Difference in concurrent stage measurements [L]
Δl	Length over which the groundwater head drop takes place [L]
ΔS	Change in storage [L^3/T]
Δt	Time step [T]
$\sum In$	$Q_{in} + R$ [L^3/T]
$\sum Out$	$Q_{out} + Q_g + ET$ [L^3/T]

List of Acronyms and Abbreviations

ac-ft	acre-feet
ac-ft/yr	acre-feet per year
CFD	computational fluid dynamics
cfs	cubic feet per second
CI	confidence interval
CL	confidence level
DBHYDRO	SFWMD's corporate environmental database
District	South Florida Water Management District
ENR	Everglades Nutrient Removal Project
ET	evapotranspiration
ETP	potential evapotranspiration
ft	feet
ft NGVD	feet National Geodetic Vertical Datum of 1929
ft/d	feet per day
HDM	Hydro Data Management Section
km	kilometer
NEXRAD	next generation radar (the National Weather Service Doppler radar network)
PREF DBKEY	DBHYDRO preferred value
SFER	South Florida Environmental Report
STA	stormwater treatment area
STA-1E	Stormwater Treatment Area 1 East
STA-1W	Stormwater Treatment Area 1 West
WCA	Water Conservation Area
WY	Water Year

1 Introduction

Previous documents and water budget analyses indicated large residual errors in the cell-by-cell water budget analyses of the District's Stormwater Treatment Areas (STAs) (Pietro 2013). Since the errors in the water budgets hinder quantification of cell performance, a team was formed to investigate the reasons for large residual errors in water budgets and recommend solutions to improve them. Cells 3A and 3B of STA-3/4 were selected for Phase I of the STA Water and Phosphorus Budget Improvements Study to review the methods used in estimation of elements of STA water budgets and recommend improvements. This report summarizes the efforts to review and improve the accuracy of the water budget analysis for Cells 3A and 3B in STA-3/4. These cells were selected due to overlapping interest from various South Florida Water Management District (District) sections in the context of the Restoration Strategies for Clean Water for the Everglades Science Plan. The findings of this phase will be expanded to STA-2 and other cells of STA-3/4 in the subsequent phases of this study.

STA-3/4 is a major structural component of the Everglades Construction Project, mandated by the 1994 Everglades Forever Act (see SFWMD 2007 for more information on location and operation of STA-3/4). STA-3/4 is divided into three north-to-south flow-ways, each consisting of two cells (**Figure 1**). When the STA was originally constructed, the Western Flow-way was one cell (Cell 3 or Flow-way 3). The cell was later divided into Cells 3A and 3B with an internal levee and the G-384 culverts. For this reason, the period of record for Cells 3A and 3B flow data is shorter than the overall Flow-way 3 and the other two flow-ways of STA-3/4.

Low head differentials across the internal control structures (G-384A–F) have been identified as the major contributor of the cell-by-cell water budget residual errors for Cells 3A and 3B (see Section 5). The large culvert cross-sections designed to pass large flows during wet conditions also have to pass low flows during low head conditions. As they operate under low head differentials, internal structures are prone to elicit spurious flow estimation, and introduce errors in water budgets. Hydro Data Management Section (HDM) staff has been working on developing a strategy to identify and apply corrections for spurious flow data generated by low head differentials. However, currently, there is no accepted general solution that can be applied to all culverts operating under low head differentials. Details of the site configuration, stage and flow data need to be investigated before a site-specific solution can be recommended. In addition to the surface water flow rates, estimation methods for all other water budget components (i.e., rainfall, evapotranspiration, and change in storage and seepage) are reviewed and presented in dedicated sections of this report. Uncertainties in culvert flow rates and water budget residuals are also evaluated.

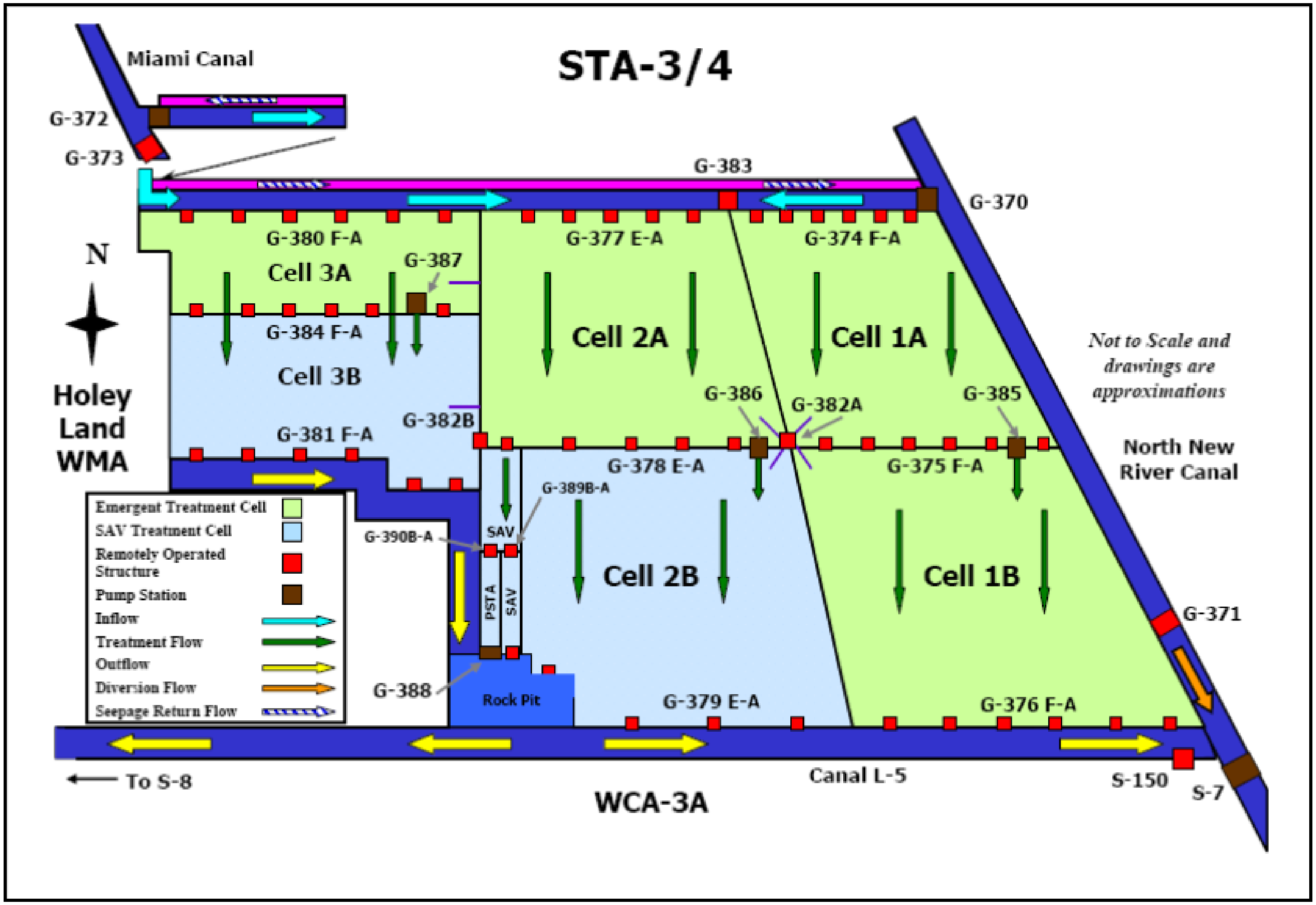

Figure 1. STA-3/4 site plan (from SFWMD 2007).

2 Objective and Scope

The objectives of this report are to review the estimation methods and historical data records involved in cell-by-cell water budgets, investigate the causes of high water budget errors for Cells 3A and 3B for Water Year (WY)2009–WY2012 (a water year begins on May 1 and ends on April 30 of the subsequent year), and revisit the water budgets for these cells. Prior to commencing work on this study, technical participants agreed upon a target annual residual error of 10% or less for a treatment cell water budget. Phase I of the study covered the following tasks:

1. Evaluate the computation of surface water flow rates.
    a. Review historical stage and flow data for Cells 3A and 3B control structures. Evaluate the status of the flow ratings at the control structures, and develop improved ratings if possible.
    b. Apply corrections for erroneous flow data caused by low head differentials.
    c. Perform flow rate uncertainty analysis.
2. Assess available rainfall estimation methods and compare variation in rain gauge and next generation radar (NEXRAD) estimates.
3. Review available evapotranspiration estimation methods, and evaluate the variability in estimates.
4. Review available seepage estimation methods. Analyze historical no flow/no rainfall periods to estimate seepage rates and apply them to Cells 3A and 3B. Conduct a sensitivity analysis to evaluate the effect of seepage on STA water budgets.
5. Develop an improved water budget analysis.
6. Perform uncertainty analysis to propagate the uncertainties in water budget components to residual errors.
7. Provide recommendations to further reduce residual errors in water budgets.

In Phase II, the scope of the study will be expanded to STA-2 Cells 1, 2, and 3 and STA-3/4 Cells 1A, 1B, 2A, and 2B, and will include development of improved phosphorus budgets for these cells using the improved water budgets.

The focus of this report is the desktop evaluation of water budget components for Cells 3A and 3B of STA-3/4. Section 3 presents an overview of STA water budget analyses. Updated effective cell treatment areas for Cells 3A and 3B are given in Section 4. For the STAs, the surface water inflows and outflows are controlled by water control structures where flow rates are monitored. The estimated flow rates for each structure are published in the District's corporate environmental database, DBHYDRO. Section 5 discusses the surface flow computation and potential improvements. Seepage into and from the STA cells is difficult to measure and is believed to display large variations. Several published seepage estimation methods were applied to STA-3/4 Cells 3A and 3B. The results and a sensitivity analysis are discussed in Section 6. The rainfall component of the water budget can be estimated from rain gauges in the vicinity of the cells. NEXRAD data, which is adjusted using the rain gauge data, can also be used to fill gaps in the historical rainfall data. These two methods of estimating rainfall are discussed in depth in Section 7. Evapotranspiration (ET) rate for the STAs is currently considered to be one of the better quantified components in the STA water budgets. An ET rate computation model developed from lysimeter experiments at the Everglades Nutrient Removal Project (ENR) is used for ET estimation. In Section 8 this method was compared against satellite-based data, indicating a good agreement and negligible differences in annual volumes. The estimation of change in storage and potential source of errors are provided in Section 9. Revisited water budgets are included in Section 11. Uncertainty analyses of flow rate computations and water budget residuals are presented in Section 10. Section 11 provides a summary of the findings of the study.

3 Water Budget Analyses for Stormwater Treatment Areas

Water budget analysis is an important tool used to understand the treatment performance of STAs. Accurate water budgets are critical to developing accurate phosphorus budgets. The water budgets for STAs can be expressed in the form of residual of the mathematical difference between all outflow (ΣOut) and inflow (ΣIn) sources plus the change in storage (ΔS) as

$$r = \Sigma Out - \Sigma In + \Delta S \qquad 1$$

The water budget residual r is used as a measure of overall accuracy of the estimates of the components contributing to the volumetric change of water in the STAs. For a given time period it can be written as

$$r = Q_{out} + Q_g + ET - Q_{in} - R + \Delta S \qquad 2$$

where Q_{out} is surface outflow, Q_g is seepage flow lost from the STA, ET is evapotranspiration, Q_{in} is surface inflow, R is precipitation, and ΔS is change in storage. All components in above equation have volumetric rate units with dimensions of [L^3/T – volume per unit time]. Customarily, acre-feet per year (ac-ft/yr) is selected as the unit of water budget components.

Error in the water budget is estimated by dividing the residual by the average of the total inflow and outflow volumetric rate (Pietro 2013).

$$\varepsilon = \frac{r}{(\sum Out + \sum In)/2} \times 100 \qquad 3$$

where ε is the percent error in water budget, $\sum Out = Q_{out} + Q_g + ET$, and $\sum In = Q_{in} + R$.

Change in storage, ΔS, is not included in the denominator of percent error equation, but included in the estimation of residual r. It can be calculated as

$$\Delta S = \frac{A_c\,(h_t - h_{t-\Delta t})}{\Delta t} \qquad 4$$

where A_c is the effective cell area, h_t is the average cell stage at a time step, and $h_{t-\Delta t}$ is the average cell stage at previous time step. Selection of the time step has an effect on the expected water budget accuracy. Typically, daily time steps are used in estimation of change in storage and all other water budget components. Daily average stages in the cells are calculated as the average of upstream and downstream stages. Instead of daily averages, end of day cell stages can be used in change in storage calculations. The impact of such subtlety was not investigated in this study. Depending on the site-specific conditions, different weights for the upstream and downstream stages can be used in calculation of the average cell stages.

3.1 Cells 3A and 3B Water Budget Analyses in the 2013 SFER

Water budget analyses for Cells 3A and 3B were included in the *2013 South Florida Environmental Report – Volume I* (SFER) (Pietro 2013) are provided in **Tables 1** through **3**. These water budgets were developed using the District's web-based Water Budget Tool. The seepage component was not independently estimated for these cells in the 2013 SFER. As shown in the tables, cell-by-cell analyses indicate large errors similar in magnitude but opposite in sign for Cells 3A and 3B. Significantly lower flow-way residuals in comparison to cell-by-cell analysis indicate that mid-levee flow rates can be a major source of water budget error. Cell-by-cell water budget analysis of Cells 3A and 3B of STA-3/4 is available after 2008 because these cells were created by adding the internal divide levee and G-384 culverts after the initial construction of STA-3/4. The summation of Cells 3A and Cell 3B is referred to as Cell 3 or Flow-way 3 in this document.

Table 1. Water budget analysis for Cell 3A in the 2013 SFER (cell area = 2,153 acres).

	Q_{in}	R	Q_g	Q_{out}	ET	ΔS	ΣIn	ΣOut	Residual, r	Residual Error, ε
	ac-ft/yr	ac-ft/yr	ac-ft/yr	ac-ft/yr	ac-ft/yr	ac-ft/yr	ac-ft/yr	ac-ft/yr	ac-ft/yr	%
WY2009	168,914	7,643	-	166,177	9,779	-2,384	176,557	175,956	-2,985	-2%
WY2010	219,526	10,934	-	358,603	9,581	3,875	230,460	368,184	141,599	47%
WY2011	112,832	6,550	-	359,101	9,918	-3,673	119,382	369,019	245,964	101%
WY2012	123,600	10,975	-	302,858	9,691	3,418	134,575	312,549	181,392	81%
Period of Record	624,872	36,102	-	1,186,739	38,969	1,236	660,974	1,225,708	565,970	60%

Table 2. Water budget analysis for Cell 3B in the 2013 SFER (cell area = 2,427 acres).

	Q_{in}	R	Q_g	Q_{out}	ET	ΔS	ΣIn	ΣOut	Residual, r	Residual Error, ε
	ac-ft/yr	ac-ft/yr	ac-ft/yr	ac-ft/yr	ac-ft/yr	ac-ft/yr	ac-ft/yr	ac-ft/yr	ac-ft/yr	%
WY2009	166,189	8,616	-	129,209	11,024	-1,725	174,805	140,233	-36,297	-23%
WY2010	358,603	12,325	-	233,842	10,800	1,242	370,928	244,642	-125,044	-41%
WY2011	360,747	7,384	-	118,737	11,180	-1,909	368,131	129,917	-240,123	-96%
WY2012	302,858	12,372	-	121,825	10,924	2,581	315,230	132,749	-179,900	-80%
Period of Record	1,188,397	40,697	-	603,613	43,928	189	1,229,094	647,541	-581,364	-62%

Table 3. Water budget analysis for Cell 3 (Flow-way 3) in the 2013 SFER (Flow-way Area 4,580 ac).

	Q_{in}	R	Q_g	Q_{out}	ET	ΔS	ΣIn	ΣOut	Residual, r	Residual Error, ε
	ac-ft/yr	ac-ft/yr	ac-ft/yr	ac-ft/yr	ac-ft/yr	ac-ft/yr	ac-ft/yr	ac-ft/yr	ac-ft/yr	%
WY2009	168,914	16,259	-	129,209	20,803	-4,109	185,173	150,012	-39,270	-23%
WY2010	219,526	23,259	-	233,842	20,381	5,117	242,785	254,223	16,555	7%
WY2011	112,832	13,934	-	118,737	21,098	-5,582	126,766	139,835	7,487	6%
WY2012	123,600	23,347	-	121,825	20,615	5,999	146,947	142,440	1,492	1%
Period of Record	624,872	76,799	-	603,613	82,897	1,425	701,671	686,510	-13,736	-2%

4 Effective Treatment Areas

The effective treatment areas for Cells 3A and 3B of STA-3/4 were revised in Piccone et al. (2014). Updated and previously used cell areas are provided in **Table 4**. As shown in the table, there is a sizeable difference between the cell areas used in the 2013 SFER and Piccone et al. (2014) reports.

Table 4. Effective treatment areas for Cells 3A and 3B.

Effective Areas for…	Cell 3A (acres)	Cell 3B (acres)	Cell 3 (acres)
Previously Published Effective Treatment Area (used in the 2013 SFER [Pietro 2013)	2,153	2,427	4,580
Updated Effective Treatment Area (Piccone et al. 2014) (used in this report)	2,415	2,087	4,502

5 Surface Water Inflow and Outflow

Structure flows are the main driver of the STA hydrology and the largest components of STA water budgets. Flows into and out of of Cells 3A and 3B are controlled by a series of culverts located along the northernmost and southernmost levees, respectively. Flow rates through culverts are computed by rating equations using the records of headwater and tailwater stages, and operation of control features, in this case, gates. When sufficient field measurements are collected, rating equations are calibrated for an improved representation of flow process through the structure.

Errors and uncertainties in stage data, structure geometry, or flow equations cause errors in the estimated flows. These uncertainties become significant when the magnitude of the monitored variable is near or lower than the monitoring instrument's precision and/or resolution. Due to exposure of the instruments to the elements of nature, sites with stage recorders need constant maintenance. The Infrastructure Management Bureau has dedicated teams to maintain the stage and gate recorders at the water control structures. Because of the high number of stations to maintain, not all issues causing error in data are addressed immediately. When an error in data is identified, the appropriate correction is applied as soon as resource scheduling allows. Once the correction is applied to the historical data, a DBHYDRO database update is performed and flow is recomputed.

Accurate stage records are essential for accurate flow computations. Quality guideline for stage recorders is accepted as ±0.03 feet (ft) by the District (SFWMD 2009). Some potential issues, such as instrument drift, well clogging and settlement at structures may cause significant errors, especially when structures operate under low head conditions. Erroneous flows can be computed when the operating head differential is near or lower than the stage sensors' precision limit. When combined with large culvert sizes, recorded low head differentials may cause significant errors in the computed flows and water budgets.

5.1 Flow Computations at Culverts

The inflow and outflow at Cells 3A and 3B are controlled by the G-380, G-381 and G-384 culverts, with intermittent operations at G-387 pump station and G-382B culvert (see **Figure 1** for structure locations). All three sets of culverts are composed of a series of six gated, reinforced concrete box culverts, operating under full-pipe flow condition. The dimensions and rating coefficients for these culverts are provided in **Table 5**. Detailed description of these structures can be found in SFWMD (2007). The flow rating equation for a culvert flowing under full-pipe condition is written as

$$Q_c = C_d A_o \sqrt{\frac{2g\Delta h}{\left(\frac{A_o}{A_G}\right)^2 + 2{C_d}^2\left(1 - \frac{A_o}{A_G} + \frac{gn^2L}{(1.49)^2 {R_o}^{4/3}}\right)}} \qquad 5$$

where Q_c is the computed flow rate, C_d is the discharge coefficient, A_o is the full barrel cross-sectional area, A_G is the area of the gate opening, g is gravitational acceleration, $\Delta h = HW - TW$ is the difference between headwater HW and tailwater TW stages, L is the length of barrel, R_o is the full barrel hydraulic radius, and n is the Manning's roughness coefficient (Wilsnack et al. 2010). To improve the accuracy of the flow rate estimates, field flow measurements can be used for calibration by fitting the model given in Equation 5 to the collected data by optimizing the parameters. For a given Manning's roughness coefficient, the only rating parameter to be calibrated in the equation is the discharge coefficient C_d.

Table 5. Hydraulic properties for Flow-way 3 culverts.

	Culvert Length (ft)	Culvert Height (ft)	Culvert Width (ft)	C_d	Manning's Roughness	Flow Record Start Date
G380A–F	111	7	7	0.75	0.012	13-Jan-2005
G384A–F	75[(1)]	8	10	0.754[(2)]	0.012	11-Apr-2008
G381A–C	40	8	8	0.831	0.012	17-Dec-2004
G381D–F	40	8	8	0.75	0.012	17-Dec-2004

[(1)] 40 ft was used before 2013 quality assessment review.

[(2)] Default value of 0.85 was used before the calibration in 2013.

5.2 Rating Status for Flow-way 3 Water Control Structures

Flow through water control structures is estimated by rating equations, typically calibrated by field measurements. HDM staff continuously update the flow ratings at water control structures. The flow ratings at the structures are revisited and improved when there is sufficient field data collected to cause a significant improvement in rating error. Quality of the rating and estimated flow rates depends on the quantity and the quality of the field flow measurements. Streamgauging data distributed within a wide range of stage and structure operation conditions is desirable for a good rating. However, at very low head differentials, even the field flow measurements become challenging.

HDM staff has been successfully implementing computational fluid dynamics (CFD) simulations to augment the field flow measurements for rating development. One of the benefits of the CFD-based flow rating is the fact that simulations are not impacted by the stage monitoring at low head conditions. It must be noted that even with a fully calibrated and verified rating equation, errors in the estimated flows can exist if the stages used in computations include errors. The optimal solution for handling the low head differentials would be to avoid them all together, unfortunately, this may not be possible with the current operational and structural conditions. Evaluation of structural and operational alternatives to minimize low head, wide gate opening and low flow events is essential. Flow uncertainty curves that can be used as guidance in operating the gates to minimize uncertainties are provided in Section 10.

Existing flow rating equations were reviewed for all inflow and outflow structures of Cells 3A and 3B (**Table 6**). Potential improvements for G-384A–F structures were identified (see Zhang 2013 for more information on the improved rating equation). Since sufficient field flow measurements were not available, CFD simulations were performed to develop an improved rating equation for G-384A–F. The newly developed rating has a discharge coefficient of 0.754 with an absolute average error of 3.8%, which represents a significant improvement over the previous rating with absolute average error of 17% (**Figure 2**).

Table 6. Flow rating status for Flow-way 3 structures.

Structure	Dominant Flow Type	Rating Coefficients	Absolute Relative Error	Rating Effective Date	Basis for Rating
G-380A–F	Full pipe flow	n = 0.012 C_d = 0.75	9.8%	1/13/2005	Calibration.
G-384A–F	Full pipe flow	n = 0.012 C_d = 0.754	3.8%	4/5/2013	Calibration. Field data supplemented by CFD.
G-381A–C	Full pipe flow	n = 0.012 C_d = 0.831	5.3%	1/1/2003	Calibration.
G-381D–F	Full pipe flow	n = 0.012 C_d = 0.75	8.4%	1/1/2003	Calibration
G-387	Case 8	A = 33.453 B = -0.1173 C = 1.6995	Not Applicable	10/22/2008	Theoretical. No field measurement available.

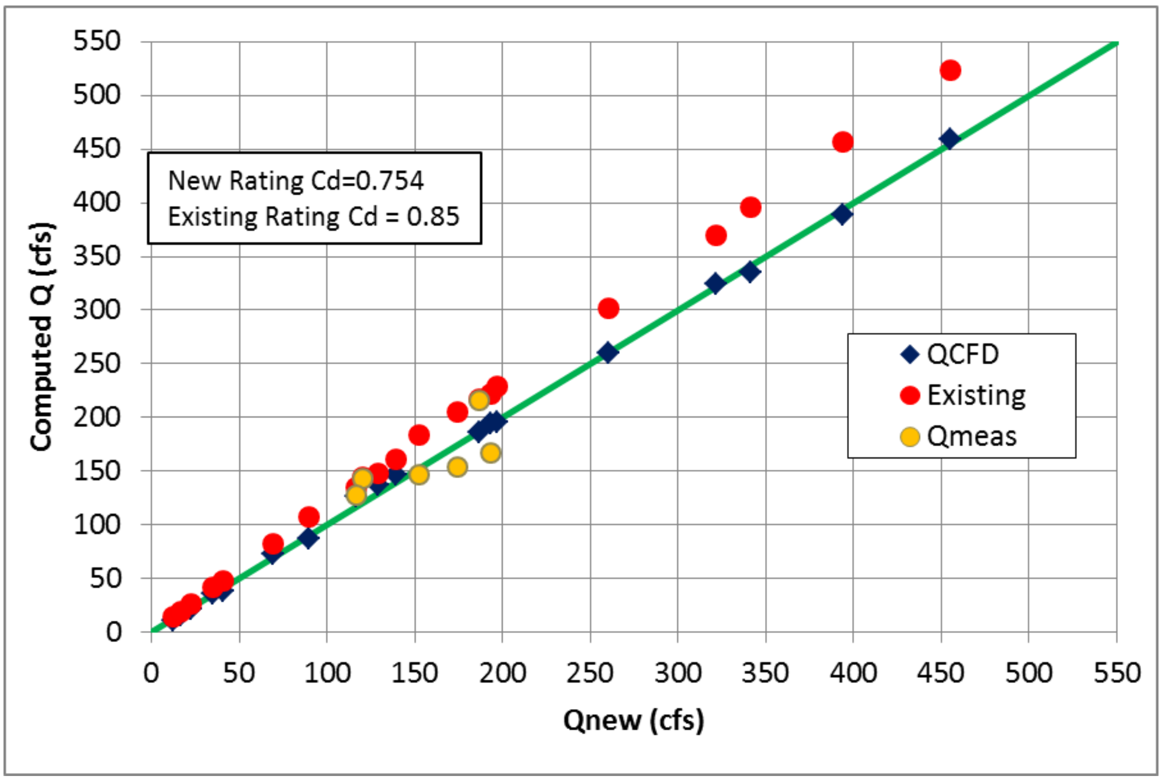

Figure 2. Comparison of existing and updated ratings for G-384 (Zhang 2013).
(Note: cfs – cubic feet per second)

5.3 Mid-Levee Culverts Flow Data Review

Culverts operating under low head differentials are known to cause large errors in the estimated flow rates. Since the original design of the internal culverts aimed at passing high flow rates, low head differentials occur frequently at these sites during low flow periods. As shown by the histograms in **Figures 3** and **4**, for the majority of the time, the G-384 culverts operate under head differentials lower than 0.03 ft with gate openings larger than 6.5 ft, generating conditions for large spurious flows.

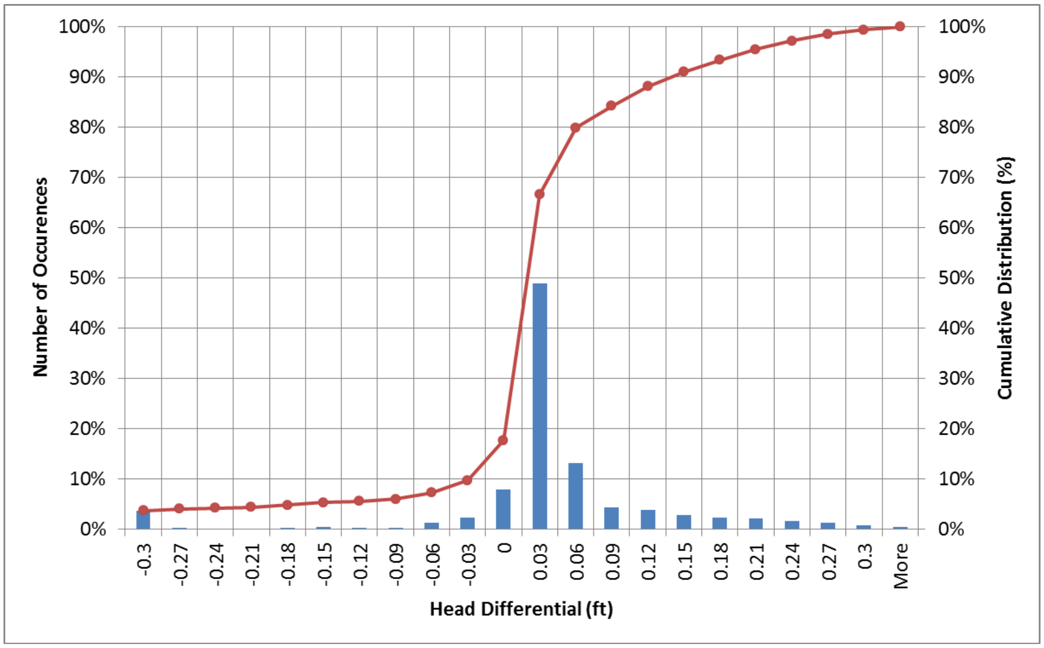

Figure 3. G-384 head differential histogram for WY2009–WY2012 based on 15-minute interpolated data.

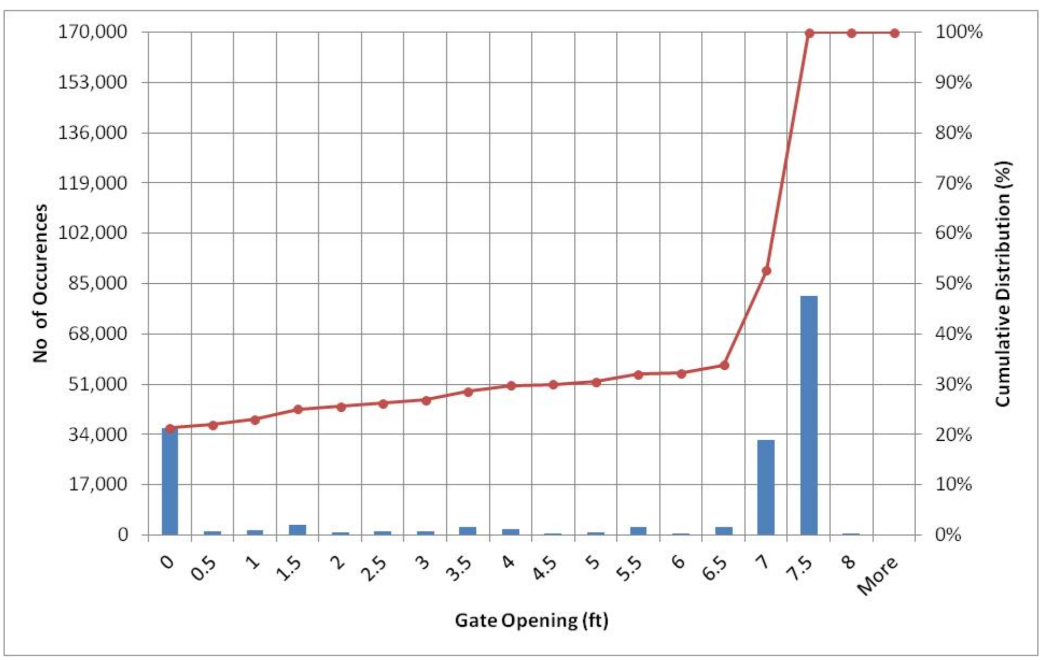

Figure 4. G-384 gate opening histogram for WY2009–2012 based on 15-minute interpolated data.

Locations for the stage monitoring sites and data acquisition protocols become very critical while the structures operate under low head differentials. HDM's *Change Management Procedures for Hydrometeorological Data* requires an accuracy of ±0.02 ft for both survey and preferred value (PREF) stage recorders, and ±0.03 ft for all other stage recorders (SFWMD 2009). The data collection protocol at the monitoring sites requires recording a new data point each time a significant change in stage occurs, where a significant change is accepted to be 0.02 ft or higher. A different sampling protocol with lower threshold or differential head measurements may help with flow computations at culverts operating under low head differentials. Calibration of the stage sensors, stage recording protocols of the sensors and survey errors (all can have a magnitude of 0.02 ft) contribute to errors in the stage readings that can be as high as 0.06 ft, causing very high relative errors for the low flow condition. Feasibility and cost-benefits of using more accurate sensors and data acquisitions protocols would need to be investigated before determining an appropriate path forward.

The G-384 culverts operate under full pipe flow condition. Inserting the information in **Table 5** into **Equation 5**, the flow curve showing the relationship between head differential and flow rate per structure can be plotted for these culverts as shown in **Figure 5**. As seen from the figure, at the stage sensors' accepted quality limit of 0.03 ft of head differential, a flow rate of 93 cubic feet per second (cfs) was computed per culvert at the G-384 structure (using a discharge coefficient of C_d = 0.85). Even though 0.03 ft of head differential corresponds to 1/267th of the culvert height, multiplied by large flow areas, they can cause significant errors in the water budgets. Such head differential could generate spurious flow rate of 558 cfs (or 1,105 ac-ft/day) across all six structures with the old rating and 486 cfs (962 ac-ft/day) with the new rating coefficient when gates are fully open. The effect of erroneous flows with such magnitude can be overwhelming in annual water budget analyses.

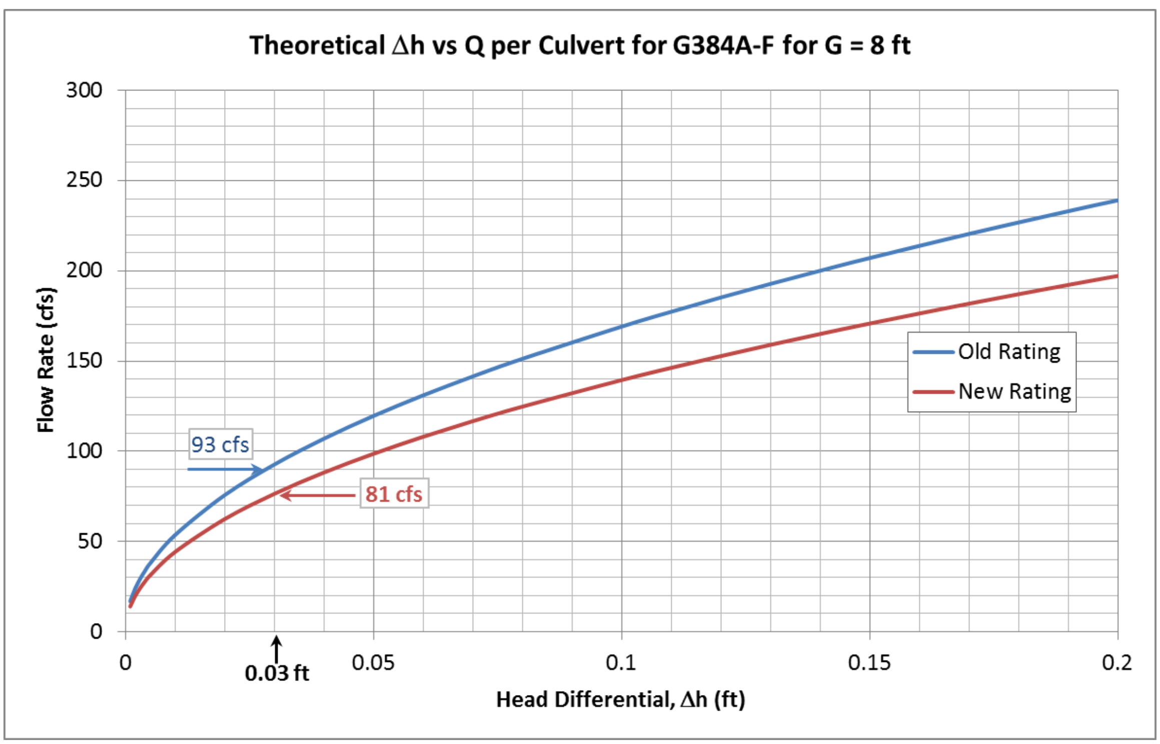

Figure 5. Δh vs Q per culvert curves for G-384A–F for the new (C_d = 0.754) and old ratings (C_d = 0.85) (with G = 8 ft, n = 0.012).

5.4 Correcting Flow Data for Mid-Levee Culverts

Visual inspection of Cell 3A inflow/outflow hydrograph given in **Figure 6** indicated potentially erroneous outflow calculations at mid-levee culverts (G-384) occurring at periods with no or very low inflow. The outflow data shown in the figure is computed using the previously used discharge coefficient C_d = 0.85. Head differential of 0.03 ft with this rating coefficient corresponds to a discharge rate of 93 cfs per structure or 558 cfs for all G-384A–F culverts for fully open gates. Coincidentally, the flow rates that were considered suspicious in the figure appear to be in the same order of magnitude as this value. In addition, the water budgets presented in **Tables 1** and **2** have residuals similar in magnitude but opposite in sign, indicating the flow rates through mid-levee culverts might have been over-estimated. The improvement in the flow rating for G-384 presented in Section 5.2 was not sufficient to explain the large residual in the water budgets of Cells 3A and 3B. Because of the reasons listed below, the cause of high cell-by-cell water budgets residuals was narrowed down to mid-levee surface flows computed at G384 structures:

1. In general, water budget errors for flow-ways are lower than those of cells.
    - ET, rainfall and seepage computations use the same data for flow-ways and cells. Surface water components for water budgets use mid-levee flows, which are not considered in flow-way water budgets.
2. Water budget residuals for the individual cells are similar in magnitude and opposite in sign.
    - Mid-levee flows appear in both cells' water budgets in opposite signs.
3. Mid-levee G-384 culverts operate under low head differentials most of the time.
    - Due to the large sizes of G-384 culverts, small spurious head differentials may cause large errors in the computed flows.
    - The suspicious flows in the historical data are of the same order of magnitude as the flow rates corresponding to stage recorder accuracy criteria of $\pm$ 0.03 ft.

These three observations were used as a rationale for the conclusion that the computed G-384 flow rates are the main reason for high errors in the cell-by-cell water budgets for Cells 3A and 3B. HDM staff continues to investigate methods to reduce errors introduced by low head differentials. Three methods to fix the historical flow rate data, one based on data correction and two on back calculation, are applied to G-384 data in this report:

Method 1: Correcting flow data by setting small head differentials to zero

Method 2: Back calculating mid-levee flows by redistributing Flow-way 3 water budget residuals

Method 3: Back calculating flows as the weighted average of Flow-way 3 inflows and outflows

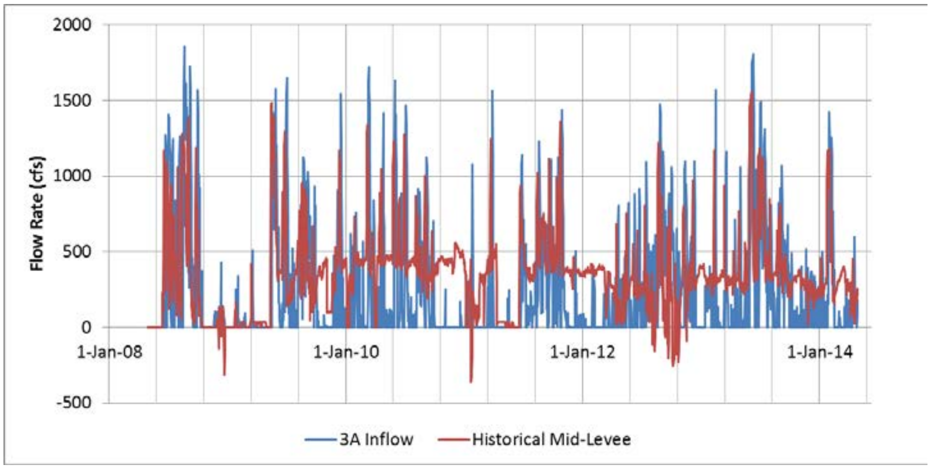

Figure 6. Historical inflow and outflow discharges for Cell 3A.

5.4.1 Method 1: Correcting Mid-Levee Flows by Setting Small Head Differentials to Zero

To correct for the erroneous flow data caused by very low head differentials, a simple correction was applied to the historical data as a desktop exercise in the form of setting the flow rates to zero at each G-384 culvert when the absolute value of the head difference is lower than 0.03 ft. The corrected flow data is plotted in **Figures 7** and **8**. It must be noted that this method does not differentiate between the actual and spurious records of low head differences; therefore, it is inherently subject to errors. In addition, since the selection of head difference threshold is arbitrary, as seen in the figure, not all potentially erroneous flows will necessarily be eliminated. Application of this method to other structures with erroneous flow data due to low head differentials needs to be considered on a case-by-case basis, and should be applied when the benefits of the applied correction outweigh the errors introduced by indiscriminately setting small flow rates to zero.

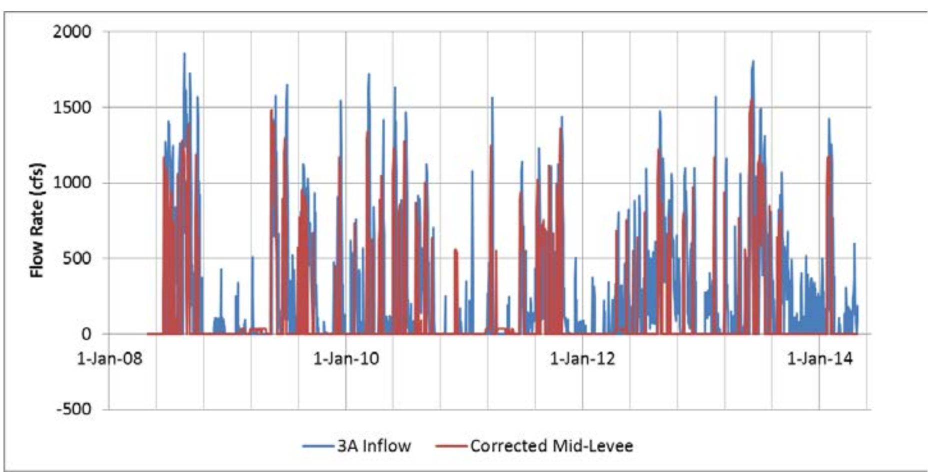

Figure 7. Historical inflow and modified outflow (Method 1) discharges for Cell 3A.

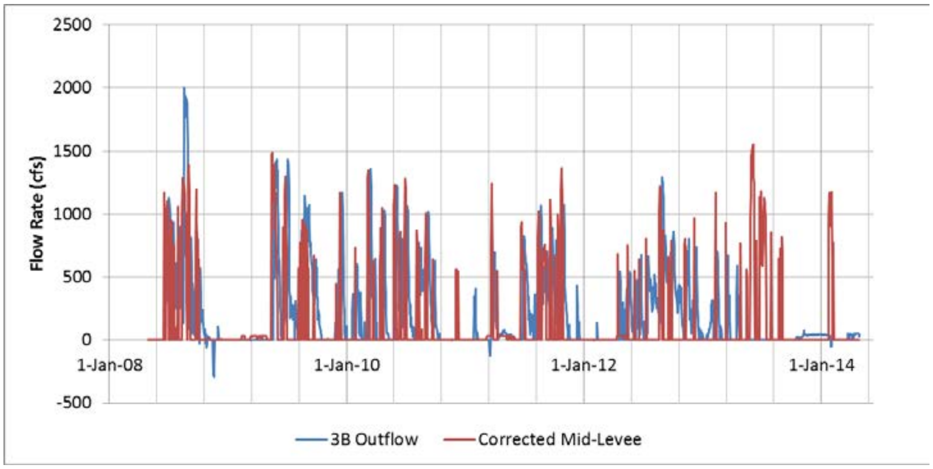

Figure 8. Modified inflow (Method 1) and historical outflow discharges for Cell 3B.

Revisited water budgets with corrected mid-levee flows are presented in **Tables 7** through **9**. Even though the errors in the updated water budgets are lower than the previously developed water budgets (**Tables 1** through **3**), they are still higher than the desired accuracy of 10% or less for individual water years. The HDM Quality Assurance Unit has started Phase II of the flow data improvement effort, and finalized corrected G-384 data will be available in DBHYDRO after December 2014. The mid-levee (G-384) data presented in this report are provisional.

Table 7. Revisited Cell 3A water budget with corrected mid-levee (G-384) flows (Method 1).

	Q_{in}	Rainfall, R	Seepage, Q_g	Q_{out} ($\boldsymbol{Q_{mid}}$)	ET	ΔS	ΣIn	ΣOut	Residual, r	Residual Error, ε
	ac-ft/yr	ac-ft/yr	ac-ft/yr	ac-ft/yr	ac-ft/yr	ac-ft/yr	ac-ft/yr	ac-ft/yr	ac-ft/yr	%
WY2009	168,618	8,573	9,112	**103,343**	10,969	-2,271	177,192	123,425	-56,038	-37%
WY2010	219,142	12,264	8,296	**164,813**	10,747	3,418	231,406	183,856	-44,132	-21%
WY2011	112,635	7,348	7,668	**139,836**	11,124	-3,187	119,982	158,629	35,460	25%
WY2012	123,384	12,310	9,956	**98,380**	10,870	3,057	135,694	119,206	-13,431	-11%
WY2013	196,068	12,218	9,507	**71,563**	10,798	-1,392	208,286	91,867	-117,811	-79%
Period of Record	819,846	52,713	44,539	**577,935**	54,508	-374	872,560	676,982	-195,952	-25%

Table 8. Revisited Cell 3B water budget with corrected mid-levee (G-384) flows (Method 1).

	Q_{in} ($\boldsymbol{Q_{mid}}$)	Rainfall, R	Seepage, Q_g	Q_{out}	ET	ΔS	ΣIn	ΣOut	Residual, r	Residual Error, ε
	ac-ft/yr	ac-ft/yr	ac-ft/yr	ac-ft/yr	ac-ft/yr	ac-ft/yr	ac-ft/yr	ac-ft/yr	ac-ft/yr	%
WY2009	**103,343**	7,409	6,272	128,970	9,479	-1,453	110,752	144,722	32,517	25%
WY2010	**164,813**	10,598	4,663	233,433	9,287	1,186	175,411	247,383	73,158	35%
WY2011	**139,836**	6,350	4,074	117,084	9,614	-1,719	146,186	130,772	-17,132	-12%
WY2012	**98,380**	10,638	5,873	119,642	9,394	2,308	109,018	134,908	28,199	23%
WY2013	**71,563**	10,558	3,544	182,107	9,331	-1,089	82,121	194,982	111,771	81%
Period of Record	**577,935**	45,554	24,426	781,237	47,105	-766	623,488	852,768	228,513	31%

Table 9. Revisited Cell 3 water budget (unaffected by mid-levee flows).

	Q_{in}	Rainfall, R	Seepage, Q_g	Q_{out}	ET	ΔS	ΣIn	ΣOut	Residual, r	Residual Error, ε
	ac-ft/yr	ac-ft/yr	ac-ft/yr	ac-ft/yr	ac-ft/yr	ac-ft/yr	ac-ft/yr	ac-ft/yr	ac-ft/yr	%
WY2009	168,618	15,982	15,385	128,970	20,448	-3,724	184,600	164,803	-23,521	-13%
WY2010	219,142	22,863	12,959	233,433	20,034	4,605	242,004	266,426	29,027	11%
WY2011	112,635	13,697	11,742	117,084	20,738	-4,905	126,332	149,564	18,327	13%
WY2012	123,384	22,949	15,829	119,642	20,264	5,366	146,332	155,734	14,768	10%
WY2013	196,068	22,776	13,051	182,107	20,129	-2,482	218,845	215,287	-6,040	-3%
Period of Record	819,846	98,267	68,965	781,237	101,613	-1,140	918,114	951,815	32,561	3%

5.4.2 Method 2: Back-Calculating Mid-Levee Flow Rates by Redistributing Flow-way 3 Water Budget Residuals

The magnitude of the head differentials plays a significant role in the flow rate errors, especially when they are very low (see Polatel et al. in prep for more information on effect of head differential on flow rate uncertainties). Culverts operating under extremely low head differentials are expected to have larger errors in estimated flow rates. Small spurious head differentials caused by the precision limits of the stage sensors may produce sizeable errors due to the large sizes of the STA culverts. Considering the abundance of contributing factors, one can suggest that, instead of trying to fix the errors in the historical data, back calculating mid-levee flow rates is more reliable.

Residual errors in water budgets are unavoidable. When the flow-way inflows and outflows are believed to be more reliable, in the absence of better information, the flow-way residuals can be distributed into constituting cells based on their areas. All of the estimated components of water budget shown in **Equation 2** other than surface flows (seepage Q_g, change in storage ΔS, evapotranspiration ET and, precipitation R) are proportional to cell area. Therefore, water budget residuals for the entire flow-way can be redistributed to the cells based on their areas to back calculate the mid-levee flows. Rewriting **Equation 2** for Flow-way 3 water budget residual results in

$$r_3 = Q_{d/s} + Q_{g3} + ET_3 + \Delta S_3 - Q_{u/s} - R_3 \qquad 6$$

where $Q_{u/s}$ and $Q_{d/s}$ are the control structure flows upstream and downstream of the flow-way, respectively. The seepage Q_{g3}, evapotranspiration ET_3, change in storage ΔS_3, and precipitation R_3 for the Flow-way 3 are simply the summations of estimated values for Cell 3A and Cell 3B as

Seepage:	$Q_{g3} = Q_{g3A} + Q_{g3B}$
Evapotranspiration:	$ET_3 = ET_{3A} + ET_{3B}$
Change in Storage:	$\Delta S_3 = \Delta S_{3A} + \Delta S_{3B}$
Precipitation:	$R_3 = R_{3A} + R_{3B}$

where subscripts 3A and 3B indicate variable estimates for these cells.

Similarly, the residuals for the individual cells can be written as

$$r_{3A} = Q_{mid} - Q_{u/s} + Q_{g3A} + ET_{3A} + \Delta S_{3A} - R_{3A} \qquad 7$$

$$r_{3B} = Q_{d/s} - Q_{mid} + Q_{g3B} + ET_{3B} + \Delta S_{3B} - R_{3B} \qquad 8$$

with

$$r_3 = r_{3A} + r_{3B} \qquad 9$$

where Q_{mid} is the flow rate through mid-levee structures, $Q_{u/s}$ is the surface water inflow to the flow-way, $Q_{\mathrm{d}/s}$ is the surface water outflow from the flow-way, and r_{3A} and r_{3B} are the water budget residuals for Cells 3A and 3B, respectively. If the residuals for the cells are assumed to be proportional to the cell area, then they can also be written as

$$r_{3A} = \frac{r_3 A_{3A}}{A_3} \qquad 10$$

$$r_{3B} = \frac{r_3 A_{3B}}{A_3} \qquad 11$$

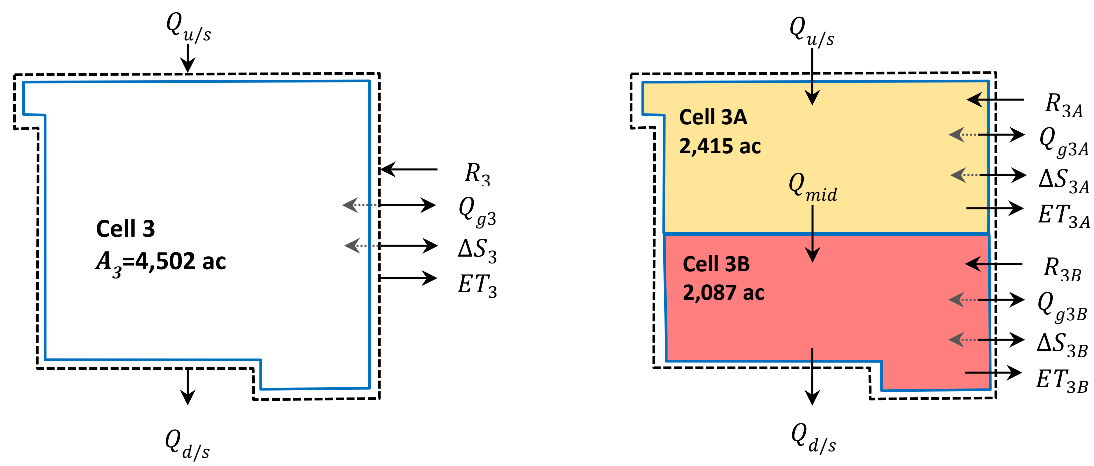

Figure 9. Components of water budgets for Flow-way 3 and Cells 3A and 3B.

For known cell areas, the water budget residuals for the flow-way can be distributed to the cells using **Equations 10** and **11**. Once the residuals for cells (r_{3A} and r_{3B}) are known, **Equation 7** or **8** can be used to estimate mid-levee flows.

From Cell 3A water budget (**Equation 7**),

$$Q_{mid} = Q_{u/s} - Q_{g3A} - ET_{3A} - \Delta S_{3A} + R_{3A} + \frac{r_3 A_{3A}}{A_3} \qquad 12$$

or, from Cell 3B water budget (**Equation 8**),

$$Q_{mid} = Q_{d/s} + Q_{g3B} + ET_{3B} + \Delta S_{3B} - R_{3B} - \frac{r_3 A_{3B}}{A_3} \qquad 13$$

The estimated mid-levee flow rates and corresponding residuals obtained by Method 2 are shown in the water budgets presented in **Tables 10** through **12**. Note that the residuals in **Table 12** for the flow-way are not the same as those of previously published values in **Table 3**. The reason for the discrepancies is the consideration of seepage losses/gains that were not considered previously in the water budgets of these cells.

The procedure followed in back calculation of mid-levee flows by Method 2 can be summarized as follows:

Step 1: Estimate r_3, the residual for the entire flow-way, from the water budget equation.

Step 2: Estimate r_{3A} and r_{3B}, the residuals for the cells, assuming their magnitude is proportional to the cell areas and their summation is equal to the flow-way residual.

Step 3: Estimate the mid-levee flows, Q_{mid}, using the residuals from the previous step in the water budget equations for individual cells.

Table 10. Cell 3A water budget with back calculated outflow (Method 2).

	Q_{in}	Rainfall, R	Seepage, Q_g	Q_{out} ($\boldsymbol{Q_{mid}}$)	ET	ΔS	ΣIn	ΣOut	Residual, r	Residual Error, ε
	ac-ft/yr	ac-ft/yr	ac-ft/yr	ac-ft/yr	ac-ft/yr	ac-ft/yr	ac-ft/yr	ac-ft/yr	ac-ft/yr	%
WY2009	168,618	8,573	9,112	**146,764**	10,969	-2,271	177,192	166,846	-12,617	-7%
WY2010	219,142	12,264	8,296	**224,515**	10,747	3,418	231,406	243,558	15,571	7%
WY2011	112,635	7,348	7,668	**114,208**	11,124	-3,187	119,982	133,000	9,831	8%
WY2012	123,384	12,310	9,956	**119,732**	10,870	3,057	135,694	140,558	7,922	6%
WY2013	196,068	12,218	9,507	**186,134**	10,798	-1,392	208,286	206,439	-3,240	-2%
Period of Record	819,846	52,713	44,539	**791,353**	54,508	-374	872,560	890,401	17,467	2%

Table 11. Cell 3B water budget with back calculated inflow (Method 2).

	Q_{in} ($\boldsymbol{Q_{mid}}$)	Rainfall, R	Seepage, Q_g	Q_{out}	ET	ΔS	ΣIn	ΣOut	Residual, r	Residual Error, ε
	ac-ft/yr	ac-ft/yr	ac-ft/yr	ac-ft/yr	ac-ft/yr	ac-ft/yr	ac-ft/yr	ac-ft/yr	ac-ft/yr	%
WY2009	**146,764**	7,409	6,272	128,970	9,479	-1,453	154,173	144,722	-10,904	-7%
WY2010	**224,515**	10,598	4,663	233,433	9,287	1,186	235,114	247,383	13,456	6%
WY2011	**114,208**	6,350	4,074	117,084	9,614	-1,719	120,558	130,772	8,496	7%
WY2012	**119,732**	10,638	5,873	119,642	9,394	2,308	130,371	134,908	6,846	5%
WY2013	**186,134**	10,558	3,544	182,107	9,331	-1,089	196,692	194,982	-2,800	-1%
Period of Record	**791,353**	45,554	24,426	781,237	47,105	-766	836,907	852,768	15,094	2%

Table 12. Cell 3 water budget (unaffected by mid-levee flows) (**Table 9** repeated).

	Q_{in}	Rainfall, R	Seepage, Q_g	Q_{out}	ET	ΔS	ΣIn	ΣOut	Residual, r	Residual Error, ε
	ac-ft/yr	ac-ft/yr	ac-ft/yr	ac-ft/yr	ac-ft/yr	ac-ft/yr	ac-ft/yr	ac-ft/yr	ac-ft/yr	%
WY2009	168,618	15,982	15,385	128,970	20,448	-3,724	184,600	164,803	-23,521	-13%
WY2010	219,142	22,863	12,959	233,433	20,034	4,605	242,004	266,426	29,027	11%
WY2011	112,635	13,697	11,742	117,084	20,738	-4,905	126,332	149,564	18,327	13%
WY2012	123,384	22,949	15,829	119,642	20,264	5,366	146,332	155,734	14,768	10%
WY2013	196,068	22,776	13,051	182,107	20,129	-2,482	218,845	215,287	-6,040	-3%
Period of Record	819,846	98,267	68,965	781,237	101,613	-1,140	918,114	951,815	32,561	3%

5.4.3 Method 3: Back-Calculating Mid-Levee Flow Rates As the Weighted Average of Flow-way 3 Inflows and Outflows

As an alternative to back-calculating the mid-levee flows by distributing the flow-way residuals, a simpler approach can be employed whereby the weighted average of daily inflows and outflows is used to estimate the mid-levee flows Q_{mid} as

$$Q_{mid} = \frac{Q_{u/s}A_{3B} + Q_{d/s}A_{3A}}{A_3} \qquad 14$$

where $Q_{u/s}$ is the inflows to the flow-way at the upstream structures, $Q_{d/s}$ is the outflows from the flow-way at downstream structures, and A_{3A}, A_{3B} and A_3 are the areas of the Cell 3A, Cell 3B and Flow-way 3, respectively. For each time step (one day) the mid-levee flows were computed as the weighted average of flow-way inflows and outflows, using the cell areas as a basis (reverse of the flow areas as the weighting coefficient). Other components of the water budget remain the same. The results of application of this method to Cells 3A and 3B for WY2009–WY2013, and resulting water budgets are presented in **Tables 13** through **15**. Computed mid-levee flow-ways using these two back calculation methods are shown in Figure 10. As seen in **Figure 10**, the back calculation methods result in more-or-less similar mid-levee flows. The mid-levee (G-384) flows computed by Method 2 are used in computations for the rest of this report. Finalized G-384 flow data will be available after September 2014.

The water budgets for cells are expected to have more errors since the mid-levee culverts operate under lower heads than the inflow and outflow culverts, which is also evident in the water budgets shown in **Tables 1** through **3**. Based on this knowledge, back calculating mid-levee flows can be recommended when the cell water budgets include potentially erroneous flows and carry significantly larger errors than the flow-ways. The pros and cons of applying back calculation methods are expected to be site specific. An evaluation of historical data, structure geometry, operational protocol and hydrogeological conditions is needed before a data correction or data reconstruction methodology is chosen.

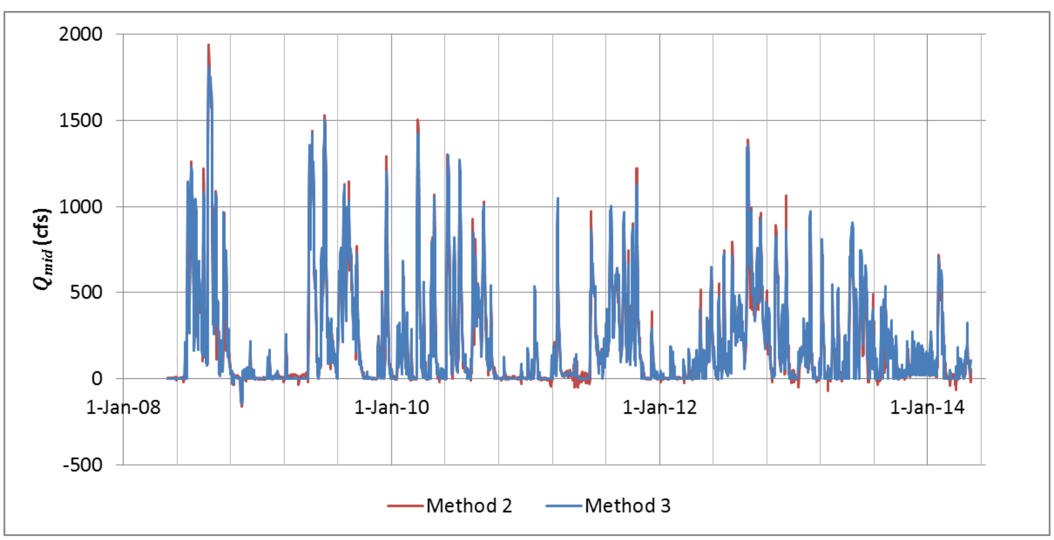

Figure 10. Comparison of mid-levee flows computed by Methods 2 and 3.

Table 13. Cell 3A water budget with back-calculated outflow (Method 3).

	Q_{in}	Rainfall, R	Seepage, Q_g	Q_{out} ($\boldsymbol{Q_{mid}}$)	ET	ΔS	ΣIn	ΣOut	Residual, r	Residual Error, ε
	ac-ft/yr	ac-ft/yr	ac-ft/yr	ac-ft/yr	ac-ft/yr	ac-ft/yr	ac-ft/yr	ac-ft/yr	ac-ft/yr	%
WY2009	168,618	8,573	9,112	**148,794**	10,969	-2,271	177,192	168,876	-10,587	-6%
WY2010	219,142	12,264	8,296	**226,288**	10,747	3,418	231,406	245,330	17,343	7%
WY2011	112,635	7,348	7,668	**114,859**	11,124	-3,187	119,982	133,652	10,483	8%
WY2012	123,384	12,310	9,956	**121,513**	10,870	3,057	135,694	142,339	9,702	7%
WY2013	196,068	12,218	9,507	**189,088**	10,798	-1,392	208,286	209,393	-286	0%
Period of Record	819,846	52,713	44,539	**800,542**	54,508	-374	872,560	899,589	26,655	3%

Table 14. Cell 3B water budget with back-calculated inflow (Method 3).

	Q_{in} ($\boldsymbol{Q_{mid}}$)	Rainfall, R	Seepage, Q_g	Q_{out}	ET	ΔS	ΣIn	ΣOut	Residual, r	Residual Error, ε
	ac-ft/yr	ac-ft/yr	ac-ft/yr	ac-ft/yr	ac-ft/yr	ac-ft/yr	ac-ft/yr	ac-ft/yr	ac-ft/yr	%
WY2009	**148,794**	7,409	6,272	128,970	9,479	-1,453	156,203	144,722	-12,934	-9%
WY2010	**226,288**	10,598	4,663	233,433	9,287	1,186	236,886	247,383	11,684	5%
WY2011	**114,859**	6,350	4,074	117,084	9,614	-1,719	121,209	130,772	7,845	6%
WY2012	**121,513**	10,638	5,873	119,642	9,394	2,308	132,151	134,908	5,065	4%
WY2013	**189,088**	10,558	3,544	182,107	9,331	-1,089	199,646	194,982	-5,754	-3%
Period of Record	**800,542**	45,554	24,426	781,237	47,105	-766	846,096	852,768	5,906	1%

Table 15. Cell 3 water budget (unaffected by mid-levee flows) (Table 9 -Repeated).

	Q_{in}	Rainfall, R	Seepage, Q_g	Q_{out}	ET	ΔS	ΣIn	ΣOut	Residual, r	Residual Error, ε
	ac-ft/yr	ac-ft/yr	ac-ft/yr	ac-ft/yr	ac-ft/yr	ac-ft/yr	ac-ft/yr	ac-ft/yr	ac-ft/yr	%
WY2009	168,618	15,982	15,385	128,970	20,448	-3,724	184,600	164,803	-23,521	-13%
WY2010	219,142	22,863	12,959	233,433	20,034	4,605	242,004	266,426	29,027	11%
WY2011	112,635	13,697	11,742	117,084	20,738	-4,905	126,332	149,564	18,327	13%
WY2012	123,384	22,949	15,829	119,642	20,264	5,366	146,332	155,734	14,768	10%
WY2013	196,068	22,776	13,051	182,107	20,129	-2,482	218,845	215,287	-6,040	-3%
Period of Record	819,846	98,267	68,965	781,237	101,613	-1,140	918,114	951,815	32,561	3%

6 Seepage

Since groundwater flow cannot be directly observed, its role in hydrology and water budgets of STAs is more difficult to understand than that of surface water. Despite the difficulties in its quantification, the interaction between the groundwater and surface water may have a sizeable effect on STA water budget analyses.

6.1 Seepage Estimation Methods

There have been various studies that attempted to estimate STA seepage to assist water budget analyses. In this report, existing seepage studies that can be applied to STA-3/4 Cells 3A and 3B were reviewed. Their findings or methodologies were applied to Cells 3A and 3B to obtain a range of seepage values. The obtained range of seepage values can be considered as an indicator of the combined effects of assumptions of the estimation methods and variations in the hydrogeology. The average of all considered methods was used to quantify potential reduction in residual errors that can be achieved by improving the seepage component of water budgets. It must be noted that reported seepage rates should not be used without understanding the limitations and assumptions of the following methods:

1. Application of the ENR flux measurements to Cells 3A and 3B (Harvey et al. 2004).
2. Seep2D model based on empirical data for STA-3/4 (Sangoyomi et al. 2011).
3. Seepage study based on measurements and calibrated numerical model for STA-3/4 design (Montgomery Watson Americas. Inc. 1999).
4. Combined water and solute mass balance (Choi and Harvey 2000).
5. Analysis of historical no inflow-outflow-rainfall periods for Cells 3A and 3B.
6. Application of the seepage coefficient currently in use by the Water Budget Tool.
7. Direct measurements (which have not been collected in the study area).

Water stages in and around the cells are the most influential variable for the direction and the magnitude of seepage flow. Available stage recorders in the vicinity of Cells 3A and 3B are shown in **Figure 11**. WY2009–WY2012 average stages for the stations shown in the figure are provided in **Table 16**.

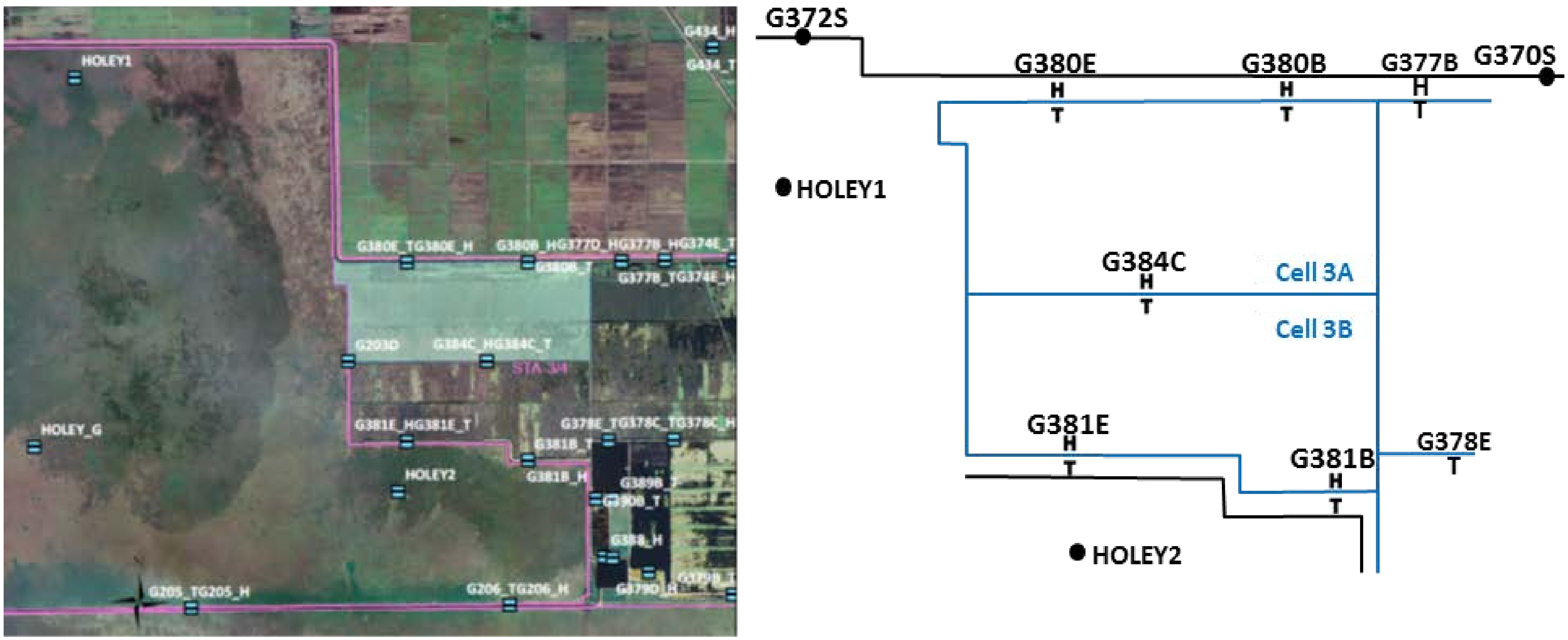

Figure 11. Locations of stage recorders in the vicinity of Flow-way 3.

Table 16. WY2009–WY2012 average stages
(in feet National Geodetic Vertical Datum of 1929 [ft NGVD]).

	Holey Land	Seepage Canal	Cell 3A		Internal Levee	Cell 3B		Neighboring Cells	
Station	HOLEY1_G	G372S_H	G380E_H	G380B_H	G384C_H	G381E_H	G381B_H	G377B_H	G378E_H
Average	11.13	8.16	12.36	12.35	11.34	11.06	11.02	12.32	Not Applicable
Station	HOLEY2_G	G370S_H	G380E_T	G380B_T	G384C_T	G381E_T	G381B_T	G377B_T	G378E_T
Average	11.19*	7.97	11.45	11.47	11.32	10.68	10.59	11.66	10.99

(*) Stage record includes periods with missing data. HOLEY1_G and HOLEY2_G historical stages follow each other closely. Due to missing data at HOLEY2_G records, HOLEY1_G data was selected to represent Holey Land stages.

Using the average stage values observed at stations shown in **Table 16**, the average WY2009–WY2012 stages for water bodies in the vicinity of Cells 3A and 3B can be found as

$$\text{Holey Land}, h_{HL} = \text{HOLEY1}_{\text{G}} = 11.13 \text{ feet National Geodetic Vertical Datum of 1929 (ft NGVD)}$$

$$\text{Seepage Canal}, h_{SC} = \text{Ave(G372S\_H, G370S\_H)} = \frac{8.16+7.97}{2} = 8.07 \text{ ft NGVD}$$

$$\text{Inflow Canal}, h_{IC} = \text{Ave(G380E\_H, G380B\_H)} = \frac{12.36+12.35}{2} = 12.36 \text{ ft NGVD}$$

$$\text{Cell 3A}, h_{3A} = \text{Ave(Ave(G380E\_T, G380B\_T), G384C\_H)} = \frac{(11.45+11.47)/2+11.34}{2} = 11.40 \text{ ft NGVD}$$

$$\text{Cell 3B}, h_{3B} = \text{Ave(Ave(G381E\_H, G381B\_H), G384C\_T)} = \frac{(11.06+11.02)/2+11.32}{2} = 11.18 \text{ ft NGVD}$$

$$\text{Cell 2A}, h_{2A} = \text{Ave(G377B\_T, G378E\_T)} = \frac{11.66+10.99}{2} = 11.33 \text{ ft NGVD}$$

$$\text{Outflow Canal}, h_{OC} = \text{Ave(G381E\_T, G381B\_T)} = \frac{10.68+10.59}{2} = 10.64 \text{ ft NGVD}$$

6.1.1 Application of Flux Measurements from ENR

Harvey et al. (2004) conducted an extensive study investigating the groundwater recharge and discharge in the ENR Project and Water Conservation Area (WCA)-2A. They monitored the groundwater and surface water stages, and collected direct seepage measurements to estimate the hydrogeological properties and vertical fluxes. They provided a range of vertical fluxes measured at various locations.

<u>Application to Cells 3A and 3B</u>

Actual vertical fluxes for wetlands can vary drastically from location to location. However, because no direct measurement data was available for STA-3/4, the direct measurements acquired for the ENR (East and West) were applied to Cells 3A and 3B as a test case. The average of observed 50% percentile vertical fluxes reported in their report for ENR East and West are 0.01115 feet per day (ft/d) and 0.02846 ft/d, respectively. These numbers were multiplied by cell areas and converted to yearly volumes in ac-ft/yr as shown in **Table 17**. While acceptable for preliminary analyses, use of the ENR fluxes reported by Harvey et al. (2004) to estimate seepage for Cells 3A and 3B is not recommended since it requires the assumption of similar hydrologic and hydrogeological conditions. It is also noted that the design and operation of WCA-2A are very different from STA-3/4, therefore, in this report, reported vertical fluxes for WCA-2A were not used to develop the Cells 3A and 3B seepage estimate.

Table 17. Estimated Seepage for Cells 3A, 3B, and Flow-way 3 using the average ENR fluxes by Harvey et al. (2004). (Note: ft^2 – square feet and ft^3/day – cubic feet per day)

Average ENR-East Flux (ft/d)	STA-3/4	Area (acres)	Area (ft^2)	Q_g (ft^3/day)	Q_g (ac-ft/day)	Q_g (ac-ft/yr)
-0.01115*	Cell 3A	2,415	105,197,400	-1,173,462	-26.94	-9,833
	Cell 3B	2,087	90,909,720	-1,014,085	-23.28	-8,497
	Cell 3	4,502	196,107,120	-2,187,547	-50.22	-18,330

Average ENR-West Flux (ft/d)	STA-3/4	Area (acres)	Area (ft^2)	Q_g (ft^3/day)	Q_g (ac-ft/day)	Q_g (ac-ft/yr)
0.02846*	Cell 3A	2,415	105,197,400	2,994,053	68.73	25,088
	Cell 3B	2,087	90,909,720	2,587,408	59.40	21,681
	Cell 3	4,502	196,107,120	5,581,461	128.13	46,768

*Fluxes mentioned in the table were collected at ENR and are not representative of STA-3/4.

6.1.2 Seep2D Model for STA-3/4

Sangoyomi et al. (2011) conducted a seepage analysis for STA-3/4 based on a SEEP2D model using previously published hydrogeological data. Approximated 3D stratigraphy was used to develop a Seep2D model to compute the seepage rates for various head conditions. Assuming a linear relationship between seepage rates and stage differences, seepage coefficients across external levees were computed. Seepage coefficients calculated here should not be confused with measured flux rates discussed in the previous section. Also seepage coefficients include the seepage through the levee and the underflow components while seepage fluxes are only the fluxes that are exchanged between the marsh surface water and groundwater.

Locations for the considered cross-sections and obtained seepage coefficients by Sangoyomi et al. (2011) are provided in **Figure 12**. Even though their analysis was not focused on cell-by-cell water budgets, estimated seepage coefficients can be used to estimate seepage rates for Cells 3A and 3B. In the figure, h_{STA} is the average stage in the STA, h_{SC} is the average stage in the seepage canal, h_{IC} is the average stage in the inflow canal, h_F is the stages in the neighboring farms, and h_{OC} is the average stage in the outflow canal.

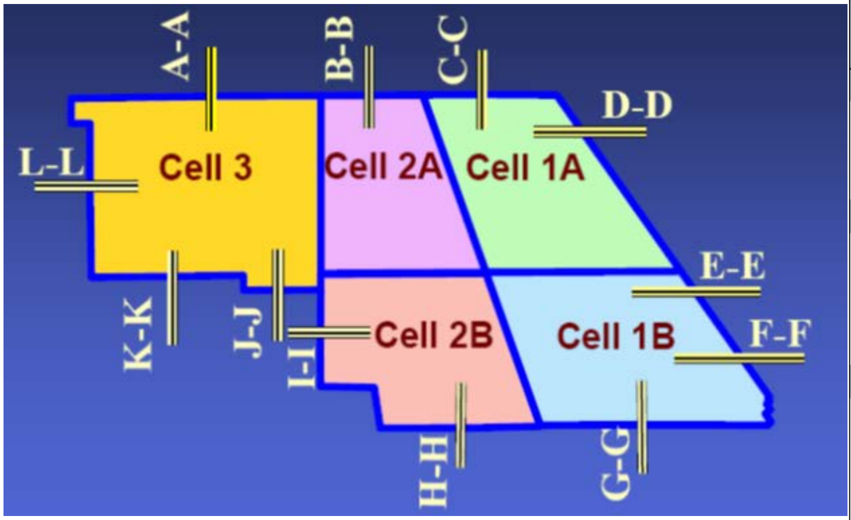

Seepage Coefficients, K_{SP} (ft^3/d/ft-levee/ft-head)		
	h_{STA}-h_{SC}	h_{IC}-h_{SC}
A-A	10.06	22.00
B-B	13.86	36.57
C-C	12.35	33.43
	h_{STA}-h_F	
D-D	19.91	
E-E	16.89	
F-F	13.06	
L-L	26.20	
	h_{STA}-h_{OC}	
G-G	44.05	
H-H	54.95	
I-I	14.02	
J-J	21.92	
K-K	59.63	

Figure 12. Locations and seepage coefficients for STA-3/4 cross-sections by Sangoyomi et al. (2011). (Note: ft^3/d/ft-levee/ft-head – cubic feet per day times height of levee time height of head.)

Estimated seepage coefficients, K_{sp}, can be used to compute the seepage rate, Q_g, by multiplying it by levee length, L_{levee}, and average difference between stages in the cells (h_c) and the neighboring water body (h_a), Δh_{c-a}, as

$$Q_g = K_{sp} L_{levee}\, \Delta h_{c-a} \qquad 155$$

<u>Application to Cells 3A and 3B</u>

To convert the reported seepage coefficients by Sangoyomi et al. (2011) to the water budget units of ac-ft/yr, the following conversion is needed:

$$1 \frac{\mathrm{ft}^3}{\mathrm{d} * \mathrm{ft.head} * \mathrm{ft.levee}} \left(\frac{5{,}280 \text{ ft}}{1 \text{ mi}} * \frac{1\mathrm{ac}}{43{,}560 \text{ ft}^2} * \frac{365\mathrm{d}}{1 \text{ yr}} \right) = 44.242 \text{ (ac.ft/yr)/(ft.head} * \text{mi.levee)}$$

Applying this factor to the values in **Figure 12**, seepage coefficients in (ac-ft/yr)/(ft-head∗mi-levee) are obtained as shown in **Table 18**. Only the cross-sections pertinent to Cells 3A and 3B are shown in the table. To apply these seepage coefficients to estimate seepage rates for Cell 3A and Cell 3B, approximate dimensions of the cells as shown in **Figure 13** are used. Seepage coefficients for internal levees are not reported in Sangoyomi et al. (2011). Considering the small differences in WY2009–WY2012 average cell stages given in the Introduction section, seepage across the internal levees can be considered negligible, and an estimate of seepage can be obtained by considering seepage across external levees only.

Table 18. Converted seepage coefficients reported by Sangoyomi et al. (2011). (Note: ac-ft/yr/mi-levee/ft-head – acre-feet per year times length of levee times height of head.)

	Seepage Coefficients, K_{sp} (ac-ft/yr/mi-levee/ft-head)	
A-A	445 (h_{STA}-h_{SC})	973(h_{IC}-h_{SC})
L-L	1,159 (h_{STA}-h_{F})	
J-J	970 (h_{STA}-h_{OC})	
K-K	2,638 (h_{STA}-h_{OC})	

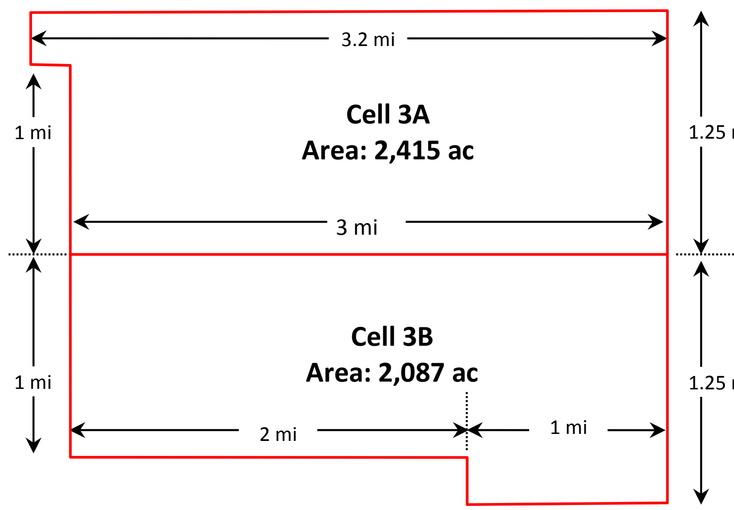

Figure 13. Approximate dimensions in acres (ac) and miles (mi) for Cells 3A and 3B.

The seepage coefficients in **Table 18** and cell dimensions shown in **Figure 1**3 can be used in **Equation 15** to estimate seepage for Cells 3A and 3B. Using the average observed stages for WY2009–WY2012, average annual seepage for these cells can be estimated as

For Cell 3A:

$$\begin{aligned} Q_{g3A} = {} & Q_{gA-A} + Q_{gL-L} \\ & = 445 * (h_{3A} - h_{SC}) * 3.2 + 1159 * (h_{3A} - h_{HL}) * 1.25 \\ & = 445 * (11.40 - 8.07) * 3.2 + 1{,}159 * (11.40 - 11.13) * 1.25 = 4{,}748 + 390 \\ & = 5{,}139 \text{ ac-ft/yr} \end{aligned}$$

For Cell 3B:

$$\begin{aligned} Q_{g3B} = {} & Q_{gL-L} + Q_{gK-K} + Q_{gJ-J} \\ & = 1{,}159 * (h_{3B} - h_{HL}) * 1 + 2{,}638 * (h_{3B} - h_{OC}) * 2 + 970 * (h_{3B} - h_{OC}) * 1 \\ & = 1{,}159 * (11.18 - 11.13) * 1 + 2{,}638 * (11.18 - 10.64) * 2 + 970 * (11.18 - 10.64) * 1 \\ & = 54 + 2{,}861 + 657 = 3{,}573 \text{ ac-ft/yr} \end{aligned}$$

These average yearly estimates for seepage rates need to be used with caution, keeping in mind that only the seepage coefficients along A-A, B-B and C-C cross-sections were calibrated using the actual seepage pump data, and the slicing technique used in draft report by Sangoyomi et al. (2011) has not been validated. Wilsnack (2013) recommended more local hydrogeological data, revisiting boundary conditions, and more rigorous uncertainty analysis to improve estimates by this method.

6.1.3 Seepage Study for STA-3/4 Design

Montgomery Watson Americas, Inc. (1999) conducted a seepage study to provide a range of seepage values for the final STA-3/4 design. Seepage rates for two scenarios, one based on geotechnical investigations and an aquifer performance test (Scenario A) and another on a calibrated MODFLOW model (Scenario B) under three stage conditions were provided. Locations for Cells 3A and 3B are roughly covered by the cell named Cell 5 in the report. Since the report was prepared to support STA design, a range of estimated seepage rates, instead of a single value, was reported. Tables below summarize the range of estimated seepage values in cubic feet per day times height of the levee (ft^3/d/[ft-levee]) for both scenarios.

Table 19. Scenario A seepage results (from Montgomery Watson Americas, Inc. 1999, Table 4.6A).

Condition	Stage			North Perimeter Loss from STA-3/4	West Perimeter Loss to Holey Land	South Perimeter Loss to Holey Land
	STA-3/4	Holey Land	Farmlands (North)			
	ft NGVD			ft^3/d/(ft-levee)		
Design Maximum	14	12	8.5	64.2	109.6	108.8
Dry Season	11	11	7.5	52.2	0	0
Wet Season	13	12	7.5	65.8	54.8	54.4

Table 20. Scenario B seepage results (from Montgomery Watson Americas, Inc. 1999, Table 4.6B).

Condition	Stage			North Perimeter Loss from STA-3/4	West Perimeter Loss to Holey Land	South Perimeter Loss to Holey Land
	STA-3/4	Holey Lands	Farmlands (North)			
	ft NGVD			ft^3/d/(ft-levee)		
Design Maximum	14	12	8.5	58.9	43.2	44.2
Dry Season	11	11	7.5	41.2	0	0
Wet Season	13	12	7.5	60.3	21.6	22.1

<u>Application to Cells 3A and 3B</u>

The seepage rates provided by Montgomery Watson Americas, Inc. (1999) are for STA-3/4 as a whole, while the current investigation focuses only on Cells 3A and 3B. In this report, seepage values in **Tables 19** and **20** were multiplied by Cells 3A and 3B levee lengths and converted to ac-ft/yr as shown in **Table 21**. Intermediate computation steps are omitted for brevity. Along the north perimeter, the values in the "Loss from STA-3/4" column were used in computations. Seepage between the STA cells was assumed negligible. The analysis provided by Montgomery and Watson Americas, Inc. (1999) was mainly for design purposes, and, as Wilsnack (2013) stated, the analyzed levee/borrow canal configuration does not exactly match what was constructed. In addition, the stages used in the analysis (shown in **Tables 19** and **20**) are different from the historical averages given above in Section 6.1.

Table 21. Application of seepage rates from Montgomery Watson Americas, Inc. (1999) to Cell 3A and Cell 3B.

	Scenario A			Scenario B		
	Cell 3A	Cell 3B	Cell 3	Cell 3A	Cell 3B	Cell 3
Condition	(ac-ft /yr)			(ac-ft /yr)		
Design Maximum	15,150	21,464	36,615	10,728	8,647	19,374
Dry Season	7,390	0	7,390	5,833	0	5,833
Wet Season	12,346	10,732	23,078	9,731	4,323	14,055

6.1.4 Combined Water and Solute Mass Balance

Choi and Harvey (2000) applied combined water and solute mass balance to estimate seepage rates for the ENR. This method assumes that seepage rates can be approximated from the residuals of water budgets. When the other components of the water budget have very large errors, this assumption may lead to erroneous seepage estimates. Application of this method to Cells 3A and 3B requires solute (chloride) concentration data for both groundwater and surface water. Currently, only surface water chloride data is being collected on a bi-weekly basis. This method was not applied to Cells 3A and 3B as not enough data is available at this time.

6.1.5 Analysis of Historical No Flow/No Rainfall Periods for Seepage Estimation

When the differences in water elevations between the STA and neighboring water bodies are high, seepage can be a significant inflow/outflow source in the water budget. Some available seepage studies assumed that the STA basins intercept the water table, resulting in negligible vertical groundwater movement. However, Harvey et al. (2004) demonstrated that the vertical flow component can be significant. When the vertical fluxes are considered as the main source of groundwater flow, instead of a nearby line source such as the inflow and outflow canals, adjacent large water bodies with significant head differences dominate the seepage flow.

Cells 3A and 3B are adjacent to Holey Land along the western and southern perimeters (**Figure 11**). Considering the small average stage differences between cells, the interaction between Holey Land and Cells 3A and 3B can be considered as the main source of groundwater flow for these two cells. The variation of stages in the cells and in Holey Land is shown in **Figures 14** and **15**. When the water levels in the cells are higher than the Holey Land stages, outflow seepage is expected. As given in Section 6.1, period of record average for differences in stages between HOLEY1_G and Cells 3A and 3B for WY2009–WY2012 period are 0.27 ft and 0.05 ft, respectively.

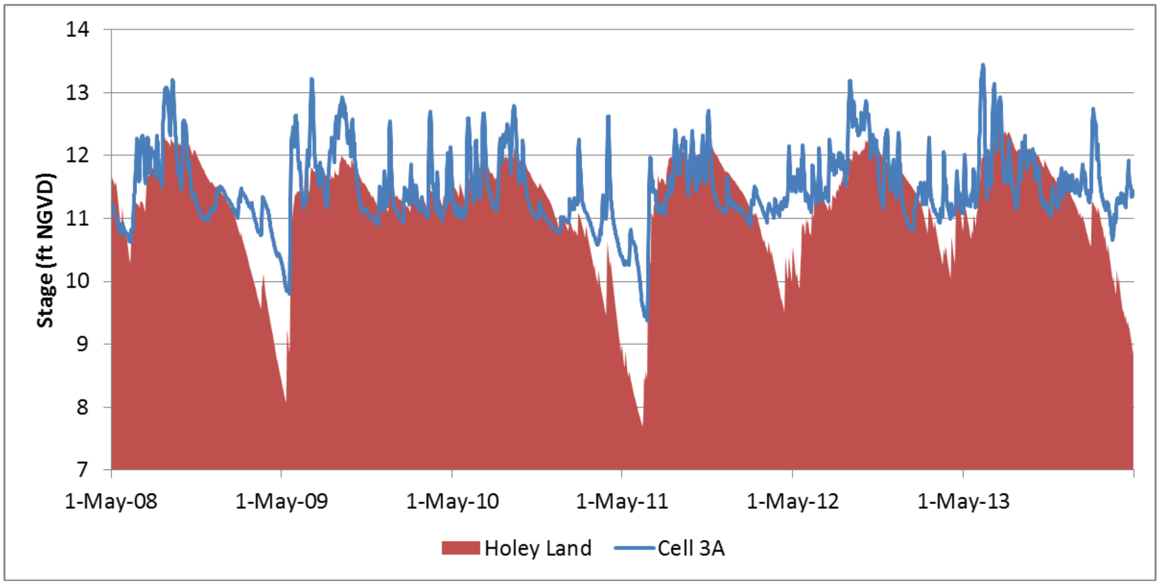

Figure 14. Holey Land and average Cell 3A stages since May 2008.

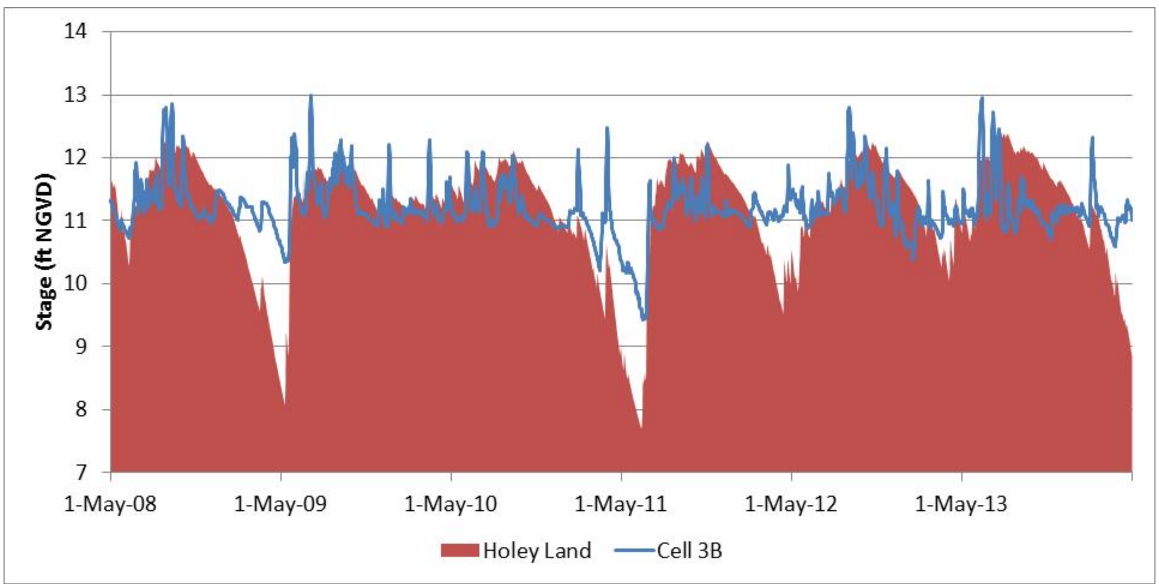

Figure 15. Holey Land and average Cell 3B stages since May 2008.

For extended dry periods with no inflow, outflow, or rainfall, the seepage rate and corresponding seepage parameters can be estimated using water mass balance. Once estimated, the seepage coefficients can be applied to the entire period of record. The water budget for STAs can be written for a given time period as

$$r = Q_{out} + Q_g + \Delta S + ET - Q_{in} - R \qquad \text{2 (repeated)}$$

where r is residual, Q_{out} is surface water outflow, Q_g is seepage flow, ΔS is change in storage, ET is evapotranspiration, Q_{in} is surface water inflow, and R is precipitation. For the periods with no inflow (Q_{in} = 0), outflow (Q_{out} = 0) and rain (R = 0), **Equation 2** can be rewritten such that the residual in the water budget is reduced to

$$r = \Delta S + Q_g + ET \qquad 16$$

Typically for the District STAs, accuracies of stage data and evapotranspiration estimates are very high in comparison to other water budget components. For a closed water budget ($r = 0$), seepage rates can be calculated from **Equation 16** as

$$Q_g = -(\Delta S + ET) \qquad 17$$

Alternatively, seepage loss for the STA cells can be computed by Darcy's law as

$$Q_g = K_e \frac{\Delta h}{\Delta l} A_g \qquad 18$$

where K_e is the effective hydraulic conductivity, Δh is the head difference between the cells and adjacent water body $(h_c - h_a)$, A_g is the cross-sectional area of the groundwater flow, and Δl is the length over which the head drop takes place. Inserting seepage flow equation (**Equation 18**) into the water budget equation for dry periods (**Equation 17**), an equation for effective hydraulic conductivity can be found as

$$K_e = -(\Delta S + ET) \frac{\Delta l}{\Delta h \, A_g} \qquad 19$$

In **Equation 19**, definition of Δl and A_g is critical for the numerical value of K_e. However, as long as the same Δl and A_g values are used during the derivation of K_e and its application to historical data, selection of Δl and A_g has no effect in the estimated conductivities and/or seepage rates. The relationship in **Equation 19** implies that effective conductivity is not constant for a given STA cell; instead it is time dependent and changes with varying stage and ET. The equation can be expanded as

$$K_e(t) = -\left(\frac{\Delta h_t}{\Delta t} A_c + \mathrm{ET}\right) \frac{\Delta l}{h_c(t) - h_a(t)} \frac{1}{A_g} \qquad 20$$

where A_c is the planar effective STA cell treatment area, h_c is the water stages in the cell, and h_a is the stages in the adjacent water body. Cross-sectional area for groundwater flow for a cell, A_g, can be found from the product of the length of the levee separating the cell from the adjacent water body and average aquifer thickness.

Application to Cells 3A and 3B

Historical stage records for the farmlands neighboring Cell 3A to the north are not available. Cell 3B, on the other hand, is surrounded by Holey Land and other STA-3/4 cells, for both of which stage data are available. Considering there is no significant head difference between Cell 3B and the adjacent cells, the head difference between this cell and the Holey Land can be used in seepage estimation. The effective conductivity given in **Equation 20** can be written for Cell 3B as

$$K_{e3B}(t) = -\left(\frac{h_{3\mathrm{B}}(t) - h_{3\mathrm{B}}(t-\Delta t)}{\Delta t} A_{c3B} + ET_{3B}\right) \frac{1}{h_{3\mathrm{B}}(t) - h_{HL}(t)} \frac{\Delta l}{A_{g3B}} \qquad 21$$

where h_{HL} is the water stage in Holey Land, and $h_{3\mathrm{B}}$ is the water stage in Cell 3B. The planar area for Cell 3B given in **Table 4** is used for A_{c3B}. For the length over which the groundwater head drop takes place, the depth for HOLEY1_G well (Δl = 12 ft) is used in this report. Ideally, vertical distance between the top of the piezometer screen to the ground surface is used as Δl; however, this information is not currently available for the HOLEY1_G well. Selection of a vertical distance as the characteristic length in Darcy's equation implies a vertical conductivity and flux. However, since the actual data from the field is used in computations, estimated conductivities consider the effects of both vertical and horizontal losses/gains. For the area of groundwater flow, the length of levees separating Cell 3B and Holey Land (4.25 miles) and an assumed aquifer thickness of 100 ft were used.

Investigation of the historical data for Cells 3A and 3B revealed that there have been very few dry periods (i.e., consecutive days of no structure flows or rainfall) since the start of individual cell operations. Considering the differences in the timescales of the processes influencing the seepage flows, only the days with fifteen or more days after a rain or flow event were chosen in determination of dry periods. Only one such period was found in the history of these two cells for the WY2009–WY2012 period. In **Figure 16**, variations of the average cell (h3A and h3B) and HOLEY1_G (hHL) stages for this period are shown. The flow data is not shown in the figure for clarity. The data recorded as S-7 rain station was used for rainfall (S7_R in the figures). During the dry period, the stages in the Holey Land are lower than those of the cells causing an outward seepage. Declining cell stages indicate reduction in storage, which is lost to evapotranspiration and seepage and replenished with rainfall.

Caution must be exercised when the average values are used at extreme hydrological conditions. Longer "no flow/no rain" records are needed to make a conclusive determination of the seepage coefficient by this method. Also, the timescale of groundwater-surface water interaction is not necessarily the same as surface water stage changes. Moving-averaging applied to stage data with a proper averaging window size needs to be used in seepage computations by this method. Directionality, head-dependence, and seasonality of seepage coefficient need further investigation before a conclusive estimation is made. The findings presented in this section should be considered provisional as more detailed analysis and longer period of record data become available.

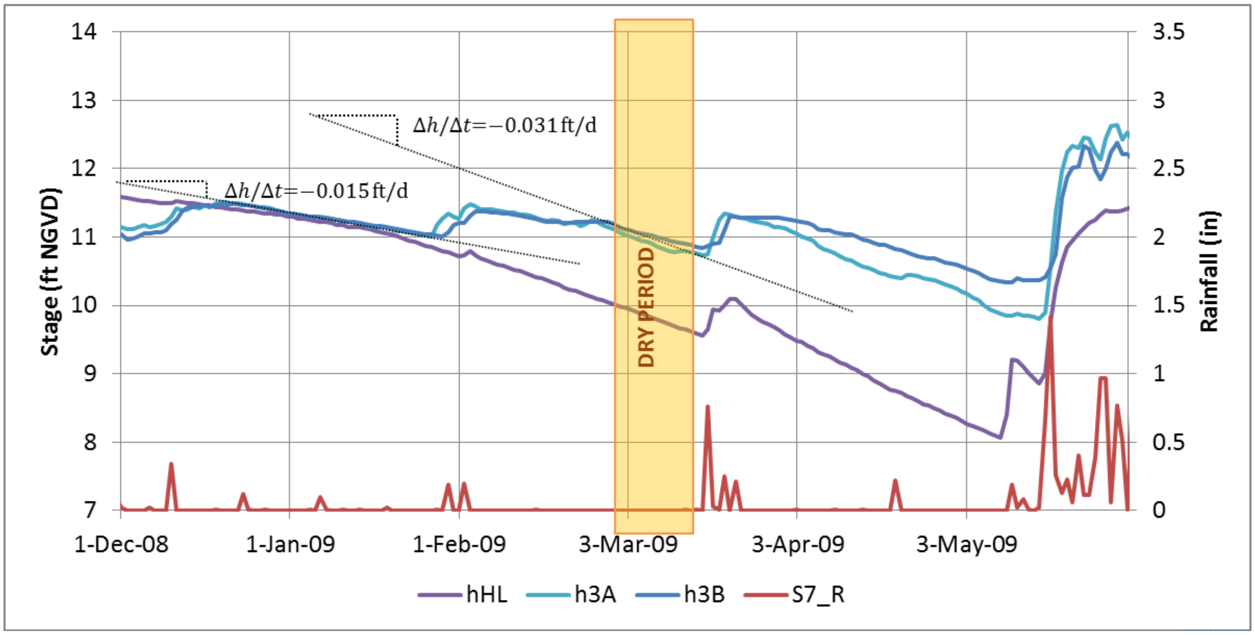

Figure 16. Holey Land and average cell stages for December 2008 to June 2009.

For the identified dry period (March 2, 2009–March 13, 2009) the average ET rate is 0.013 ft/d and average head difference $h_{3\mathrm{B}}(t) - h_{HL}(t)$ is 1.2 ft. Using these values in **Equation 21**

$$K_{e3B}(t) = -(-0.031\,A_{c3B} + 0.013\,A_{c3B}\,)\,\frac{1}{1.2}\,\frac{\Delta l}{A_{g3B}} = 0.015\,A_{c3B}\,\frac{\Delta l}{A_{g3B}} \qquad 22$$

Inserting the obtained effective conductivity in the flow equation, a relationship for seepage flow as a function of cell and Holey Land stage differences can be obtained as

$$Q_g = K_{e3B}\,\frac{\Delta h_{3B-HL}}{\Delta l}\,A_{g3B} = \left(0.015\,A_{c3B}\,\frac{\Delta l}{A_{g3B}}\right)\frac{\Delta h_{3B-HL}}{\Delta l}\,A_{g3B} = 0.015\,A_{c3B}\,\Delta h_{3B-HL} \qquad 23$$

Using the historical data for evapotranspiration, and average cell stages, water volume lost through seepage is computed. Using Darcy's law, effective conductivity, K_e, can be computed using the average stage difference between the cells and Holey Land, $h_{3B} - h_{HL}$. The accuracy of this method of computing effective conductivities largely depends on the validity of the assumption that the head differences between Holey Land and the cell is the main driver of the seepage losses. However, as seen in **Figure 16**, there is a 0.015 ft/d stage drop, even when the cell and Holey Land stages are the same (mid-December 2008 to mid-January 2009). The average ET rate for this period is 0.009 ft/day. Therefore, it can be assumed that difference of 0.006 ft/d is lost to the regional groundwater even when there is no head difference between the cells and Holey Land.

The effective conductivity estimated by this method is sensitive to various factors. There is not enough information available on applicability of the seepage coefficients derived for dry periods to wet periods.

Seepage coefficient and hydraulic conductivities are most likely anisotropic with varying magnitudes depending on loss or gain. More dry periods are needed to accurately estimate the effective conductivity. The information provided in this section should be regarded as provisional, as it is subject to change as more data become available.

Table 22. Seepage rates for Cells 3A and 3B for WY2009–WY2012 estimated from an analysis of dry periods.

	Cell 3A	Cell 3B	Cell 3
Average seepage rate for WY2009–WY2012 (ac-ft/yr)	8,758	5,221	13,979

6.1.6 Water Budget Tool

Currently the Water Budget Tool employs a methodology similar to Sangoyomi et al. (2011) using the differences in stages in the STA and surrounding canals to estimate seepage. A seepage coefficient of 1.74 cfs/mile-levee/ft-head (or 1,260 ac-ft/yr/mile-levee/ft-head) is used in the water budget analysis for the entire STA. The tool currently does not estimate the seepage for individual cells, however, Phase II will include adding this capability. In this review, the STA seepage coefficient was applied to the historical data for Cells 3A and 3B. Assuming no seepage occurs between cells, the seepage for the cells can be estimated as shown in **Table 23**.

Table 23. Seepage coefficient currently in use by the Water Budget Tool for the STA-3/4 and corresponding average yearly seepage rates for Cells 3A and 3B during WY2009–WY2012.

	Cell 3A	Cell 3B	Cell 3
Seepage Coefficient (ac-ft/yr/mile-levee/ft-head)	1,260	1,260	1,260
Average seepage rate (ac-ft/yr)	13,820	2,240	16,060

6.1.7 Direct Measurements

No direct measurement of seepage has been conducted for Cells 3A and 3B. Affordable meters that measure the direct seepage fluxes are available if needed in future phases of this study (Rosenberry and LaBaugh 2008). Combined with the hydraulic head measurements, the seepage meters can also provide information on the hydraulic conductivity of the soil matrix. Frequent field measurements to capture the effect of varying hydrological conditions may be needed. Indirect measurements using conductance and stage data can facilitate seepage monitoring.

6.2 Effect of Seepage on Water Budget

In this section, a desktop review of the available groundwater and seepage data for STA-3/4 and Cells 3A and 3B is provided. An initial review of the existing data indicated that no physical seepage measurements (in situ) were conducted during the design phase and no new seepage study has been done since the STA-3/4 seepage analysis was conducted by Montgomery Watson Americas, Inc. in 1999. This 1999 seepage analysis did include an aquifer performance test. The rates for vertical seepage were approximated from that aquifer performance test and subsequent modeling work. In addition, even though they provide a range of expected fluxes, due to the differences in the hydrogeological conditions, the field measurements conducted at the ENR cannot be directly used to estimate seepage for STA-3/4.

A summary of the estimated seepage values obtained by the methods reviewed in Section 6.1 is provided in **Table 24**. As seen in the table, estimated seepage rates display a significant variation with a large standard deviation. These large differences in the estimated values can be considered as an indicator of the effects of assumptions and approximation in followed methods. In the absence of better-justified data, the standard deviations shown in the table can be used as the basis for standard deviation and, consequently, the uncertainty of seepage estimates.

Table 25 shows the mean seepage estimate and its basic statistics using the values presented in **Table 24**. Confidence interval (CI) for the mean was computed assuming a normal distribution at 95% certainty as $\pm 1.96(s/\sqrt{N})$, where s is the standard deviation of the estimated seepage values by different methods and N is the sample size. Upper and lower confidence limits (CL) of the mean average yearly seepage rate, $\overline{Q_g}$, are estimated as $\overline{Q_g} \pm \mathrm{CI}$.

Tables 26 through **28** show the water budgets for Cells 3A and 3B for WY 2009–WY2012 period of record averages. The seepage estimates at lower CL, mean, and upper CL are shown in the tables. Surface flow rate through the structures on the internal levee (G-384A-F) is currently under quality assurance/quality control investigation, and is expected to be finalized in approximately December 2014. Provisional values estimated by Method 2 of Section 5.4.2 are used in the tables. Changes in the mid-levee flows (G-384A-F) may appreciably change the relative magnitude of other water budget components.

Table 24. Estimated average yearly seepage rates by all reviewed methods.

	Montgomery Watson Americas, Inc. 1999						ENR Study		Seep2D Model	Water Budget Tool	From Dry Periods
	Scenario A			Scenario B							
Condition:	Design Maximum	Dry	Wet	Design Maximum	Dry	Wet	ENR East	ENR West			
Location	ac-ft/yr										
Cell 3A	15,150	7,390	12,346	10,728	5,833	9,731	-9,833	25,089	5,139	13,820	8,758
Cell 3B	21,464	0	10,732	8,647	0	4,323	-8,496	21,677	3,573	2,240	5,221
Cell 3	36,614	7,390	23,078	19,375	5,833	14,054	-18,329	46,766	8,712	16,060	13,979

Table 25. Summary statistics of the estimated average yearly seepage rates by all reviewed methods.

	Mean, $\overline{Q_g}$	Standard Deviation	Coefficient of Variation	CI	Lower CL, $\overline{Q_g} - \mathrm{CI}$	Upper CL, $\overline{Q_g} + \mathrm{CI}$
	ac-ft/yr	ac-ft/yr	-	ac-ft/yr	ac-ft/yr	ac-ft/yr
Cell 3A	9,468	8,453	0.893	4,995	4,473	14,463
Cell 3B	6,307	9,049	1.435	5,348	960	11,655
Cell 3	15,776	16,880	1.070	9,975	5,800	25,751

Table 26. WY2009–WY2012 average yearly water budgets with seepage values at the lower CL.

	Q_{in}	Rainfall, R	Seepage, Q_g (Lower CL)	Q_{out}	ET	ΔS	ΣIn	ΣOut	Residual, r	Residual Error, ε
	ac-ft/yr	ac-ft/yr	ac-ft/yr	ac-ft/yr	ac-ft/yr	ac-ft/yr	ac-ft/yr	ac-ft/yr	ac-ft/yr	(%)
Cell 3A	155,944	10,124	4,473	151,305	10,928	254	166,068	166,706	892	1%
Cell 3B	151,305	8,749	960	149,782	9,443	81	160,054	160,186	213	0%
Cell 3	155,944	18,873	5,800	149,782	20,371	335	174,817	175,954	1,472	1%

Table 27. WY2009–WY2012 average yearly water budgets with mean seepage values.

	Q_{in}	Rainfall, R	Seepage, Q_g (Mean)	Q_{out}	ET	ΔS	ΣIn	ΣOut	Residual, r	Residual Error, ε
	ac-ft/yr	ac-ft/yr	ac-ft/yr	ac-ft/yr	ac-ft/yr	ac-ft/yr	ac-ft/yr	ac-ft/yr	ac-ft/yr	(%)
Cell 3A	155,944	10,124	9,468	151,305	10,928	254	166,068	171,701	5,887	3%
Cell 3B	151,305	8,749	6,307	149,782	9,443	81	160,054	165,533	5,560	3%
Cell 3	155,944	18,873	15,776	149,782	20,371	335	174,817	185,929	11,447	6%

Table 28. WY2009–WY2012 average yearly water budgets with seepage values at the upper CL.

	Q_{in}	Rainfall, R	Seepage, Q_g (Upper CL)	Q_{out}	ET	ΔS	ΣIn	ΣOut	Residual, r	Residual Error, ε
	ac-ft/yr	ac-ft/yr	ac-ft/yr	ac-ft/yr	ac-ft/yr	ac-ft/yr	ac-ft/yr	ac-ft/yr	ac-ft/yr	(%)
Cell 3A	155,944	10,124	14,463	151,305	10,928	254	166,068	176,696	10,882	6%
Cell 3B	151,305	8,749	11,655	149,782	9,443	81	160,054	170,881	10,908	7%
Cell 3	155,944	18,873	25,751	149,782	20,371	335	174,817	195,904	21,422	12%

Using the values provided in **Tables 26** through **28**, percent contributions from each water budget component can be computed as an indicator of their relative effect on water budget, and its residual error. **Tables 29** through **31** show the relative contribution from each component with seepage estimates at lower CL, mean, and upper CL. Percent contributions for the WY2009–WY2012 were computed by dividing the values shown in **Tables 26** through **28** by ΣIn and ΣOut for inflow and outflow components, respectively.

Table 29. WY2009–WY2012 percent contributions of water budget components with seepage values at the lower CL.

	Inflow		**Outflow**			
	Q_{in}	R	Q_g (Lower CL)	Q_{out}	ET	ΔS
Cell 3A	93.9%	6.1%	2.7%	90.8%	6.6%	0.2%
Cell 3B	94.5%	5.5%	0.6%	93.5%	5.9%	0.1%
Cell 3	89.2%	10.8%	3.3%	85.0%	11.5%	0.2%

Table 30. WY2009–WY2012 percentage contributions of water budget components with mean seepage values.

	Inflow			Outflow		
	Q_{in}	R	Q_g (Mean)	Q_{out}	ET	ΔS
Cell 3A	93.9%	6.1%	5.5%	88.1%	6.3%	0.1%
Cell 3B	94.5%	5.5%	3.8%	90.5%	5.7%	0.0%
Cell 3	89.2%	10.8%	8.5%	80.5%	10.9%	0.2%

Table 31. WY2009–WY2012 percentage contributions of water budget components with seepage values at the upper CL.

	Inflow			Outflow		
	Q_{in}	R	Q_g (Upper CL)	Q_{out}	ET	ΔS
Cell 3A	93.9%	6.1%	8.1%	85.6%	6.2%	0.1%
Cell 3B	94.5%	5.5%	6.8%	87.7%	5.5%	0.0%
Cell 3	89.2%	10.8%	13.1%	76.4%	10.3%	0.2%

Using the information in **Tables 29** through **31**, the findings of the review can be summarized in the form of expected percent contributions from the seepage estimates as shown in **Table 32**.

Table 32. Contribution of seepage to the water budgets for WY2009–WY2012.

STA Compartment	Seepage Contribution to Water Budget
Cell 3A	5.5% $\pm$ 2.9%
Cell 3B	3.8% $\pm$ 3.2%
Cell 3	8.5% $\pm$ 5.4%

For cells with larger treatment areas, the relative size of surface water flows is smaller as the seepage, ET, and rainfall volumes increase linearly with increasing cell areas. Because Cells 3A and 3B are the smallest of the STA-3/4 cells, significantly different percent contributions may be obtained if similar analysis is applied to a different flow-way.

Table 33. WY2009–WY2012 percentage contributions of water budget components for average rainfall, ET and mean seepage values.

	Rainfall	Seepage	ET
Cell 3A	6.1%	5.5%	6.4%
Cell 3B	5.5%	3.8%	5.7%
Cell 3	10.8%	8.5%	11.0%

Based on results presented in **Table 33**, in terms of contribution to the water budgets, ET and rainfall have a similar contribution, which is higher than that of seepage for Cell 3 (Flow-way 3). Improved estimates of groundwater flux may reduce the uncertainty and, hence, the residuals in STA water and nutrient budget calculations. A seepage model targeting cell-by-cell water budget analysis, using refined hydrogeological data, can be developed to produce more robust estimates. However, direct field measurements are considered the most reliable method for seepage estimation. If resources allow, a program for locating the existing wells and evaluating their condition, and installation of groundwater wells, and direct seepage measurements or monitoring would be very helpful in investigating the interaction between the groundwater and STA cells.

7 Rainfall

In this section, available rainfall estimation methods, spatial and temporal variations in these estimates, and their effect on water budgets of Cells 3A and 3B are discussed. In STAs, where the surface water flows through the control structures are the main driver of the hydrology, rainfall is a relatively small component of the annual water budget. The rainfall component of STA water budgets is currently estimated from rain gauges in the STAs or the nearest gauges in the surrounding area. NEXRAD rainfall estimates are also available for 2 kilometer (km) by 2 km pixels and have been used to fill the gaps in the rain gauge data. Both rain gauge and NEXRAD data are available in District databases. There are also point rainfall time series based on NEXRAD in DBHYDRO for select rain gauge locations.

Even though the NEXRAD rainfall estimates are adjusted using available rain gauges, evaluation of the NEXRAD and gauge rainfall shows the two data sets can have notable differences. It is currently not possible to determine which data set is superior; therefore, it is recommended that STA water budget analyses continue using rain gauges when available with NEXRAD data used to fill gaps. Rain gauges are considered as the standard method of estimating rainfall; however, localized rainstorms that are common in South Florida, can introduce significant estimation errors. In this report, densely located rain gauges in STA-1 West (STA-1W) are used to compare NEXRAD and rain gauge estimates. The results of this comparison were used as a basis to determine the variability in rainfall estimates for Cells 3A and 3B of STA-3/4. A more intensive evaluation of NEXRAD and gauge rainfall to see which set represents a better estimation of the actual rainfall over the STAs is outside the scope of this study.

7.1 Comparison of Rainfall Estimation Methods

The exact volume of rainfall that falls on a specific area is unknown. All rainfall measurements are estimates with errors. Rain gauges, despite being considered a standard method of rainfall measurement, involve many sources of error. There have been numerous studies evaluating errors in rainfall measurements (Winter 1981). Rain gauge data has errors associated with gauge dimension, gauge density, areal rainfall estimation from gauges, gauge maintenance, data transfer and recording. Errors in estimates of rainfall decrease as the time over which accumulation is considered. Spatial analysis for daily and monthly rainfall in South Florida showed that fivefold rain gauge spacing may be needed to estimate daily rainfall with about the same error as a monthly rainfall estimate (Abtew et al. 1993, 1995).

Real-time radar rainfall estimates are important for water management operations. Spatial distribution of rainstorms and information gained on the relative magnitude of rainfall from radar estimates is critical for water management decision making as shown during Tropical Storm Isaac, which passed over South Florida in late August 2012 (Abtew and Ciuca 2014).

Gauge-adjusted NEXRAD rainfall data is a radar-based rainfall estimate that is adjusted with gauge observations. NEXRAD, also known as Weather Surveillance Radar 88 Doppler, is a network of weather radar stations over the United States. The District's area is covered by three of the radar stations: KAMX in Miami, KMLB in Melbourne and KBTW in Tampa. Radar rainfall estimates are obtained near-real-time and generally used for water management decisions. At a later time, comparison is made to the network of rain gauge readings and gauge-to-radar ratio is developed to adjust the radar estimates and produce gauge-adjusted NEXRAD rainfall data by the data provider. As Skinner et al. (2009) reported, the quality of radar-rainfall measurements remains largely unknown. They compared gauge and NEXRAD data in the Upper and Lower Kissimmee basins and concluded that radar-rainfall demonstrates localized bias, and overestimates low-end and underestimates high-end rainfall. They recommended further study for an exhaustive evaluation of NEXRAD errors.

Conclusive literature on analysis of rain gauge and radar rainfall and recommendations as to which one best represents actual rainfall over the region were not found during preparation of this report. For this study, for the purpose of areal rainfall estimation over the STAs, a simple comparison was made between gridded NEXRAD rainfall and gauge rainfall estimates. For the NEXRAD-rain gauge comparison, STA-1W was selected as it has a relatively high density of rainfall gauges. The five existing rainfall gauges at STA-1W are ENR101, ENR203, ENR301, ENR308 and ENR401. Eight NEXRAD 2 km by 2 km pixels cover the STA fully or partially (**Figure 17**). NEXRAD gauge-adjusted rainfall data, average of pixels covering STA-1W, (**Figure 17**) was compared to Thiessen-weighted areal average of the five gauges for twelve water years (WY2001–WY2012). The result indicates that average water year NEXRAD rainfall estimates are 9 percent higher than the rain gauge values (**Table 34**). The monthly difference between NEXRAD and Thiessen-weighted gauge average ranges from -5.43 to 4.85 inches (**Figure 18**). The highest monthly difference was 4.86 inches in August 2004. Most of the differences have a positive bias, since in most months, NEXRAD rainfall estimates are higher than gauge values in this case.

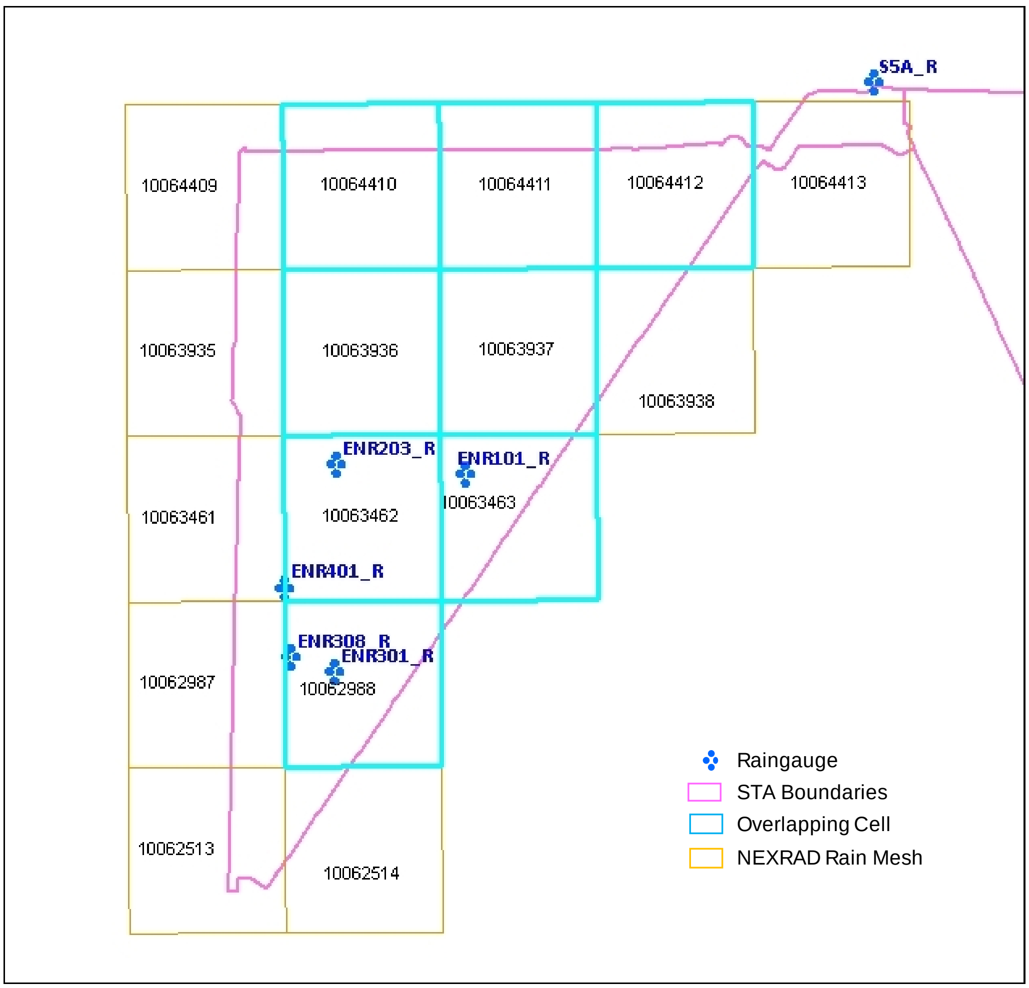

Figure 17. STA-1W rainfall gauges and NEXRAD pixels.

Table 34. Comparison of water year rainfall estimates over STA-1W by NEXRAD (8 cells) rainfall and five-gauge Thiessen average.

Water Year	NEXRAD (8 cells)	Five-gauge (Thiessen average)	Difference	Difference
	(inches)	(inches)	(inches)	(%)
WY2001	40.51	35.02	5.48	16%
WY2002	58.69	52.63	6.06	12%
WY2003	37.17	42.30	-5.13	-12%
WY2004	36.48	34.09	2.39	7%
WY2005	48.28	41.85	6.42	15%
WY2006	51.17	43.82	7.35	17%
WY2007	41.87	38.20	3.68	10%
WY2008	55.91	46.74	9.16	20%
WY2009	58.49	51.31	7.17	14%
WY2010	62.55	57.96	4.58	8%
WY2011	40.78	37.50	3.28	9%
WY2012	42.54	43.32	-0.78	-2%
Average	47.87	43.73	4.14	**9%**

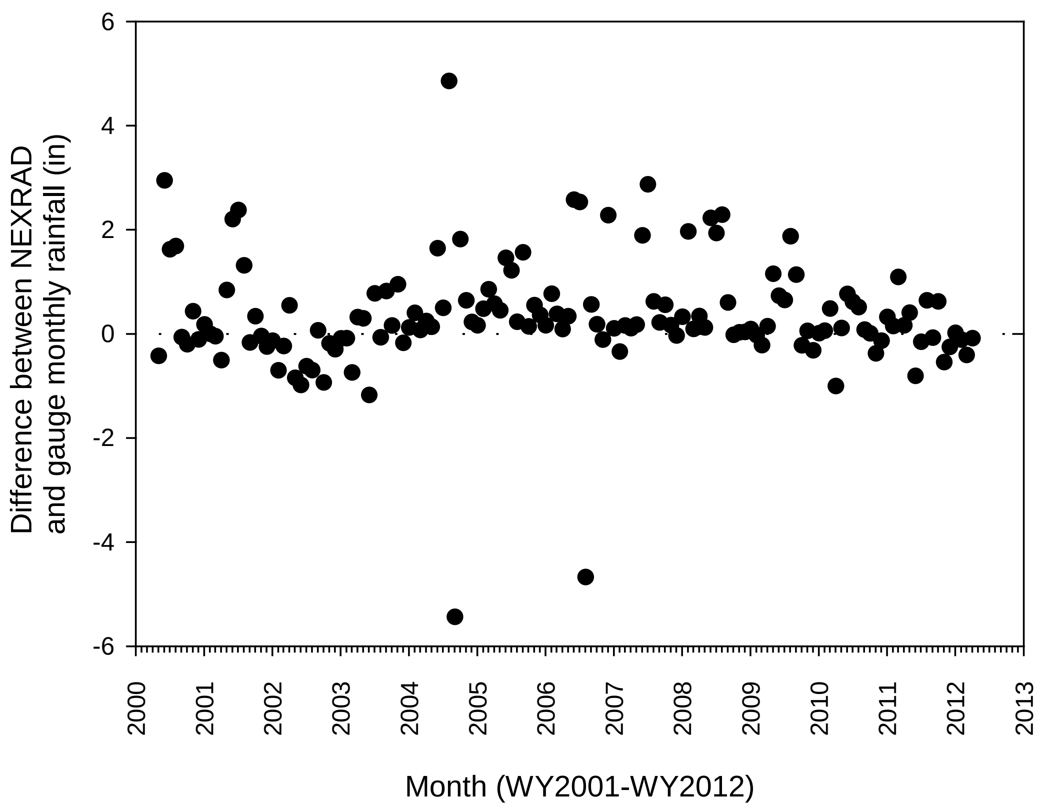

Figure 18. Difference between NEXRAD and gauge monthly average areal rainfall in STA-1W.

Difference between the mean monthly rainfall NEXRAD areal estimates and the Thiessen-weighted five-gauge estimate is shown in **Figure 19**. Mean difference in September is negligible and differences for April, January, December, November, October, February and May are small. August, June and July have 0.71, 1.12 and 1.19 inches monthly mean difference, respectively. The figure indicates that when the differences between the NEXRAD and gauge rainfall data are evaluated, seasonality should also be considered.

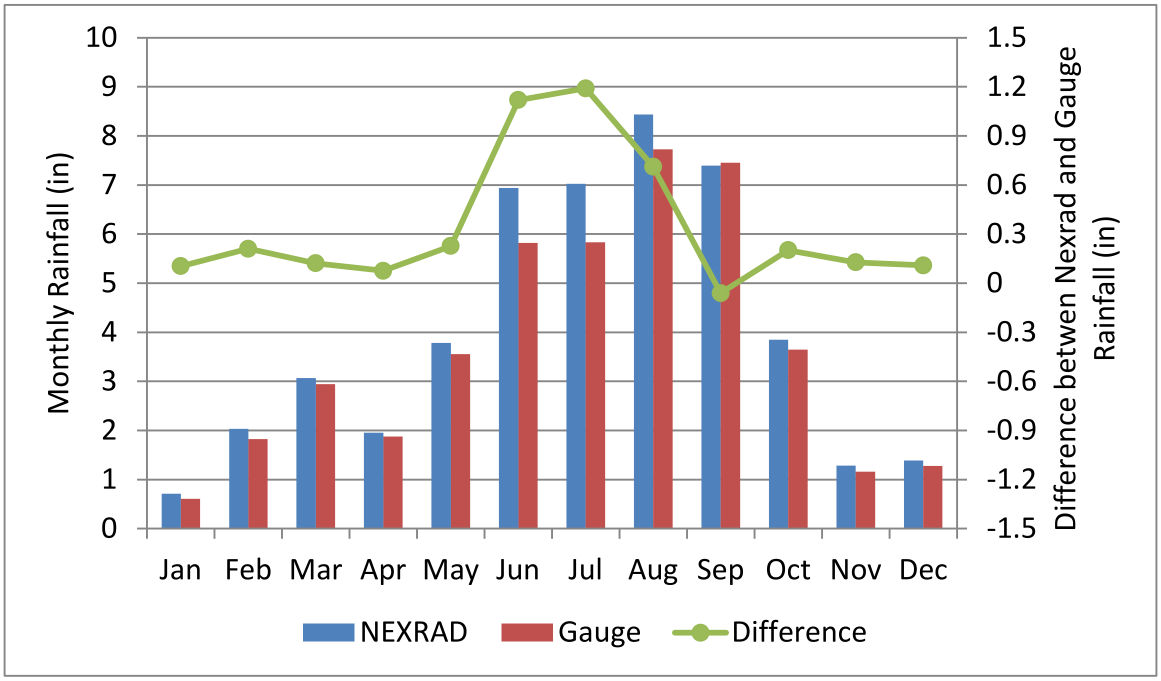

Figure 19. Mean monthly NEXRAD and gauge areal average rainfall for STA-1W (WY2001–WY2012).

In addition to temporal/seasonal variation, the difference in NEXRAD and gauge data can vary drastically from location to location. **Figure 20** shows NEXRAD rainfall estimates for the water bodies in the vicinity of WCA-1 for August 2004. While NEXRAD data over STA-1W indicates 10.05 inches rainfall, the rainfall observed at the five STA-1W gauges had an average of 5.08 inches, demonstrating a 100% difference in rainfall estimates by these two methods.

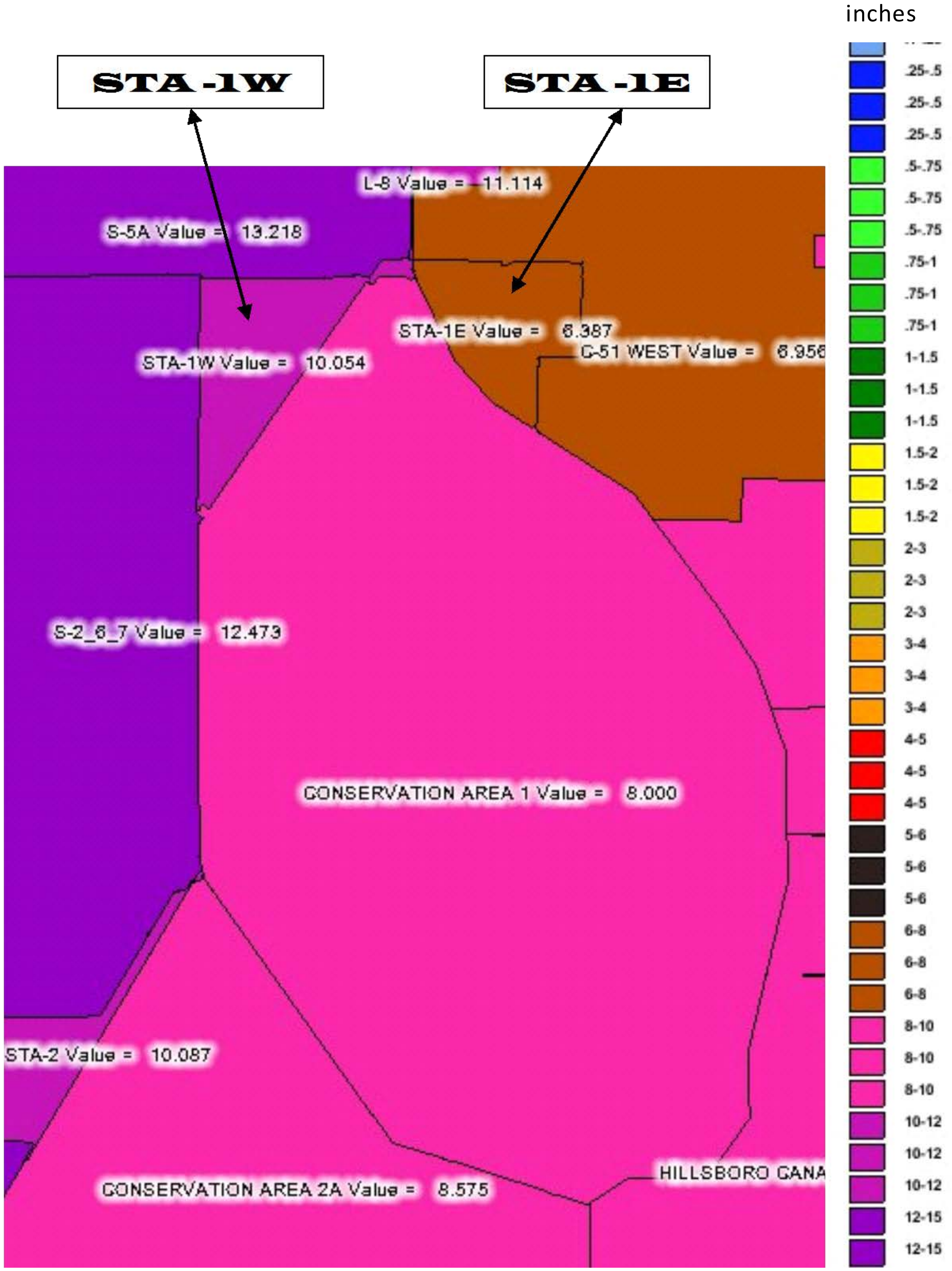

Figure 20. August 2004 NEXRAD rainfall estimate (10.05 inches) for STA-1W when gauge Thiessen average estimate was 5.08 inches.

In addition to spatial and temporal averages, as a further evaluation of the comparison of NEXRAD and gauge rainfall estimates, rainfall from a NEXRAD pixel (# 10062988) was compared to a gauge (ENR308) inside the pixel for 16 water years (WY1997–WY2012). The result indicates that average water year NEXRAD pixel rainfall estimate is 9% higher than the rain gauge values (**Table 35**). The average monthly difference between NEXRAD pixel rainfall and a rain gauge in the pixel ranges from -0.13 to 1.47 inches (**Figure 21**). The mean difference in April, December and January is negative (NEXRAD estimates lower than gauge). Generally, the higher differences are in the wet season. But this result could change depending on pixel, gauge and period of record used. As stated previously, the assumption that gauge data has no measurement error is not correct, as there are many missing and partial observation data that had to be filled.

Table 35. Comparison of annual rainfall estimates in STA-1W by NEXRAD (one cell) and ENR308 gauge.

Water Year	NEXRAD (Single cell) (in)	Rain gauge (ENR308) (in)	Difference (in)	Difference (%)
WY1997	59.63	57.79	1.84	3%
WY1998	63.43	59.94	3.49	6%
WY1999	49.67	49.77	-0.10	0%
WY2000	51.97	56.13	-4.16	-8%
WY2001	39.45	34.74	4.71	12%
WY2002	57.33	50.81	6.52	11%
WY2003	38.71	39.81	-1.10	-3%
WY2004	37.46	34.23	3.23	9%
WY2005	53.45	40.71	12.74	24%
WY2006	52.00	42.62	9.38	18%
WY2007	41.48	35.54	5.94	14%
WY2008	57.82	42.98	14.84	26%
WY2009	58.50	56.16	2.34	4%
WY2010	59.70	57.52	2.18	4%
WY2011	39.80	34.00	5.80	15%
WY2012	45.88	42.24	3.64	8%
Average	50.39	45.94	4.45	**9%**

In the interest of STA water budget analysis, water budget errors were evaluated with NEXRAD and gauge rainfall over STA-2, STA-5 and STA-6 by Huebner et al. (2007). For each STA for WY2003 and WY2004, weighted areal average daily NEXRAD rainfall from pixels fully or partially covering each STA was computed. Average rainfall from gauges used for each STA was also computed (**Table 36**). Annual water budget errors were compared using the NEXRAD and gauge rainfall data. In Huebner et al. (2007), water budget error was marginally reduced for STA-2 while no difference was shown for STA-5 and STA-6 by using NEXRAD data. It should be noted however that these results do not prove which data better represents actual rainfall over the STAs. The comparison in **Table 36** and **Figure 21** indicates that NEXRAD rainfall was lower than gauges by 10% on average.

Table 36. Comparison of water year NEXRAD rainfall and gauge rainfall estimates over STA-2, STA-5 and STA-6 (From Huebner et al., 2007).

STA	Water Year	NEXRAD Weighted Areal Average (inches)	Rain Gauge Average (inches)	Difference (inches)	Difference (%)
STA-2	WY2003	39.21	50.43	-11.22	-29%
	WY2004	38.03	45.75	-7.72	-20%
STA-5	WY2003	46.42	47.64	-1.22	-3%
	WY2004	46.18	45.55	0.63	1%
STA-6	WY2003	47.32	48.70	-1.38	-3%
	WY2004	50.87	55.08	-4.21	-8%
	Average	44.67	48.86	-4.19	**-10%**

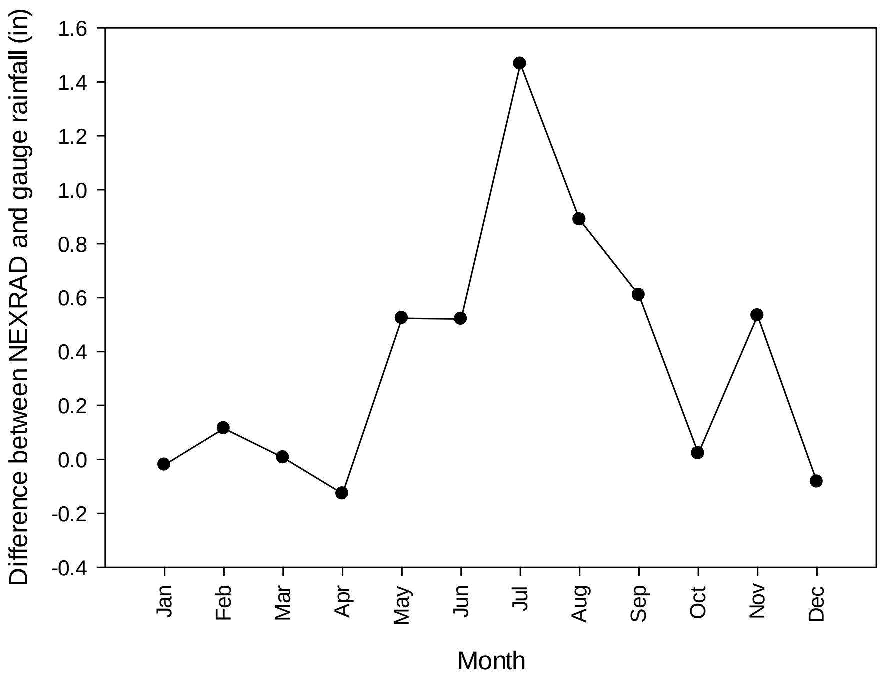

Figure 21. Mean monthly difference in a NEXRAD pixel and a gauge rainfall.

There are times where NEXRAD rainfall observations are more representative than gauges. This was the case during Tropical Storm Isaac (**Figures 22a** and **22b**). The storm dividing line was between STA-1 East (STA-1E) and STA-1W with NEXRAD rainfall of 20.5 and 14.6 inches, respectively. The rain gauge average rainfall at STA-1W was 14.1 inches. Due to its proximity, rainfall from STA-1W rain gauges is also used for STA-1E water budget analysis. In this case, the major storm was over STA-1E. By using estimates from gauges at STA-1W for STA-1E, a major underestimation occurs. There is a difference of 6.4 inches between NEXRAD at STA-1E and the gauges at STA-1W for August 2012. For the WY2013 STA-1E water budget, NEXRAD rainfall estimates should be substituted for gauge estimates for August 2012. Otherwise, an additional error of about 3,099 acre-feet (ac-ft) will be generated in the water budget for August 2012. There are ongoing efforts (external to this study) to address the question of whether the rain gauge or NEXRAD data better represents the actual volume of rainfall over an area. Future water budget analyses can utilize the results of these efforts once they are available.

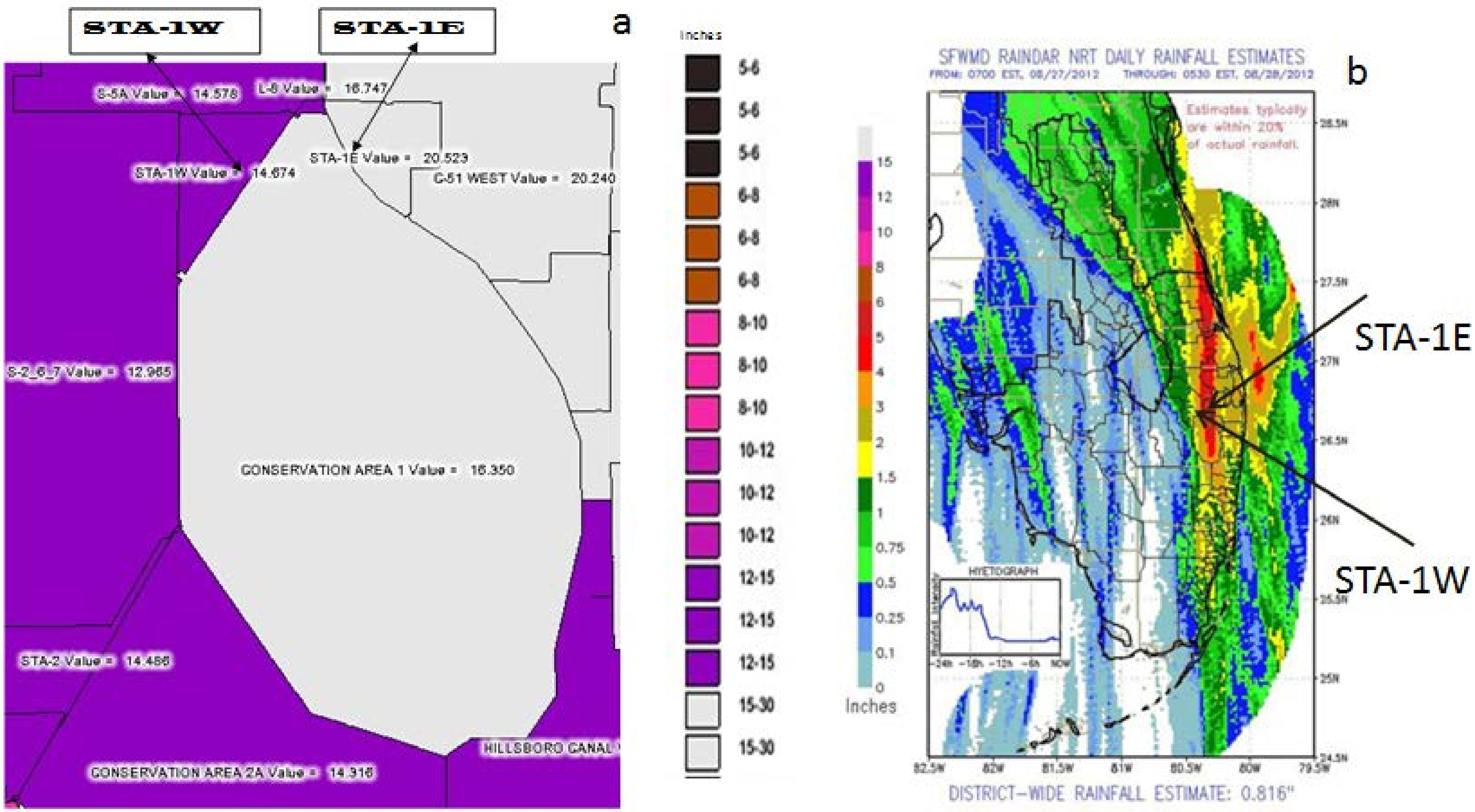

Figure 22. a) August 2012 NEXRAD rainfall estimates, for STA-1E (20.52 inches) and for STA-1W (14.67 inches); b) main rainfall band on STA-1E (Tropical Storm Isaac August 25–28, 2014).

7.2 Rainfall Data for Cells 3A and 3B

Locations for the rainfall stations in the vicinity of Cell 3A of STA-3/4 and their distance from the centroid of Cell 3A are shown in **Figure 23**. Previous water budget analysis for Cells 3A and 3B used either rainfall data from the S7 rainfall station or the average of data from the S7 and EAA5 rainfall stations. EAA5 is the closest rainfall station to Flow-way 3, which is 4.5 miles away from Cell 3A.

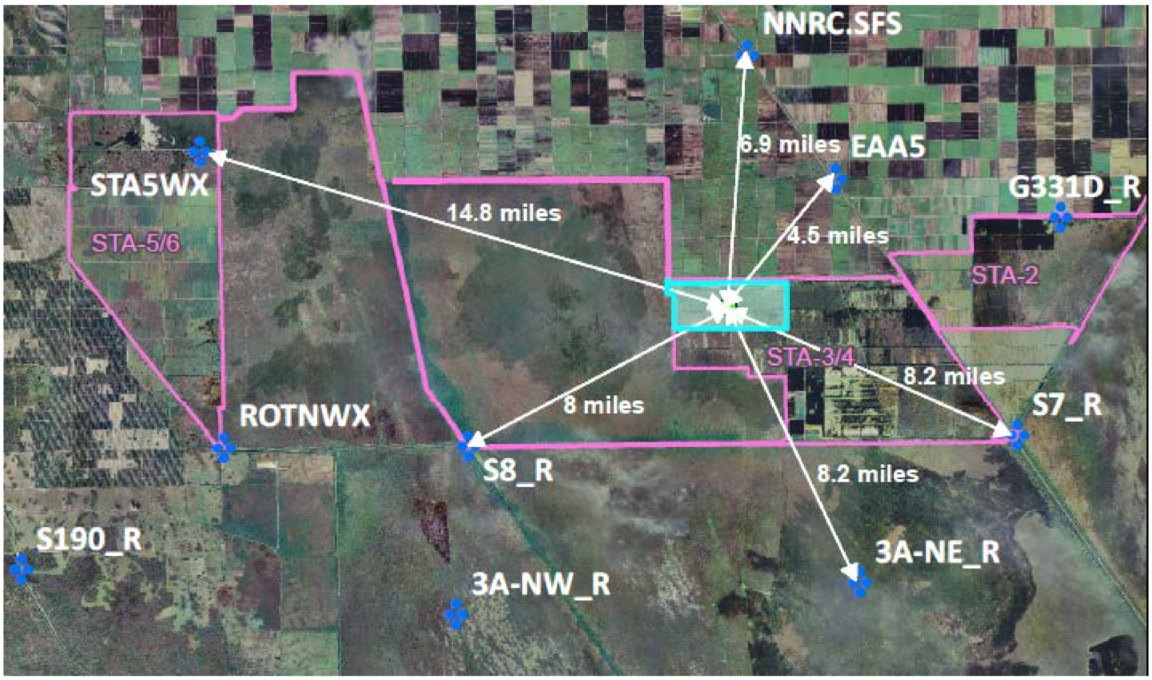

Figure 23. Rain stations in the vicinity of STA-3/4 Cell 3A.

Localized events can cause a significant difference in the recorded rainfalls at locations 4 to 8 miles apart in South Florida. Spatial variations can be muted when large time periods are chosen for consideration. Variations in the monthly rainfall data for Cell 3A from the closest five stations for WY2012 are shown in **Figure 24**. As seen in the graph, the range of monthly variation can be as high as 1,500 ac-ft. Annual rainfall for these stations for WY2009–WY2012 is compared in **Table 37**. As shown in the table, the range of variations in the recorded rainfall data varies between 1,647 ac-ft for WY2011 to 4,793 ac-ft for WY2009. **Table 37** also shows that when longer periods are considered, the variations in the averages get smaller. The period of record averages from all four rain stations have very similar values, even when annual rainfalls vary considerably.

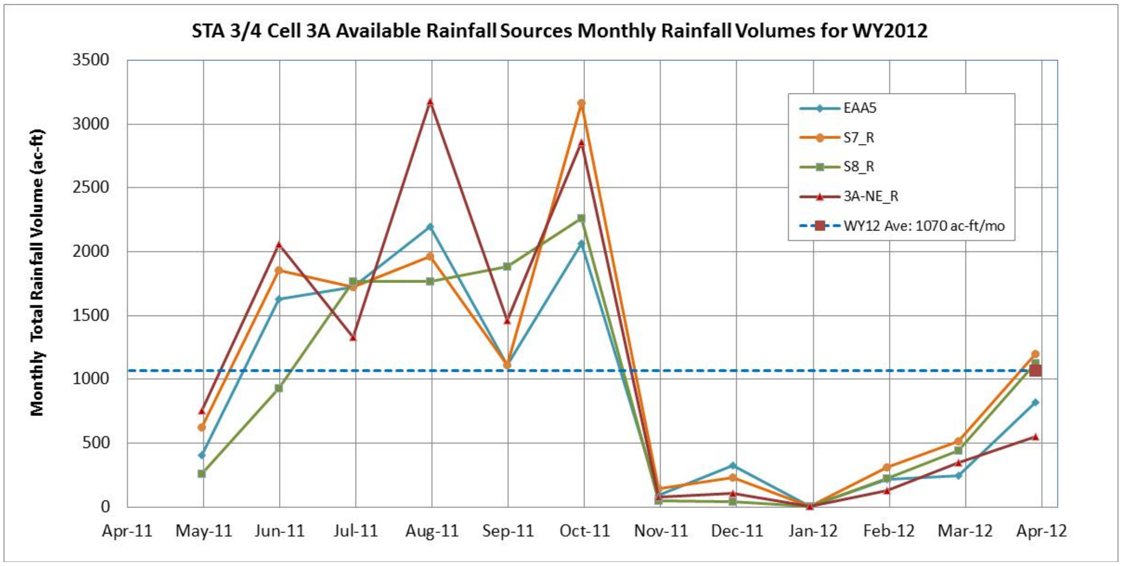

Figure 24. Variations in rainfall from various rain stations for STA-3/4 Cell 3A for WY2012.

Table 37. Variation in total water year rainfall from available stations for Cell 3A (2,415 acres).

Station:	EAA5	S7_R*	S8_R	3A-NE_R	Range Maximum-Minimum	Average of all stations	Stand. Deviation	Coefficient of Variation	NEXRAD
DBKEY:	15184	15204	15205	LX283					
Water Year	ac-ft	ac-ft	ac-ft	ac-ft	ac-ft	ac-ft	ac-ft	%	ac-ft
WY2009	10,726	8,573	8,658	6,130	4,596	8,520	1,880	22%	10,148
WY2010	11,333	12,264	13,447	12,403	2,115	12,363	866	7%	12,493
WY2011	8,150	7,348	8,935	8,619	1,584	8,264	689	8%	8,314
WY2012	10,394	12,310	10,321	13,266	2,945	11,572	1,456	13%	11,726
WY2013	12,384	12,218	10,307	11,607	2,076	11,628	942	8%	10,817
Period of Record Average	10,597	10,541	10,334	10,405	264	10,469	121	1%	10,699

* Rainfall data from S7 rainfall station was used in the water budget analyses presented in this report.

The comparison of rain gauge data collected at various locations shown in **Table 37** indicates that, even though period of record averages do not display significant variations, yearly rainfall measured at locations 15 miles apart can have variations as high as 22%. The water budgets developed in this report use rain gauge data from the S7 rain station. **Figure 25** shows the NEXRAD pixels covering Cells 3A and 3B. Coverage by cell footprint for each pixel is also shown in the figure. The table in the figure was used in estimation of NEXRAD rainfall shown in **Tables 37** and **38**. A comparison of rain gauge (S7) versus NEXRAD data in **Table 39** indicates significant differences in annual rainfall estimates by these methods. The differences in annual estimates are reduced to 2% for the considered period of record of five water years. As stated previously, there are ongoing efforts to address the question of whether the rain gauge or NEXRAD data better represents the actual volume of rainfall over an area. Future water budget analyses can utilize the results of these efforts once they are available.

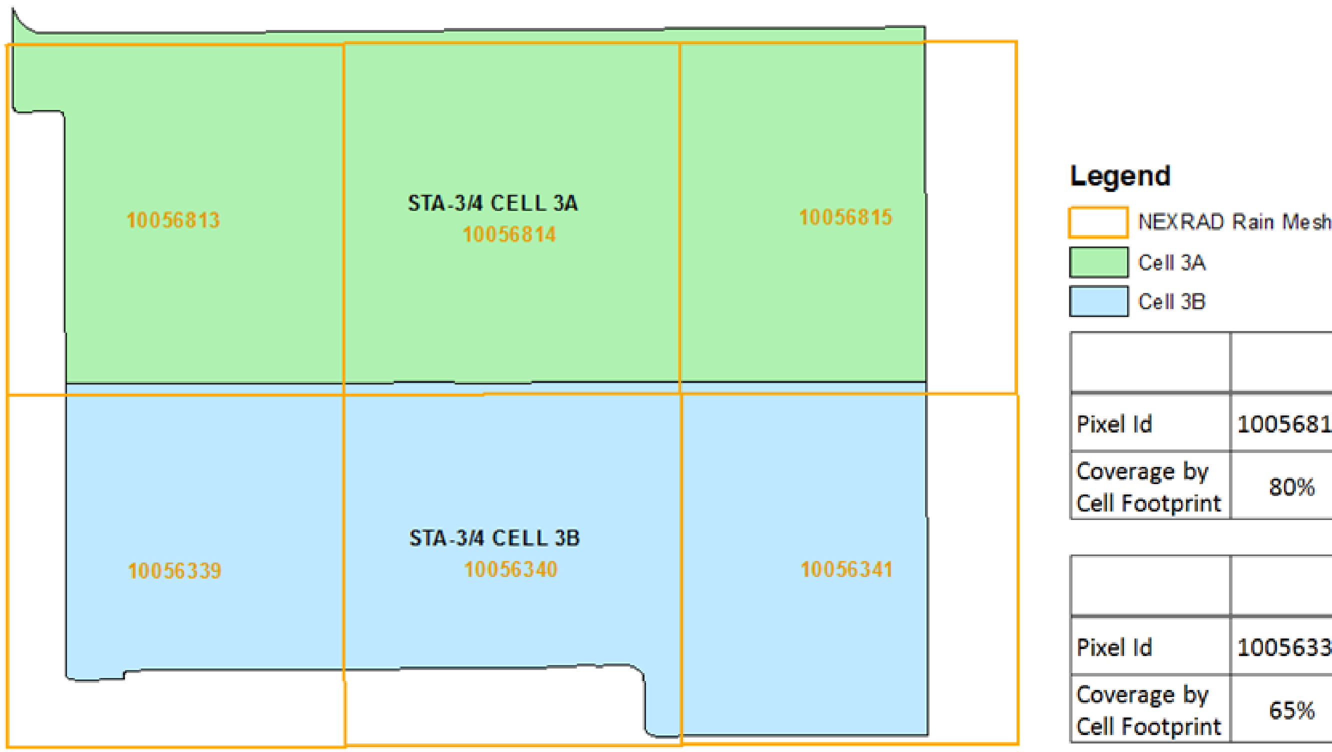

	Cell 3A		
Pixel Id	10056813	10056814	10056815
Coverage by Cell Footprint	80%	100%	70%

	Cell 3B		
Pixel Id	10056339	10056340	10056341
Coverage by Cell Footprint	65%	80%	70%

Figure 25. NEXRAD pixels covering Cells 3A and 3B.

Table 38. Variation in total water year rainfall from available stations for Cell 3B (2,087 acres).

Station:	EAA5	S7_R*	S8_R	3A-NE_R	Range Maximum-Minimum	Average of all stations	Stand. Deviation	Coefficient of Variation	NEXRAD
DBKEY:	15184	15204	15205	LX283					
Water Year	ac-ft	ac-ft	ac-ft	ac-ft	ac-ft	ac-ft	ac-ft	%	ac-ft
WY2009	9,269	7,409	7,482	5,297	3,972	7,363	1,624	22%	8,556
WY2010	9,793	10,598	11,621	10,718	1,828	10,684	748	7%	11,077
WY2011	7,043	6,350	7,721	7,449	1,369	7,141	595	8%	7,621
WY2012	8,982	10,638	8,919	11,464	2,545	10,000	1,259	13%	10,037
WY2013	10,702	10,558	8,907	10,031	1,794	10,049	814	8%	9,001
Period of Record Average	9,158	9,111	8,930	8,992	228	9,047	105	1%	9,258

* Rainfall data from the S7 rainfall station was used in the water budget analyses presented in this report.

Table 39. Differences in rainfall data measured at the S7 rain station and by NEXRAD for Cells 3A and 3B.

	(S7_R-NEXRAD) (ac-ft)		(S7_R-NEXRAD)/S7_R (%)	
	Cell 3A	Cell 3B	Cell 3A	Cell 3B
WY2009	-1,575	-1,147	-18%	-15%
WY2010	-229	-479	-2%	-5%
WY2011	-966	-1,271	-13%	-20%
WY2012	584	601	5%	6%
WY2013	1,401	1,557	11%	15%
Period of Record	-158	-147	-2%	-2%

8 Evapotranspiration

The direct measurement of ET rate, which requires measuring how much water is being transpired by plants on a daily basis in addition to evaporation, is difficult to make. Equations allowing adjustments based on site-specific data are used in estimations. ET is currently considered to be one of the better quantified components in the STA water budgets. DBHYDRO has PREF data for potential ET (ETP), which is defined as evaporation and ET from wetlands and water bodies. The model for ET computation was developed from lysimeter experiments associated with the ENR Project. This model has been published in many peer reviewed journals and books and is applied in several countries. Any additional effort to estimate ET rates for the STA water budgets might not significantly change their accuracy. The STA ET data are derived from a model (the Simple Method) that uses input data from the closest weather station (Abtew 1996). The weather station associated with each STA is given in **Table 40**. As seen from **Figure 26**, S7WX location is closer to the cells under discussion in this report; however, since this data set was discontinued in 2009, ET values from ROTNWX weather station is used in the analyses. Alternatively, satellite-based ET values are also available in the District databases. Satellite-based ET estimation is based on GOES-8 satellite total solar radiation measurement and application of the Priestley-Taylor ET Estimation Model. The method has been applied with the Simple Method giving comparable results (Jacobs et al. 2008).

Table 40. Weather stations used in ET rate estimates for District STAs.

STA	Weather Station
STA-1E	ENR308
STA-1W	ENR308
STA-2	ROTNWX
STA-3/4	ROTNWX
STA-5	STA5WX
STA-6	ROTNWX

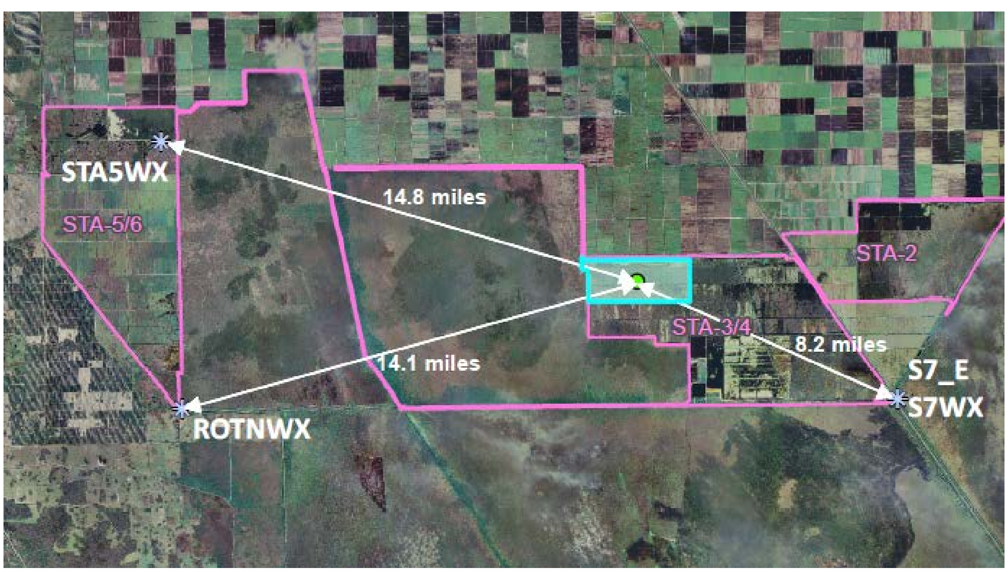

Figure 26. Map of available ET stations in the vicinity of Flow-way 3.

8.1 Spatial Variations

Monthly ET rate estimates from the weather stations in the vicinity of Cells 3A and 3B are shown in **Table 41** and plotted in **Figure 27**. The period of record for availability of data from all three stations is February 2007 to March 2009. Even though the S7 station is closer to Cells 3A and 3B, since the ET data for this site was discontinued in March 2009, data from the Rotenberger weather station was used in the water budgets developed in this report. For the overlapping record length shown in **Table 41**, the annual ET rate estimates from these two stations differ by 4%, indicating ET rate does not show a significant spatial variation assuming data quality is similar. The difference in the estimated ET rates would be lower if the comparison period were longer.

Table 41. Variation in ET rate estimates from different weather stations.

Station:	ROTNWX	S7WX	STA5WX
Date	ETP (inches)	ETP (inches)	ETP (inches)
February 2007	3.38	3.25	3.29
March 2007	4.91	4.79	4.87
April 2007	5.73	5.44	5.64
May 2007	5.42	5.30	5.42
June 2007	5.27	4.83	5.02
July 2007	5.04	4.62	4.95
August 2007	5.20	5.04	4.83
September 2007	4.30	4.27	4.14
October 2007	3.75	3.68	3.77
November 2007	3.53	3.51	3.37
December 2007	3.26	3.18	2.96
January 2008	3.34	3.24	3.30
February 2008	3.79	3.55	3.59
March 2008	4.69	4.45	4.56
April 2008	5.52	5.42	5.54
May 2008	6.06	5.91	5.93
June 2008	5.02	4.71	5.09
July 2008	4.89	4.87	5.21
August 2008	4.58	4.40	4.62
September 2008	4.49	4.33	4.50
October 2008	4.15	4.03	4.16
November 2008	3.90	3.71	3.90
December 2008	3.27	3.15	3.24
January 2009	3.56	3.53	3.31
February 2009	4.16	3.97	3.79
March 2009	3.31	3.29	3.32
Annual ET	53.52	51.62	52.61
Difference from ROTNWX	0%	-4%	-2%

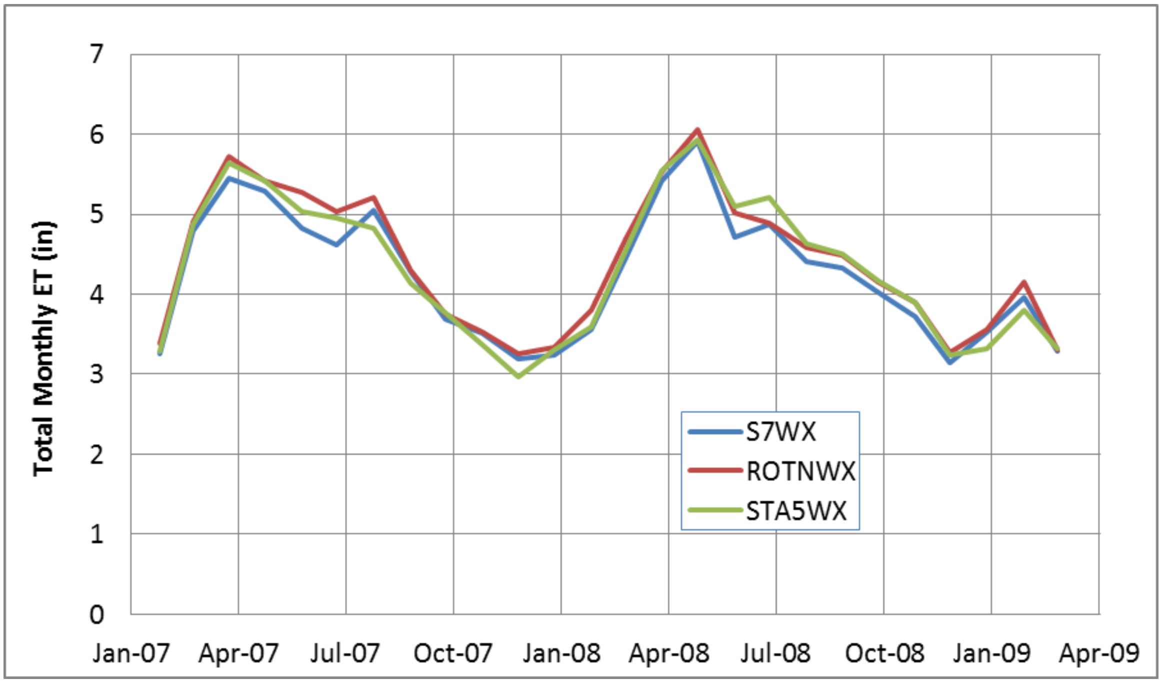

Figure 27. Comparison of monthly ET measurements at weather stations in the vicinity of STA-3/4 Cell 3A.

8.2 Comparison of Evapotranspiration Estimation Methods

Figure 28 depicts monthly ET over STA-3/4 Cell 3A as estimated using the ET data from DBHYDRO and by averaging satellite-based ET estimates for three cells covering Cell 3A (**Figure 25**) for the period of 2008 to 2011. Monthly mean ET is estimated as 4.53 and 4.56 inches for the two methods, respectively. As shown in **Figure 28**, seasonal variation exists in the monthly ET data both from ROTNWX station and satellite-based data. The range and spread of the satellite-based method is higher. However, as summarized in **Tables 41** and **42**, the differences in the average annual volumes and ET rates from these two sources are negligibly small (less than 1%). Therefore, no changes are needed to improve the ET component of STA water budgets.

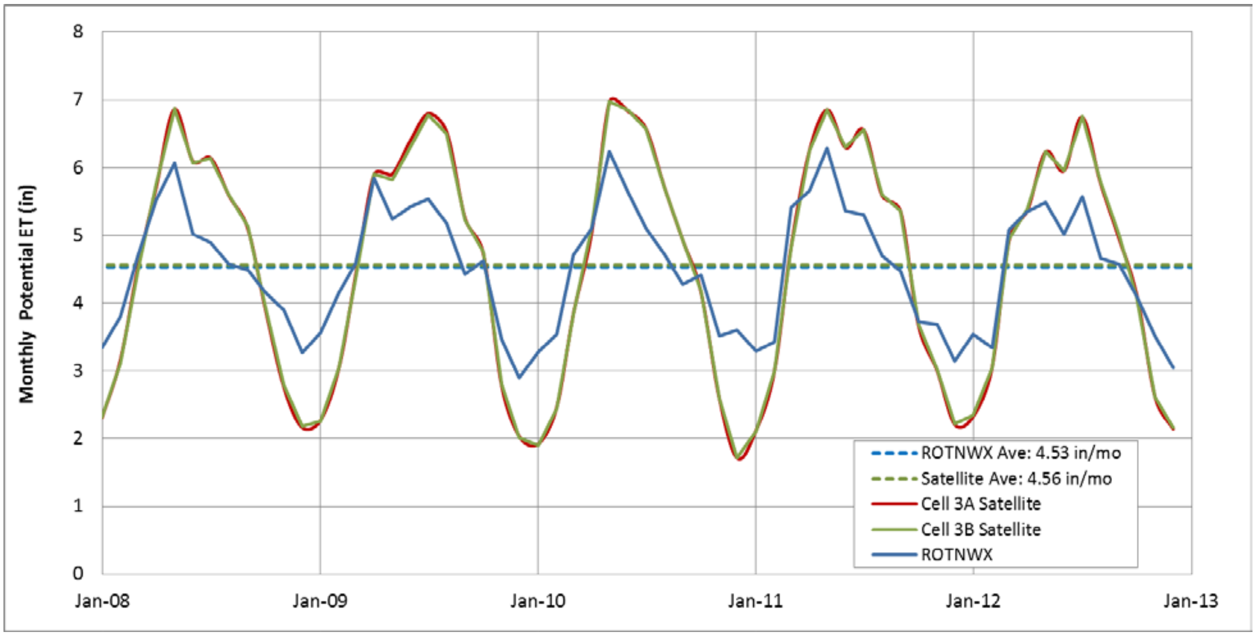

Figure 28. Comparison of monthly ET over STA-3/4 Cells 3A and 3B with DBHYDRO ET and satellite-based ET data for January 2008 to December 2012.

Table 41. Variations in annual ET volumes from ROTNWX and satellite based data for Cell 3A (2,415 acres).

Station:	ROTNWX	Satellite
DBKEY/Pixel:	RW486	Weighted Average of 3 Pixels
Water Year	ac-ft	ac-ft
WY2009	10,969	10,908
WY2010	10,747	10,796
WY2011	11,124	11,193
WY2012	10,870	11,105
Period of Record Mean (ac-ft/yr)	10,928	11,001
Period of Record Mean (inches/year)	54.31	54.68
Annual ET Difference	0.7%	

Table 42. Variations in annual ET volumes from ROTNWX and satellite-based data for Cell 3B (2,087 acres).

Station:	ROTNWX	Satellite
DBKEY/Pixel:	RW486	Weighted average of 3 pixels
Water Year	ac-ft	ac-ft
WY2009	9,480	9,434
WY2010	9,287	9,303
WY2011	9,614	9,684
WY2012	9,394	9,619
Period of Record Mean (ac-ft/yr)	9,443	9,510
Period of Record Mean (inches/year)	54.31	54.67
Annual ET Difference	0.7%	

8.3 Relative Magnitude of Rainfall and ET in STA Water Budgets

It is important to evaluate the relative magnitude of each water budget parameter to evaluate the effort to improve data quality and the benefit of reducing water budget errors. As stated earlier, the relative contribution of rainfall and ET to the STA water budget is expected to be smaller than those of surface water components (Abtew et al. in prep). To show the ranges of magnitudes of rainfall and ET in the STA water budget, an analysis was performed with expected ranges of rainfall and ET and actual historical data. **Figure 29a** indicates the percent contribution of range of rainfall and ET to each STA water budget with a reference of expected annual inflows to each STA as shown in the operation plans. Annual average, 90% and 110% of rainfall and ET were used to demonstrate average, dry and wet conditions. The percentage varies from STA to STA based on operational hydraulic loading and rainfall and ET variation in each STA. Ranges vary from 9% to 19%. **Figure 29b** shows the actual percentage of contributions by rainfall and ET in water budgets of each STA for several years when compared to actual inflow. Ranges vary from 3% to 32%. Rainfall and ET have a higher percentage contribution to the water budget during low inflow years, and a lower percentage contribution during high inflow years.

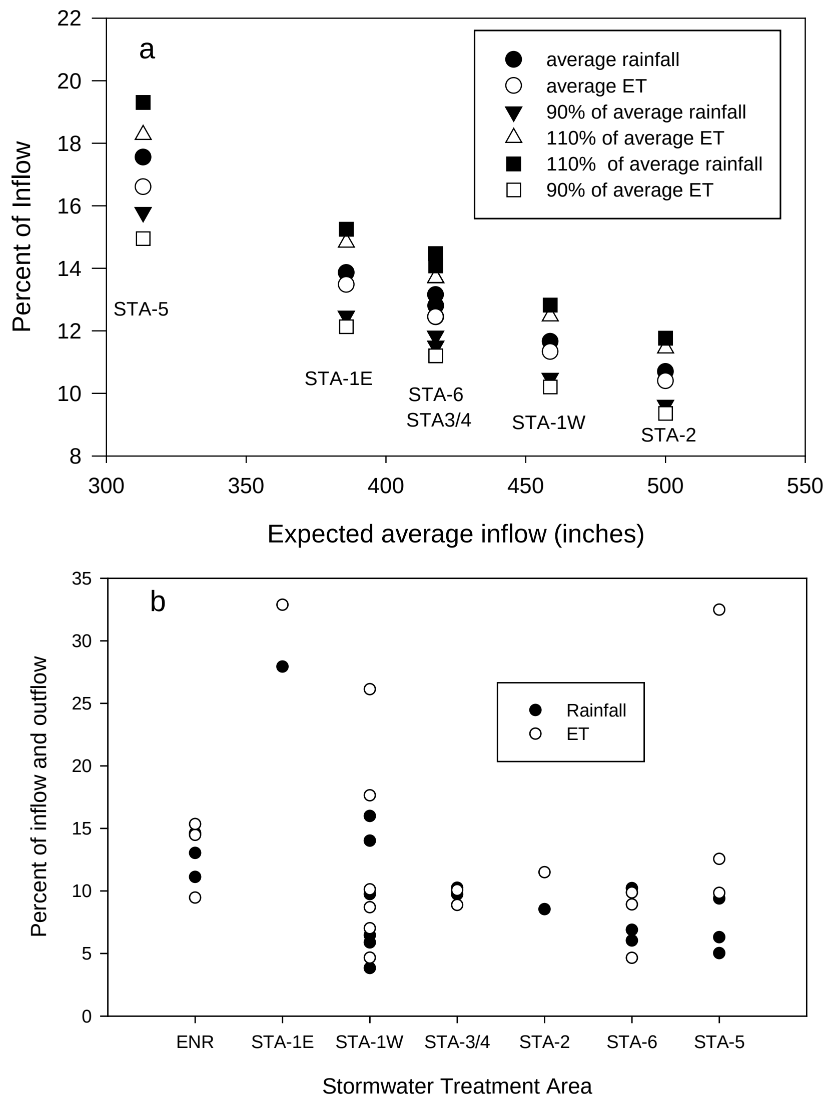

Figure 29. Rainfall and ET as percentage of inflow a) expected average inflow and b) historical inflows.

9 Change in Storage

Storage in an STA is computed as the product of average water depth and surface area. Surface areas of the treatment cells vary with flow depth, especially when the flow depth is very low. This is particularly an issue in treatment cells with high variability in the bottom elevation. Flow depth is calculated from a few water surface elevations and the average ground elevation based on field survey measurements. Depending on irregularities in the cell floor, water depth estimation error could be high. Subsurface storage may change during dry-outs, for which it is not easy to account. The presence of dense vegetation in wetlands, although commonly not factored in storage calculation, will influence the precision of the storage calculation. The volume occupied by vegetation is assumed negligible because it is difficult to measure (Kadlec and Wallace 2009). The "change in storage" component of the STA water budgets is an estimate of change in the volume of water retained in the STA between start and end of the considered time step. There are several assumptions in estimating change in storage:

1. Wetland bottom is smooth and floor elevation is well measured.
2. Depth measurements at inflow and outflow represent water depth in a cell.
3. Stage-area and stage-volume relationships are linear.
4. Volume occupied by vegetation is negligible.

If seepage can be estimated with an acceptable accuracy, change in storage can be derived from the water budget equation. Errors that can be introduced by inaccurate wetland depth estimations of 0.1, 0.2, 0.3 and 0.4 ft for each STA are provided in **Figure 30**. In general, change in storage is expected to be a small percentage of the annual water budget. Site-specific conditions need to be considered when selecting the stage data to be used in storage volume computation. Stage monitoring at internal locations or numerical modeling could reduce the uncertainties introduced by storage computations.

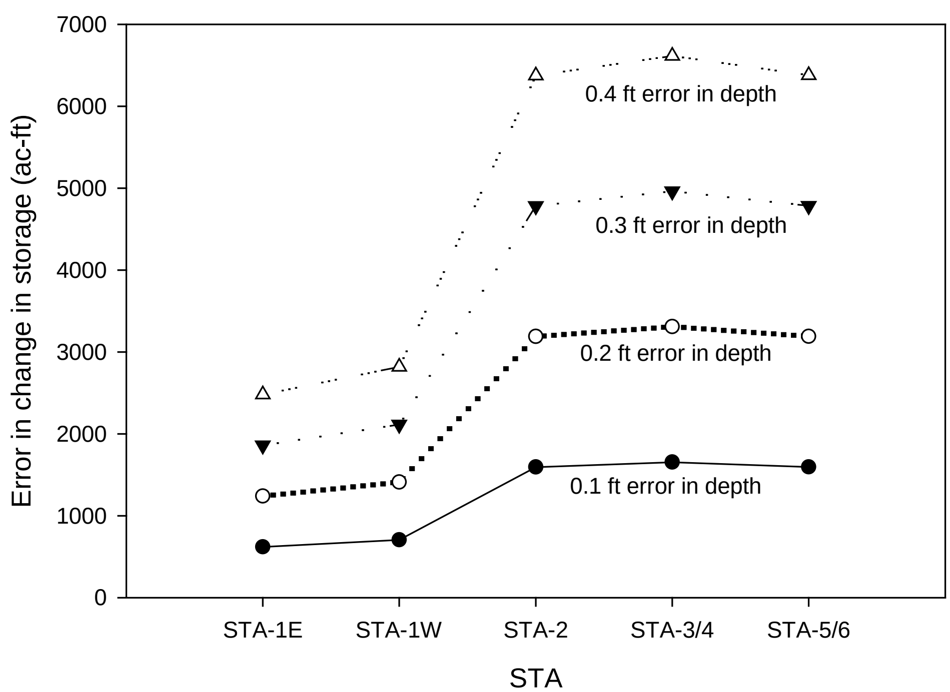

Figure 30. Errors in change in storage due to depth estimation errors of 0.1, 0.2, 0.3 and 0.4 ft.

10 STA Water Budget Uncertainty Analysis

The development of water budgets involves uncertainties and results in residual errors. Observed residual errors may vary dramatically seasonally and from one wetland to another. In addition to the errors involved in the measurement or estimation of water budget components, varying time and spatial scale of the processes considered in water budget analysis also introduce errors. Furthermore, selection of the time step and length of period of record for the analysis significantly affects the relative contribution and uncertainties introduced by each component. This study focuses on annual water budgets, based on mean daily estimates of contributing components. The period of record starting from WY2009 is considered in the analyses. If the uncertainties in the components of the water budget are known, first order Taylor series approximation to the variance can be used to propagate these uncertainties to estimate uncertainties in water budget residuals.

The true value of any measurement is not known as there are always uncertainties in measurements. Uncertainty is the quantified expectation for dispersion and unknowns of a measurement. Uncertainties in the measured quantities are divided into two categories: systematic and random. Random errors, non-repeatable inaccuracies caused by unknown or uncontrollable factors, can be expressed as the dispersion of repeated observations. If identified, systematic errors need to be corrected instead of being propagated through data reduction equations. Identifying the systematic and random uncertainties in the components of water budget is not straightforward. When it is difficult or impossible to identify uncertainties, an estimate based on scientific and engineering judgment can be used. Estimated spatial or temporal variations in the observed values, or deviations from a standard measurement method can be used as a basis for uncertainty estimation. Historical averages and associated standard deviations estimated in the previous sections can be used to analyze uncertainties, and identify their relative contributions to the residual errors.

10.1 Flow Rate Uncertainty Analysis

Quantifying uncertainties in flow rate estimates is not straightforward. Even though widely accepted statistical/mathematical tools to address uncertainties are available, use of scientific judgment is the backbone of uncertainty analysis. Some rough guidelines providing wide brackets for expected uncertainties in measurement are available for a range of flow measurement devices. Flow rate accuracy requirement for gated culverts flowing under full pipe flow condition is determined as ±10–15% by Gonzalez and Damisse (2008) for typical flow ranges, which can be used in the absence of case-specific uncertainty information. HDM staff has been developing a strategy to account for the uncertainties introduced during rating development and by the stage and operations data used in computation of instantaneous flow rates (Polatel et al. in prep). Once estimated, the total uncertainty limits of the computed flows provide the most rigorous indicator of uncertainty in computed flow data.

Once the flow equation is determined, the uncertainties in stage, gate opening, structure geometry, and rating parameters can be propagated to estimate the flow rate uncertainties. The flow equation currently used by the District to estimate flow rates through culverts flowing full is

$$Q_c = C_d A_o \sqrt{\frac{2g\Delta h}{\left(\frac{A_o}{A_G}\right)^2 + 2{C_d}^2\left(1 - \frac{A_o}{A_G} + \frac{gn^2L}{(1.49)^2 {R_o}^{4/3}}\right)}} \qquad \text{5 (repeated)}$$

where Q_c is the computed flow rate (cfs), C_d is the discharge coefficient, $A_o = BD$ is the full barrel cross-sectional area (square feet [ft^2]), B is barrel width (ft), D is barrel depth (ft), $A_G = GB$ is the area under the gate (ft^2), G is the gate opening (ft), $\Delta h = HW - TW$ is the difference between headwater (HW) and tailwater (TW) stages (ft), L is the length of barrel (ft), $R_o = \frac{BD}{2(B+D)}$ is the full barrel hydraulic radius (ft), and n is the Manning's roughness coefficient (Wilsnack et al. 2010). To improve the accuracy of the flow rate estimates, field flow measurements can be used for calibration by fitting the model given in **Equation 5** by optimizing the parameters in the equation. If the Manning's roughness coefficient is assumed constant, the only rating parameter to be calibrated in the equation is the discharge coefficient C_d. All variables of the flow equation are subject to uncertainties. Static variables (B, D, L and n), dynamic variables (Δh and G), rating parameter C_d, and the equation model itself introduce uncertainties that propagate to the computed flow rates. When the flow data from culverts flowing under low head differentials are used in water budget analyses, major contribution to the uncertainties are expected to come from surface water components. Under these conditions, even though rating model and coefficients introduce uncertainties, the main source of error in estimated flows is the low head differentials.

10.1.1 Law of Propagation of Uncertainty

The standard uncertainty of the measurement result y, designated $u(y)$ and taken to represent the estimated standard deviation of the result, is the positive square root of the estimated variance $u^2(y)$ obtained from

$$u^2(y) = \sum_{i=1}^{N} \left(\frac{\partial f}{\partial x_i}\right)^2 u^2(x_i) + \sum_{i=1}^{N-1} \sum_{j=i+1}^{N} \frac{\partial f}{\partial x_i} \frac{\partial f}{\partial x_j} u\left(x_i, x_j\right) \qquad 24$$

where the output estimate y is obtained by using N input estimates $x_1, x_2, \ldots, x_N$ through the functional relation f as $y = f\ (x_1, x_2, \ldots, x_N\ )$. **Equation 24** is based on first-order Taylor series approximation and is referred to as the *Law of Propagation of Uncertainty* (Taylor 1997). The partial derivatives $\partial f / \partial x_i$ are often referred to as *sensitivity coefficients*, $u(x_i)$ is the standard uncertainty associated with the input estimate x_i, and $u\left(x_i, x_j\right)$ is the estimated covariance associated with x_i and x_j.

10.1.2 Propagation of Uncertainty for Culverts Flowing Full

Once the flow equation is determined and the standard uncertainties of input quantities are decided, the uncertainties can be propagated using **Equation 24**. Flow rate through culverts is not measured directly, but is determined from other quantities through a functional relation f

$$Q = f\ (L, B, D, n\ , C_D, G, \Delta h\ ) \qquad 25$$

which can be approximated by the flow equation given in **Equation 5** for culverts flowing full. Inserting the flow equation into the uncertainty propagation equation given in **Equation 24**, the flow rate uncertainty equation for culverts flowing full can be written as

$$u(Q) = \sqrt{\left(\frac{\partial Q}{\partial L}\right)^2 u_L^2 + \left(\frac{\partial Q}{\partial B}\right)^2 u_B^2 + \left(\frac{\partial Q}{\partial D}\right)^2 u_D^2 + \left(\frac{\partial Q}{\partial n}\right)^2 u_n^2 + \left(\frac{\partial Q}{\partial C_d}\right)^2 u_{C_d}^2 + \left(\frac{\partial Q}{\partial G}\right) u_G{}^2 + \left(\frac{\partial Q}{\partial \Delta h}\right)^2 u_{\Delta h}^2} \quad 26$$

The expanded forms of the sensitivity coefficients, as the partial derivatives shown in **Equation 26**, are given in Polatel et al. (in prep) and not included here for brevity. Once the standard uncertainty $u(Q)$ is estimated, the expanded uncertainty can be estimated using a coverage factor corresponding to 95% CL

$$U(Q) = k\, u(Q) \quad 27$$

For given culvert properties (B, D, L and n) and rating coefficient (C_d), $u(Q)$ and $U(Q)$ can be computed as a function of dynamic variables (G and Δh). With changing operating head (Δh), the effect of other input quantities on flow uncertainty change as Δh appears in all sensitivity coefficients. However, as Polatel et al. (in prep) showed, effect of Δh increases exponentially with decreasing Δh for its very low values. For very low operating heads, its contribution becomes so large that the variations in the culvert properties, rating coefficient and gate opening become relatively insignificant.

The analysis presented above was applied to mid-levee (G-384) flows for WY2009–WY2012 period, before any corrections to historical flow rates were applied. The uncertainties in instantaneous flow rates were estimated by propagating the uncertainties in elemental input variables, rating coefficients, and structure geometry by First Order Taylor Series Approximation method, and then the uncertainties in time-averaged flow rates were computed while accounting for correlations (see Nayak et al. 2012 for more details on algorithm used). A histogram of the computed mean daily flow rate uncertainties at G-384 structure is shown in **Figure 31** indicating high uncertainties.

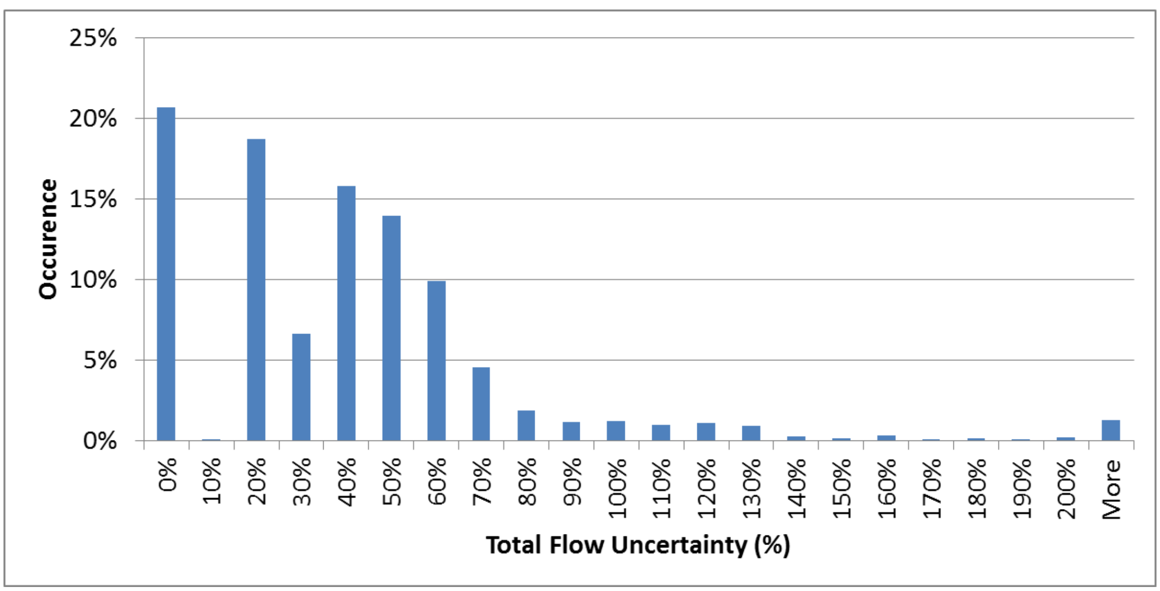

Figure 31. Histogram of percent uncertainties in G-384 daily flow rates before corrections were applied.

10.2 Managing Flow Rate Uncertainty for Culverts Flowing Full

A generalized flow uncertainty equation for culverts is not possible due to variations in geometry and hydraulic properties in the field. However, considering the dominant effect of head differential on flow uncertainty for very low values, a general behavior can be identified to be used as a guide in determination of desirable operating conditions. To investigate the presence of such general behavior, two fictitious culverts were chosen as shown in **Table 43** to represents the range of typical culvert geometries in District STAs. In the table, Culverts C1 and C2 represent the upper and lower limits of STA culvert sizes, respectively.

The standard uncertainties in the static and dynamic variables shown in **Table 43** are estimated using the published reports and standards, considering random errors negligible. The standard error of the rating parameter C_d is site-specific and may change significantly from location to location. It must be noted that the standard uncertainty for the C_d reported in **Table 43** is based on limited number of culverts analyzed as a part of HDM's Flow Rate Uncertainty Analysis Project, and should be considered provisional; it is expected to be modified as more data become available.

Table 43. Input variables and their uncertainties for culverts flowing full.

Symbol:	*L* (ft)	*B* (ft)	*D* (ft)	*n*	C_d	*G* (ft)	Δh (ft)
Culvert 1 (C1) Large, Smooth, Short	30	10	10	0.012	0.85	Variable	Variable
Culvert 2 (C2) Small, Rough, Long	100	5	5	0.024	0.70	Variable	Variable
Standard Uncertainty $u(x_i)$	0.0082	0.0082	0.0082	0.0008*	0.005*	0.0289	0.0115

* Uncertainties in n and C_d can vary significantly from culvert to culvert. The results should be interpreted with caution because of the limited sample size used in estimation of these numbers.

Using the flow rate uncertainty equation given in **Equation 26**, variation of relative flow rate uncertainty ($U(Q)/Q$) with operating head Δh and gate opening G_o can be obtained for given culvert properties. For Culverts C1 and C2, the variation of relative flow rate uncertainty with operating head for fully open gates is plotted in **Figure 32**. Considering C1 and C2 are representing limiting culvert sizes, variation of relative flow uncertainty with operating head for fully open gates is expected to fall between the C1, G=10 ft and C2, G=5 ft curves for most of the STA culverts. As expected, the curves in **Figure 32** follow each other closely for low head differentials, with no significant disagreement for Δh < 0.1 ft. Considering the dominant effect of head differential on flow uncertainty for its low values, some generalization based on **Figure 32** is possible. The figure can be used to estimate threshold head differential that should trigger the lowering the gate opening for a desired relative flow rate uncertainty. For example, for fully open gates with given culvert properties, a relative flow rate uncertainty of 10% can be achieved only when the head difference is 0.12 ft or higher. In **Table 44**, minimum operating head for 10%, 15%, 20%, 25% and 30% flow rate uncertainties for fully open gate conditions are provided. The minimum Δh values shown in the table are the threshold values that should trigger the lowering of the gate openings. It must be noted that the minimum head differentials shown in **Table 44** are for fully open gates, and they will not be sufficient to ensure the shown flow rate uncertainties for lower gate openings.

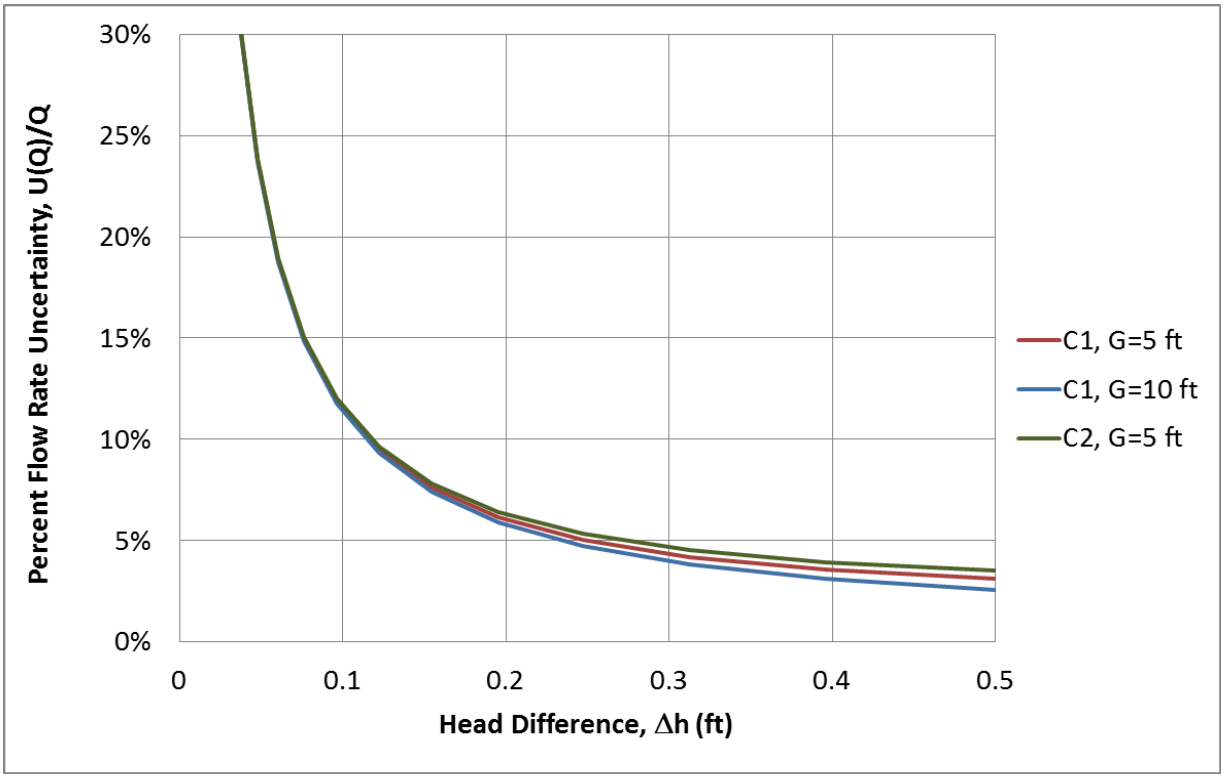

Figure 32. Comparison of variation of relative flow rate uncertainty with operating head Δh for fully open gates and G_o= 5 ft for culvert 1 (C1).

Table 44. Threshold operating head ($\boldsymbol{\Delta h}$) for various relative flow uncertainties for fully open gates.

Desired $U(Q)/Q$ (%)	10%	15%	20%	25%	30%
Min Δh (ft)	0.12	0.08	0.06	0.05	0.04

For gate openings lower than fully open, a parametric flow rate uncertainty equation can be derived, which can be used to back-calculate sets of gate opening and operating head conditions required to maintain flow rate uncertainty below a desired value as shown in **Figure 33**. The relationships between the flow uncertainty and the dynamic variables given in **Equation 26** can be converted to a different form to facilitate management of flow uncertainty through control operations. To construct this practical form, a range of (Δh, G) pairs were calculated for varying target total uncertainties. Required gate openings for a range of head differentials are back calculated for select target flow rate uncertainties. In **Figure 33**, calculated (Δh, G) pairs are plotted for 5%, 10% and 15% uncertainties in estimated flow rates for culverts C1 and C2. **Figure 33** can be used to estimate the minimum head differential and/or gate opening required to maintain the flow rate uncertainty below a desired value. By relating flow uncertainty to easy-to-control variables, these curves enable the conversion of uncertainty analysis results to a practical form that can be used to control the uncertainties in the estimated flow rates.

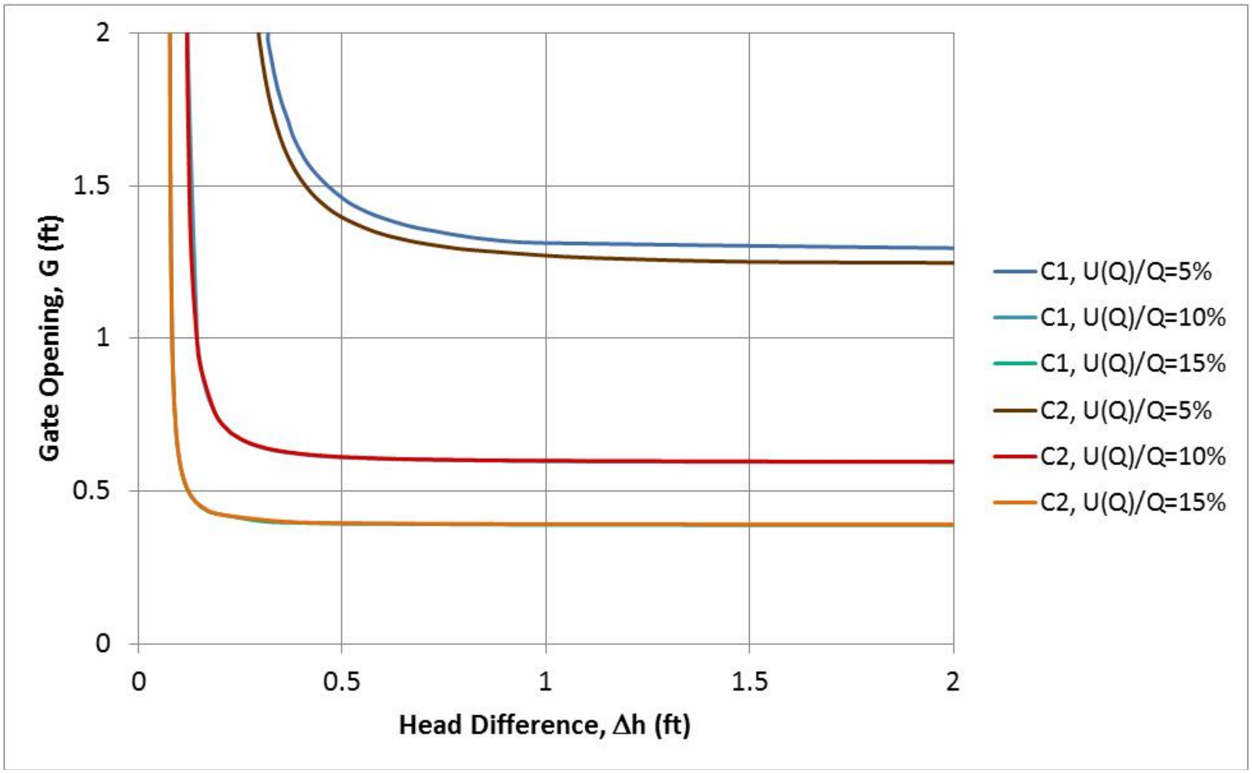

Figure 33. Flow rate uncertainty curves for culverts 1 and 2 (C1 and C2).

The results shown in this section should be regarded as general information since elemental standard uncertainties used in the computations are based on the limited number of culverts analyzed as a part of Flow Rate Uncertainty Analysis Project. A site-specific analysis, using specific culvert geometry and collected field data, is needed for a more robust analysis. The results shown should be taken as a guideline while site-specific uncertainty curves are being developed. Note that plotted curve in **Figures 32** and **33** are only for the culverts operating under full-pipe flow condition. The effect of geometry and calibration process may be more dominant for other structures, rendering development of a general behavior impossible.

10.3 Propagation of Uncertainties to the Water Budget Residual

As mentioned in the previous sections, there are many sources of error and uncertainties in the STA water budgets. Uncertainties cannot be eliminated, but can be reduced by changing measurement methods and/or protocols. In general, however, the lower the error in the measured value the higher the cost of measurements. In addition to the operational requirements, methods followed in measurement of STA water budget components are typically constrained by the availability of the resources. Any attempt at reducing the STA water budgets needs specification of how much error is acceptable for the intended purpose. If the uncertainties in the components are known, expected uncertainty in the water budget residual can be estimated by using the error propagation equation discussed in Section 10.1.2.

For a given time period water budget residual can be written as

$$r = Q_{out} + Q_g + ET - Q_{in} - R + \Delta S \qquad \text{2 (repeated)}$$

where r is the residual, Q_{out} is the surface outflow, Q_g is the seepage flow lost from the STA, ET is the evapotranspiration, Q_{in} is the surface inflow, R is the precipitation, and ΔS is the change in storage. Using the error propagation equation given in **Equation 24**, assuming no correlation between the uncertainties of the components, the uncertainties in the water budget residual can be written as

$$u(r) = \sqrt{\left(\frac{\partial r}{\partial Q_{out}}\right)^2 u_{Q_{out}}^2 + \left(\frac{\partial r}{\partial Q_g}\right)^2 u_{Q_g}^2 + \left(\frac{\partial r}{\partial ET}\right)^2 u_{ET}^2 + \left(\frac{\partial r}{\partial Q_{in}}\right)^2 u_{Q_{in}}^2 + \left(\frac{\partial r}{\partial R}\right)^2 u_R^2 + \left(\frac{\partial r}{\partial \Delta S}\right)^2 u_{\Delta S}^2} \qquad 28$$

Considering all sensitivity coefficients in **Equation 28** have an absolute value of 1 ($\partial r/(\partial x_i) = 1$), standard uncertainty in the water budget residual can be rewritten as

$$u(r) = \sqrt{u_{Q_{out}}^2 + u_{Q_g}^2 + u_{ET}^2 + u_{Q_{in}}^2 + u_R^2 + u_{\Delta S}^2} \qquad 29$$

The components of water budgets (i.e., surface water flows, seepage, ET, rainfall and change in storage) include uncertainties from various sources including the temporal and spatial resolutions of the observations, limitations of measuring instrument and method, calibration and data reduction, and installation and maintenance of the measurement devices. Quantifying the uncertainties in the water budget components is not straightforward. When it is difficult or impossible to calculate this type of error, an estimate based on scientific and engineering judgment can be used. In the previous sections, average values for expected variations in the components of the water budget were provided as some percentage of each component. Using the results of the analyses presented in the previous sections, approximate uncertainties in each water budget component can be summarized as shown in **Table 45** as the percent value of the measured/estimated value. Higher errors were assigned to surface water flow estimates at mid-levee structures compared to those of flow-way inflow and outflow structures.

Table 45. Approximate uncertainties in water budget component estimates for 1 water year.

	$u_{Q_{in}}$	u_R	u_{Q_g}	$u_{Q_{out}}$	u_{ET}	$u_{\Delta S}$
Cell 3A	10% Q_{in}	9% R	100% Q_g	15% Q_{out}	1% ET	0% ΔS
Cell 3B	15% Q_{in}	9% R	100% Q_g	10% Q_{out}	1% ET	0% ΔS
Cell 3	10% Q_{in}	9% R	100% Q_g	10% Q_{out}	1% ET	0% ΔS
Typical STA cell	10% Q_{in}	9% R	100% Q_g	10% Q_{out}	1% ET	0% ΔS

As reviewed in Section 3, error in the water budgets is estimated by dividing the residuals by the average of the total inflow and outflow volumetric rates as

$$\varepsilon = \frac{r}{(\sum Out + \sum In)/2} \times 100 \qquad 3 \text{ (repeated)}$$

where ε is the percent error in water budget, $\sum Out = Q_{out} + Q_g + ET$, and $\sum In = Q_{in} + R$. To quantify the contribution of each component, the magnitude of each component can be expressed relative to the average of outflow and inflow volumes as shown in **Table 46**. Inserting the values in **Table 46** into **Table 45**, uncertainties in the components as a function of $(\sum Out + \sum In)/2$ will be obtained. Using **Equation 29** for each row of **Table 45**, the expected uncertainties in the water budget residuals can be estimated as shown in **Table 47**. The table also includes the expected uncertainties for 4, 5, 10, 15 and 20 year long period of records. The contribution from each component to the uncertainties in the water budget residual is provided in **Table 48**. As expected, contributions from surface water flows decrease as the cells get larger. In the presented uncertainty analysis, all uncertainties were treated as total uncertainties. The expected residual error for the considered cells was 17% or less for any given water year and 9% or less for a 4-year period of record. More detailed uncertainty analysis is recommended for future studies.

Table 46. Sizes of water budget components relative to $(\sum \boldsymbol{Out} + \sum \boldsymbol{In})/\mathbf{2}$.

Component:	Q_{in}	R	Q_g	Q_{out}	ET	ΔS
Cell 3A	93%	6%	5%	90%	6%	0%
Cell 3B	94%	5%	3%	92%	6%	0%
Cell 3	88%	11%	7%	84%	11%	0%
Typical STA cell	90%	10%	5%	85%	10%	0%

Table 47. Approximate uncertainties in water budget residuals for various length of record.

			$\boldsymbol{u}(\boldsymbol{r})/[(\sum Out + \sum In)/2]$			
Period of Record Length:	1 year	4 year	5 year	10 year	15 year	20 year
Cell 3A	17%	9%	8%	5%	4%	4%
Cell 3B	17%	9%	8%	5%	4%	4%
Cell 3	14%	7%	6%	4%	4%	3%
Typical STA cell	13%	7%	6%	4%	3%	3%

Table 48. Contribution of water budget components to residual uncertainty.

Component:	Q_{in}	R	Q_g	Q_{out}	ET	ΔS
Cell 3A	29%	0%	9%	62%	0%	0%
Cell 3B	68%	0%	3%	29%	0%	0%
Cell 3	38%	0%	27%	35%	0%	0%
Typical STA cell	45%	1%	14%	40%	0%	0%

Considering the larger contribution of surface flows in the water budget, lower errors can be expected if inflow and outflows are well monitored as the relative sizes of the remaining parameters are smaller. Depending on the site characteristics such as soils, levee construction, depth and water level difference with surroundings, vertical and lateral seepage can be a sizeable factor in accuracy of water budgets. Seepage collection and recirculation may minimize the effect of seepage on water budget. Rainfall and ET contribute relatively small percentage of the annual water budget. Change in storage is expected to be a smaller percentage of the annual water budget. For larger cells, the contribution from seepage, rainfall and ET are expected to be higher.

11 Key Findings and Improved Water Budgets

Each component of the STA water budgets was reviewed in dedicated sections of this report. Available methods were compared, and an evaluation of expected variations in the estimates was provided. The key findings of this study that would benefit future water budget improvement efforts are as follows:

- Surface water flows are generally the largest component of the STA water budgets and the largest source of uncertainty in the residuals. Methods to reduce or eliminate errors in their estimation should be effected to the extent feasible. The errors in stage data used in flow computation should be minimized.
- Seepage estimation can contribute significantly to the water budget residual. When field data is not available, historical no flow/no rainfall periods can be investigated to develop seepage estimates.
- An uncertainty analysis of each inflow and outflow component and an estimate for an acceptable residual error should accompany water budget improvement efforts.

During the preparation of this report a conclusive comparison of rain gauge and radar rainfall, for use in providing a recommendation on which one more closely relates to actual rainfall over the region, was not found. The recommended methods to estimate the water budget components and the associated uncertainties for Cells 3A and 3B are summarized in **Table 49**.

Table 49. Summary of recommendations for Cells 3A and 3B water budget components.

Component	Recommended Method	Estimated/Assumed Uncertainty in Annual Volumes
Flow-way inflows	Rating equation – Data published in DBHYDRO	10%
Flow-way outflows	Rating equation – Data published in DBHYDRO	10%
Mid-levee flows	Back calculation based on residual redistribution (Method 2)	15%
Seepage	Darcy's law with conductivities estimated from historical no flow/no rainfall periods	100%
Rainfall	Rain gauge readings	9%
ET	Measurements at weather stations	1%
Change in storage	Product of cell areas and average of daily downstream and upstream stages	0%

Improved water budgets provided in **Tables 50** through **52** use the mid-levee flows estimated by the back calculation method based on redistributing flow-way residuals to the cells (Method 2), ET rate estimates from the Rotenberger weather station, and rainfall from the S-7 rain station. Seepage estimates based on effective conductivities found during dry periods are used in the tables. The mid-levee flows (G-384s) used in the tables are provisional and are subject to revision. The presented water budgets will be revisited after G-384 flows are finalized in the second phase of the study.

Table 50. Improved Cell 3A water budget (**Table 10** repeated).

	Q_{in}	Rainfall, R	Seepage, Q_g	Q_{out} (Q_{mid})	ET	ΔS	ΣIn	ΣOut	Residual, r	Residual Error, ε
	ac-ft/yr	ac-ft/yr	ac-ft/yr	ac-ft/yr	ac-ft/yr	ac-ft/yr	ac-ft/yr	ac-ft/yr	ac-ft/yr	%
WY2009	168,618	8,573	9,112	146,764	10,969	-2,271	177,192	166,846	-12,617	-7%
WY2010	219,142	12,264	8,296	224,515	10,747	3,418	231,406	243,558	15,571	7%
WY2011	112,635	7,348	7,668	114,208	11,124	-3,187	119,982	133,000	9,831	8%
WY2012	123,384	12,310	9,956	119,732	10,870	3,057	135,694	140,558	7,922	6%
WY2013	196,068	12,218	9,507	186,134	10,798	-1,392	208,286	206,439	-3,240	-2%
Period of Record	819,846	52,713	44,539	791,353	54,508	-374	872,560	890,401	17,467	2%

Table 51. Improved Cell 3B water budget (**Table 11** repeated).

	Q_{in} (Q_{mid})	Rainfall, R	Seepage, Q_g	Q_{out}	ET	ΔS	ΣIn	ΣOut	Residual, r	Residual Error, ε
	ac-ft/yr	ac-ft/yr	ac-ft/yr	ac-ft/yr	ac-ft/yr	ac-ft/yr	ac-ft/yr	ac-ft/yr	ac-ft/yr	%
WY2009	146,764	7,409	6,272	128,970	9,479	-1,453	154,173	144,722	-10,904	-7%
WY2010	224,515	10,598	4,663	233,433	9,287	1,186	235,114	247,383	13,456	6%
WY2011	114,208	6,350	4,074	117,084	9,614	-1,719	120,558	130,772	8,496	7%
WY2012	119,732	10,638	5,873	119,642	9,394	2,308	130,371	134,908	6,846	5%
WY2013	186,134	10,558	3,544	182,107	9,331	-1,089	196,692	194,982	-2,800	-1%
Period of Record	791,353	45,554	24,426	781,237	47,105	-766	836,907	852,768	15,094	2%

Table 52. Improved Flow-way 3 water budget (**Table 12** repeated).

	Q_{in}	Rainfall, R	Seepage, Q_g	Q_{out}	ET	ΔS	ΣIn	ΣOut	Residual, r	Residual Error, ε
	ac-ft/yr	ac-ft/yr	ac-ft/yr	ac-ft/yr	ac-ft/yr	ac-ft/yr	ac-ft/yr	ac-ft/yr	ac-ft/yr	%
WY2009	168,618	15,982	15,385	128,970	20,448	-3,724	184,600	164,803	-23,521	-13%
WY2010	219,142	22,863	12,959	233,433	20,034	4,605	242,004	266,426	29,027	11%
WY2011	112,635	13,697	11,742	117,084	20,738	-4,905	126,332	149,564	18,327	13%
WY2012	123,384	22,949	15,829	119,642	20,264	5,366	146,332	155,734	14,768	10%
WY2013	196,068	22,776	13,051	182,107	20,129	-2,482	218,845	215,287	-6,040	-3%
Period of Record	819,846	98,267	68,965	781,237	101,613	-1,140	918,114	951,815	32,561	3%

12 Conclusions

Water budget analysis is one of the basic tools used in evaluating treatment performance of STAs; therefore large quantities of unaccounted water hinder the effective evaluation of STA performance. This report was prepared to evaluate the methods used in estimation of water budget components and investigate the source of errors in the data, recommend solutions to correct for identified errors, and provide recommendations to help reduce the errors in water budget for Cells 3A and 3B of STA-3/4. Phase II of the study will extend the presented analysis to other cells of STA-3/4 and STA-2, and will consider phosphorus budgets.

In this report, currently used and alternative methods to estimate the components of the water budgets were reviewed for potential improvements. The spatial and temporal variability of rainfall and ET data, and the differences in data from various sources were investigated. A comparison of NEXRAD and rain gauge data found a notable difference in the rainfall estimates by these two methods. It is currently not possible to determine which data set is superior; therefore, it is recommended that STA water budget analyses continue using rain gauges when available with NEXRAD data used to fill gaps. The results of ongoing efforts (external to this study) to address the question of whether the rain gauge or NEXRAD data better represents the actual volume of rainfall over an area can be applied to future water budget analyses. Satellite and lysimeter-based ET methods were compared. No significant difference in the effect of these two methods on the annual water budgets was found. Updated treatment cell effective areas were used in the analyses. Available methods to estimate seepage were reviewed and applied to Cells 3A and 3B. An impact analysis to quantify the effect of seepage was conducted. The factors affecting the accuracy of change in storage estimates were identified. Data collection and surface water flow computation protocols and procedures were reviewed. Historical stage and flow data were examined for errors. Corrections were applied to stage data for flow-way inflow (G-380) and mid-levee (G-384) structures by HDM Staff. Datum adjustment and sensor calibration corrections were applied to stage data at G-384. Corrections due to a clogged well were applied at G-380. The accuracy of the current flow ratings at the Cells 3A and 3B control structures was reviewed. A CFD-based flow rating equation was developed for G-384A-F culverts.

Low head differentials at internal water control structures were identified as the main source of high errors for the Cells 3A and 3B water budgets. Spurious flow data generated by low head differentials were identified at the G-384 culverts. Three methods to fix the historical flow rate data, one based on data correction and two on back calculation, were applied. The back calculation method (Method 2) that was based on redistribution of Flow-way 3 water budget residuals to the cells was chosen to be used in the improved cell-by-cell water budgets for this report. The mid-levee flows (G-384s) used in this effort are provisional and are subject to revision. The presented water budget analyses will be revisited in Phase II of this study after the G-384 flows are improved.

The review of computation processes indicated that the flow computations for the internal culverts may currently be at the limits of potential accuracy without structural or operational changes. Evaluation of structural and operational means to minimize low head, wide gate opening and low flow events is essential. If additional improvements in flow estimates are required, structural changes such as augmenting internal structures with pumps and retrofitting culvert inlets to install v-notch weirs may be needed. More field measurements at low head conditions are recommended to improve the accuracy of the flow estimates. Considering the sensitivity of the estimated flows to small variations in stage records, conducting periodic structure and stilling well surveys are advised. Use of filtered headwater and tailwater data can also be considered. Changes in data acquisition and analysis, including installation of more than one set of stage sensors for internal structures, changes in the sampling protocols, use of differential head measurements, and periodic inspection and calibrations of the sensors are recommended. Improvements in the data analysis including reporting uncertainty limits or quality indicators for flow data and using PREF DBKEYs for internal structures are also suggested.

An uncertainty analysis was performed to estimate the expected uncertainties in the water budget residuals. Estimated uncertainties and relative sizes of each water budget components were propagated through the water budget equation. The biggest source of uncertainties in the residuals was identified as the surface water flows. Despite constituting a small fraction of water budgets, due to large uncertainties in its estimate, seepage was found to be a major contributor of residual uncertainty. It is expected that future potential efforts of reducing the uncertainties in seepage estimates would help reduce errors in water budgets. During dry periods where surface water inflows and outflows are below average, the effects of smaller water budget components, such as rainfall, ET and change in storage, can be magnified. As a result of the water budget uncertainty analysis, expected residual errors for the considered cells were found to be ±17% or less for any given water year and ±9% or less for a 4-year period of record.

In the second phase of the study, investigation of methods to eliminate and correct for spurious flow rates in the mid-levees will continue. The presented analysis will be expanded to other cells of STA-3/4 and STA-2, and improved phosphorus budgets will also be developed using the improved water budget results. The variables and equations used in the Water Budget Tool will be reviewed and the capability to compute seepage for individual cells will be added.

13 References

Abtew, W. 1996. Evapotranspiration measurements and modeling for three wetland systems in South Florida. *Journal of the American Water Resources Association* 32(3):465-473.

Abtew, W. and V. Ciuca. 2014. Chapter 2: South Florida Hydrology and Water Management. In *2014 South Florida Environmental Report – Volume I*. South Florida Water Management District, West Palm Beach, FL.

Abtew, W., J. Obeysekera and G. Shih. 1993. Spatial analysis for monthly rainfall in South Florida. *Water Resources Bulletin* 29(2):179-188.

Abtew, W., J. Obeysekera and G. Shih. 1995. Spatial variation of daily rainfall and network design. *American Society of Agricultural Engineers* 38(3):843-845.

Abtew, W., T. Piccone, K. Pietro and S.K. Xue. In prep. Hydrologic and Treatment Performance of Constructed Wetlands: The Everglades Stormwater Treatment Areas. In: B. Middleton (ed.). *Encyclopedia of Wetlands: Structure and Function, Volume 1: Wetlands Structure and Function*. Article ID:355202, Chapter ID:62, Springer, New York.

Choi, J. and J.W. Harvey. 2000. Quantifying time-varying groundwater discharge and recharge in wetlands – A comparison of methods in the Florida Everglades. *Wetlands* 20(3):500-511.

Gonzalez, J. and E. Damisse . 2008. SHDM Quality Requirements for Flow at Monitoring Sites Derived from Ratings. Technical Memorandum. South Florida Water Management District. West Palm Beach, FL.

Harvey, J. W., S.L. Krupa and J.M. Krest. 2004. Groundwater recharge and discharge in the central Everglades. *Ground Water* 42(7):1090-1102.

Huebner, R. S., W. Abtew and C. Pathak. 2007. Impact of using radar rainfall data in water budget for South Florida stormwater treatment areas. In K.C. Kabbes (ed.), Proceedings of the World Water and Environmental Resources Congress 2007, American Society of Civil Engineers, May 15–19, 2007, Tampa, FL.

Jacobs, J., J. Mecikalski and S. Paech. 2008. Satellite-based solar radiation, net radiation and potential and reference evapotranspiration estimates over Florida. Technical Report, University of New Hampshire, Department of Civil Engineering, Durham, NH.

Kadlec, R. H., and S.D. Wallace. 2009. *Treatment Wetlands, 2nd Edition*, CRC Press, Boca Raton, FL.

Montgomery Watson Americas, Inc. 1999. STA-3/4 Field Investigations and Seepage Analysis. Lake Worth, FL.

Nayak, A., C. Polatel and E. Damisse 2012. Flow uncertainty evaluation program (FUN): A software tool for evaluating flow rate uncertainty. American Society of Civil Engineers/Environmental & Water Resources Institute 2012 Hydraulic Measurement & Experimental Methods Conference, August 12–15, 2012, Snowbird, UT.

Piccone, T., J. McBryan, H. Zhao and Y. Yan. 2014. Updated Everglades Stormwater Treatment Area Average Ground Elevations, Stage-Area/Stage-Volume Relationships and Effective Treatment Areas. Technical Publication ASB-WQTT-12-002, South Florida Water Management District, West Palm Beach, FL..

Pietro, K. 2013. Appendix 5-2: Water Budgets, Total Phosphorus Budgets and Treatment Performance in STA Treatment Cells and Flow-ways. In *2013 South Florida Environmental Report – Volume I*, South Florida Water Management District, West Palm Beach, FL.

Polatel, C., A. Nayak and E. Damisse. In prep. Integration of flow uncertainty analysis into operational decisions of water control structures: Application to a culvert flowing full. Submitted to *Journal of Hydraulic Engineering*.

Rosenberry, D.O. and J W. LaBaugh. 2008. Field Techniques for Estimating Water Fluxes between Surface Water and Ground Water. Techniques and Methods 4–D2, United States Geological Survey, United States Department of the Interior, Reston, VA.

Sangoyomi, T., A. Nayak, G. Huang and S. Xiao 2011. 2011. Levee Seepage Analysis at Stormwater Treatment Area 3/4. South Florida Water Management District, West Palm Beach, FL.

SFWMD. 2007. Operation Plan Stormwater Treatment Area 3/4. South Florida Water Management District, West Palm Beach, FL.

SFWMD. 2009. Change Management Procedures for Hydrometeorological Data (Draft). OHDM Technical Report, SFWMD Q100-01, South Florida Water Management District, West Palm Beach, FL.

Skinner, C., F. Bloetscher and C. S. Pathak. 2009. Comparison of NEXRAD and rain gauge precipitation measurements in South Florida. *Journal of Hydraulic Engineering* 14(3):248-260.

Taylor, J.R. 1997. *An Introduction to Error Analysis: The Study of Uncertainties in Physical Measurements*. University Science Books, Sausalito, CA. Pages 45–92.

Wilsnack, M.M., J. Zeng and L. Zhang. 2010. Atlas of Flow Computations at Hydraulic Structures in the SFWMD. SHDM Report # 2009-005, South Florida Water Management District, West Palm Beach, FL.

Wilsnack, M. 2013. RE: STA-3/4 Seepage Reports. E-mail to Tracey Piccone, Ceyda Polatel and Luis Cadavid dated February 13, 2013.

Winter, T.C. 1981. Uncertainties in estimating the water balance of lakes. *Water Resources Bulletin* 17(1):82-115.

Zhang, L. 2013. Flow Rating Improvement for Culverts G384A-F in STA-3/4. Technical Note, Hydro Data Management Section, South Florida Water Management District, West Palm Beach, FL.

APPENDIX: List of Completed Tasks and Recommendations

Completed tasks in Phase I are as follows:

- Historical stage and flow data for Cells 3A and 3B control structures were examined and errors were corrected. Data collection and surface water flow computation protocols and procedures were reviewed.
- Status of the flow ratings at the control structures was reviewed. A CFD-based flow rating was developed for G-384. The CFD simulation results significantly lowered the absolute average errors of the rating equation.
- Spurious flow data at G-384 structures due to low head differentials were identified as the main reason for high residual errors in Cell 3A and 3B water budgets.
- Three methods to fix the historical flow rate data, one based on data correction and two on back calculation, were applied. Recommendations were made to the quality assurance group to improve flow data quality. Generation of corrected G-384 flow data in DBHYDRO is expected by approximately December 2014.
- Improved water budgets with improved mid-levee flows were developed.
- An uncertainly analysis of flow through culverts was performed.
- The Water Budget Tool was tested and found to be working properly if correct parameters are used in computations. The DBKEYs used in the water budgets and seepage estimation methods need to be reviewed.
- Available seepage estimation methods were applied to Cells 3A and 3B. A seepage estimation method based on reconciliation of the water budget for historical "no flow, no rainfall" periods was developed.
- An impact analysis showing the effect of seepage on water budget was conducted.
- Spatial and temporal variability in rainfall estimates were investigated. NEXRAD versus gauge rainfall data was compared. A noticeable difference was observed.
- Variability of ET estimation was investigated. Seasonal variations and slight differences, which are cancelled out in annual analyses, in lysimeter- and satellite-based data were found.
- The factors affecting the accuracy of change in storage estimates were identified.
- Effects of selected time steps and period of record were discussed.
- Improved water budget analyses based on provisional mid-levee flow rates were provided.
- Errors in components of water budgets were evaluated. Recommendations to reduce errors in surface water flows were provided.
- An uncertainty analysis was performed to quantify contributions from each component to the residual uncertainty.

The following items are provided for future implementation to further improve water budget analyses. The recommendations mentioned below, not listed according to importance or feasibility, are expected to improve the flow computations and water budget residual errors. Many items on this list are being implemented in Phase II:

- Review DBKEYs and cell areas used in water budget tool to ensure most up-to-date data is used in the analyses.
- Include seepage estimation capability for individual cells in the Water Budget Tool.
- Automate the gate operations at structures as a function of head differential using the flow rate uncertainty curves.
- Develop a seepage program to refine the estimate of seepage and the associated loading to each cell.
- Use and maintain PREF DBKEYS for internal structures.
- Collect more field flow data at low head conditions.
- Develop methods to rate flows under low head differential conditions.
- Evaluation of structural and operational means to minimize low head, wide gate opening and low flow events is essential.
- If possible, change the timing of discharges by operating the structures for shorter periods with higher discharge rates, or operate fewer structures.
- Install more than one set of stage recorders at internal structures.
- Consider differential head measurements for culverts to eliminate the errors introduced by surveys.
- Perform periodic inspections and calibrations to correct for sensor drift, sensor malfunctions, or reference elevation. Perform yearly resurveys for the stilling wells.
- Warn users of high uncertainties when the flow is computed with low head differentials. Put uncertainty bands around the flow data or include tags indicating the quality of flow estimates.
- Consider use of time-filtered headwater and tailwater data (time averaged and/or more complex data filtering techniques) to estimate flow during low head differential conditions.